Arctic worming:
Human-facilitated earthworm invasion transforms soil organic matter budgets and pools in Fennoscandian forests

A Thesis
SUBMITTED TO THE FACULTY OF
UNIVERSITY OF MINNESOTA
BY

Adrian Allan Wackett

IN PARTIAL FULFILLMENT OF THE REQUIREMENTS
FOR THE DEGREE OF
MASTER OF SCIENCE

Adviser Kyungsoo Yoo

December 2018

Acknowledgements

There are many people who have made this project and my participation in this work possible, and it would be impossible to acknowledge all of them adequately in this short section. Kyungsoo Yoo and Jonatan Klaminder deserve particular recognition for bringing this work to fruition. Their long-running friendship and collaboration is what conceived the idea of extending this ecological approach to academic study of earthworm invasion into Fennoscandia.

I cannot express the gratitude I have towards Kyungsoo for putting his faith in me to 'lead' this project and giving me the freedom to spend nearly half of my time in the LAAS program overseas. Our time traveling across the world chasing exciting research questions has inspired me at many levels and has vigorously stoked my passion for researching our planet and the myriad of organisms that inhabit it. These last three years have been memorable, and the kindness, passion, and overall joy you bring to the work you do and share with those around you has contributed greatly to my experience.

On the other end, I have a deep appreciation and respect for Jonatan Klaminder, Johan Olofsson, Carolina Olid, and all of the faculty and graduate students in the Department of Ecology and Environmental Sciences at Umeå University. Daily conversations at fika (and after hours in the EMG pub) were fountains of personal and academic growth, and some of these discussions inspired the subsequent work conducted here. Jonatan in particular deserves recognition for being a fantastic guide and host during my time in Sweden, and his self-described 'eccentric' approach to studying the natural world has made a strong impression on my approach towards research.

The list of those who have contributed in countless other ways is lengthy. I would like to thank my committee here at UMN – Brandy Toner, Nicolas Jelinski, and Lee Frelich – for their guidance and support over these years. I am so grateful to have been able to work with you all. Nic deserves additional recognition for the countless hours you have spent discussing soils and GIS with me: much of the mapping I have done for this work would not have been possible without your guidance and expertise.

I thank Doreen Huang and Carolina Olid at Umeå University for their guidance and assistance in the laboratory. Erin Cameron at University of Helsinki has also been a great inspiration and close collaborator on this work. Her extensive mapping of earthworm communities across Finland and willingness to share sites and resources is what made much of the work in Finland possible. I thank my friend Aku Korhonen for his tireless help in the field, Marjut Wollner for her help in the laboratory, and Visa Nuutinen for his creative and inspiring insights on earthworm ecology and Fennoscandian soils. Nate Looker has also become a close friend and colleague over these years, and his contributions and insights to this work have proven invaluable.

Last but certainly not least, I sincerely thank the friends and family who have supported me over the course of my life and in particular during this most recent journey. Thank you, mom and dad, for your unceasing love and support, and for teaching me to chase my passions in life and work. I can't adequately thank my partner, Holly Bolstad, for always believing in me and putting up with the countless late nights and vacations spent searching for earthworms and soils across the world. I dedicate this thesis to everyone who has helped me along the way.

Abstract

Earth's high latitude ecosystems are already under dire threat from climate warming, permafrost thaw, and intensifying natural resource exploitation. In addition to these ongoing concerns, accelerating urbanization, agricultural expansion, and greater opportunities for recreation in high-latitude regions are likely to introduce a less conspicuous but potentially potent threat: non-native geoengineering earthworms. Earthworms were eradicated from northern N. America (including Minnesota) during the last glaciation, and it is now established that humans are (re-) introducing exotic earthworm species into these forests with dramatic consequences on soil and ecosystem functioning. However, their invasiveness and capacity to modify high-latitude boreal and arctic forests like those in Fennoscandia remains largely unknown. Here I explore two inter-related hypotheses concerning earthworms and soils in Fennoscandian forests: H1) despite their different human history and proximity to the native range of *Lumbricidae* earthworms (Southern and Central Europe), I predicted that Pleistocene glaciations also extirpated earthworms from Fennoscandia, suggesting that European earthworms (if present) are also non-native and invasive in these landscapes; and H2) if introduced by humans, the invasive earthworms transform Fennoscandian forest soil morphologies and soil organic matter (SOM) dynamics by removing thick organic layers at the forest floor and forming A-horizon (mineral topsoil) in their wake.

To address H1, I tested a series of sub-hypotheses stating that: 1) earthworms did not colonize the Fennoscandian landscape via dispersal by brackish seawater, nor were they introduced by early indigenous peoples (Sami) who followed the retreating glaciers

into northern Fennoscandia; and 2) earthworms are spreading into Fennoscandian forests from 'worm point sources' created by modern human-mediated dispersal vectors such as farming, fishing, gardening, and logging (among others). Although I could not dispel the possibility that small epigeic-type earthworms may have entered the Fennoscandian landscape considerably earlier via water-mediated dispersal and/or by 'hitch-hiking' along with Sami settlers, I found that more impactful 'geoengineering' species are only present in arctic landscapes associated with more modern (i.e. last two centuries) human disturbance (supporting H1) and are radiating outward from these anthropogenic point sources into virgin arctic and boreal forests. Furthermore, in line with H2, expansion of these geoengineers into adjacent forests consistently induced changes to forest soil morphologies and nutrient cycling regimes, including rapid reduction of the SOM pool in organic horizons and re-allocation of this SOM into mineral horizons: wherein it is sorbed onto mineral surfaces and/or occluded within aggregates.

This belowground transformation likely has significant aboveground consequences as well as implications for the long-term carbon balance of boreal and arctic ecosystems, which store more than half (~ 53%) of earth's soil carbon. Furthermore, based on results from N. America, this 'unseen' invasion may also have cascading effects on fungal and microbial associations, plant communities, and overall ecosystem functioning. Considering that the arctic is already being disproportionately affected by climate change and that human activities in these regions are likely to accelerate as these regions warm, additional research assessing the ecological impacts of arctic w<u>o</u>rming is urgently needed.

Table of Contents

List of Tables

List of Figures

Chapter 1

Human-mediated introduction of geoengineering earthworms in the Fennoscandian arctic

"*Peregrine [worms] … those species which possess some power of migration over the sea, denied to the majority of worms, and probably due to the direct interference of man.*"

– Frank E. Beddard, 1912

Chapter Overview

It is now well established that European earthworms are re-shaping formerly glaciated forests in North America with dramatic ecological consequences. However, few have considered the potential invasiveness of this species assemblage in the European arctic. Here we argue that some earthworm species (*Lumbricus rubellus, Lumbricus terrestris* and *Aporrectodea* sp.) with great geomorphological impact (geoengineering species) are non-native and invasive in the Fennoscandian arctic birch forests, where they have been introduced by agrarian settlers and most recently through recreational fishing and gardening. Our exploratory surveys indicate no obvious historical dispersal mechanism that can explain early arrival of these earthworms into the Fennoscandian arctic: that is, these species do not appear to establish naturally along coastlines mimicking conditions following deglaciation in Fennoscandia, nor were they spread by early native (Sami) cultures. The importance of anthropogenic sources and the invasive characteristics of *L. rubellus* and *Aporrectodea* sp. in the arctic is evident from their radiation outwards from abandoned farms and modern cabin lawns into adjacent arctic birch forests. They appear to outcompete previously established litter-dwelling earthworm species (i.e. *Dendrobaena octaedra*) that likely colonized the Fennoscandian landscape rapidly following deglaciation via hydrochory and/or dispersal by early Sami settlements. The high geoengineering earthworm biomasses, their recognized ecological impact in other formerly glaciated environments, and their persistence once established leads us to suggest that geoengineering earthworms may pose a potent threat to some of the most remote and protected arctic environments in northern Europe.

1. Introduction

Hidden underfoot, earthworms are powerful ecosystem engineers and the best-known soil macrofauna. Earthworms are found on all continents except Antarctica, but non-native earthworm populations have drawn renewed scientific interest in recent years due to their large-scale invasive properties (Hendrix *et al.,* 2008). Introductions and ecological impacts of non-native earthworms are particularly well studied in the formerly glaciated forests of North America, where it is now established that earthworms were eradicated during the last glaciation (Gates, 1982), but have since been reintroduced by farming, fishing, and other human activities (Cameron *et al.,* 2007; Eisenhauer *et al.,* 2007). Here, invasive European earthworm species (*Lumbricidae*) have resulted in dramatic transformations to forest soil morphologies (Alban and Berry 1994; Hale *et al.,* 2005), inorganic nutrient availability (Resner *et al.,* 2015), carbon cycling (Lyttle *et al.,* 2015), understory plant communities (Hale *et al.,* 2006), and overall ecosystem biodiversity and functioning (Craven *et al.,* 2017). Earthworms dwelling within the organic soil horizons and the upper few cm of the mineral soil (epi-endogeic, i.e. *Lumbricus rubellus*), or those that burrow deeply (vertically or horizontally) into mineral soil (anecic *Lumbricus terrestris* and endogeic *Aporrectodea* sp., respectively) are recognized as the main 'geoengineers' and drivers of ecosystem change (e.g. Hale *et al.,* 2005, 2006; Resner *et al.,* 2015). These earthworms are henceforth in the text referred to as 'geoengineering earthworms'.

In Fennoscandia, earthworms have historically not been viewed as invasive. One possible reason for this differing perspective is the five millennia longer European agrarian history, for instance in southern parts of Sweden (Skoglund *et al.,* 2012), which

with the North American examples in mind likely induced a much older migration history of geoengineering earthworms. However, the alpine region of Fennoscandia (the Scandes) represents one of the last European environments where earthworm dispersal by agrarian cultures has historically been very limited. As a result, this biome likely represents one of the last northern European landscapes where peregrine earthworm communities have yet to establish. That epi-endogeic and anecic *Lumbricus* sp. and/or endogeic *Aporrectodea* sp. have the capacity to establish in the arctic climate of the Scandes is evident given that *L. rubellus* has been reported in similar climates within Fennoscandia (Terhivuo, 1988) and Southeast Alaska (Costello *et al.,* 2011), while various *Aporrectodea* sp. have also been documented in man-made biotopes at similar latitudes in Finland and Norway (Terhivuo, 1988).

In this study, we test the idea that *Lumbricus* and *Aporrectodea* sp. are non-native and invasive (i.e. occurring in abundances causing significant impact on the native environment) in the Fennoscandian arctic (Figure 1.1). This overall hypothesis was tested by a series of sub-hypotheses stating that these geoengineering earthworms: (1) did not enter northern boreal and arctic ecosystems via natural dispersal with brackish waters (conditions mimicking those following deglaciation); (2) did not arrive to the Scandes with traditional Fennoscandian native (Sami) cultures—in the North American analog native agrarian populations did not involve tillage and animal husbandry in the glaciated regions (Pleasant, 2011) that could have facilitated earthworm introduction; and (3) are currently spreading into Fennoscandian arctic birch forests from anthropogenic point sources such as abandoned farms, cabin yards, composts, and fishing sites.

2. Methods

2.1. Field methods and site description

Possible historical dispersal routes for geoengineering earthworms to enter the Fennoscandian arctic (Hypotheses 1 and 2) were assessed by surveying earthworm populations in primary succession gradients largely resembling those following deglaciation of Scandinavia where water in the Baltic alternated between brackish and freshwater stages (Figures 1.1, 1.2), as well as within ancient Sami cultural soils. Hypothesis 1 was tested using primary succession gradients forming along the shoreline of the weakly brackish Gulf of Bothnia in response to isostatic uplift rates of ~ 0.8 cm yr^{-1} (Figure 1.2). These vegetation gradients are described in detail in Svensson and Jeglum (2003). In short, two distinct temporal vegetation zones (*Alnus incana*, soil age ~20–50 years; *Picea abies*, >200 years) in undisturbed forests were surveyed for earthworms presumably entering the landscape via water transport (i.e. hydrochory), even though migration from adjacent terrestrial sources cannot be fully excluded. Spatial gradients traversing the *Alnus* and *Picea* forest were divided into two types: (1) gradients (N = 3) with no evident human sources of earthworms adjacent (referred to as 'natural'); and (2) anthropogenic gradients (N = 3) developing adjacent to human earthworm sources (cabins with flowerbeds, composts and lawns).

In these gradients, earthworm populations were surveyed at six sites located along each gradient. Each site, located between ca. 10–110 m apart, was surveyed using three replicated sub-plots (0.07 m^2). For each sampling, the common liquid mustard extraction technique (Gunn, 1992) was coupled with hand sorting of the organic soil or humus (if present) down to 15 cm depth. In addition to the natural gradients, three

gradients within the same temporal zones were traversed adjacent to known anthropogenic sources (cabins with lawns, flower beds, gardens, composts) to test whether geoengineering *Lumbricus* and *Aporrectodea* sp. could migrate into and survive in this environment if introduced (i.e. serving as positive controls, Figure 1.2c–2e).

Hypothesis 2 was tested at meadows (historical milking grounds) generated by nomadic Sami peoples within Padjelanta national park (Figures 1.1, 1.3a, 1.3e), where nomadic Sami cultures gathered reindeer for milking for centuries (1600–1900). The more nutrient (nitrogen) rich soils in the historical milking grounds are likely to be suitable for soil-dwelling *Lumbricidae*; thus, if Sami cultural practices facilitated their dispersal to the landscape, these geoengineering species should be present in these areas. The unique vegetation and soils of these milking grounds are described in detail elsewhere (Egelkraut *et al.,* 2018a, 2018b). Milking ground sites (N = 4) were surveyed for earthworms (methods as described previously) using 3–4 subplots (0.07 m^2) per site. At each site we used a similar set of control sites (N = 4) representing the adjacent tundra and sub-alpine birch (*var. tortuosa* and *Betula pubescens*, respectively) forest soils to allow quantification of the impact of anthropogenic disturbances on earthworm communities.

To test hypothesis 3, we surveyed potential anthropogenic point sources situated in alpine environments within the Abisko area and Padjelanta national park during the summer and autumn (July through September) of 2016 and 2017. In 2016, three presumed earthworm invasion gradients extending from farms established by homesteading farmers in the late nineteenth century (Kopparåsen and Jierpen, Figure 1.3b–3.d respectively) as well as a modern compost (Staloloukta, Padjelanta) (Figure 1.3a) were surveyed for earthworms (methods as described previously). Here, at subjectively chosen distances

from the point source, earthworm populations were surveyed using one to three replicates per distance. The gradient at Jierpen was surveyed again in 2017 to cope with eventual between-year differences. During this survey, an additional control gradient was established running in parallel to the gradient intersecting with the anthropogenic source (farm), but separated from this former gradient by a stream restricting species unable to migrate via hydrochory. In these two surveys (summer 2017), we also sorted mineral soils down to a depth of 25 cm following liquid mustard extraction, to cope with eventual under-selecting for endogeic (i.e. *Aporrectodea*) species.

Site selective surveys of earthworm species introduced from potential anthropogenic sources were also conducted (sampled as described earlier) along parts of the hiking trail Kungsleden (the King's trail), at abandoned farms and station homes along the Kiruna-Narvik railway line, and in the villages of Abisko (lawns and composts) and Stalologukta (lawns and helicopter landing ground) (Figure 1.1b). The validity of hypothesis 3 was tested statistically using a regression analysis (data normal distributed) between distances from the point source versus total biomass of geo-engineering (epi-endogeic, endogeic, and anecic) earthworm species for the three gradients sampled in detail (Jierpen, Kopparåsen and Stalologukta).

2.2. Laboratory analysis

2.2.1. Earthworm identification

Following sampling, earthworms were identified down to species level using the keys of Sims and Gerard (1999) and Hale (2007) and were grouped by functional type according to Hale (2007). Measured length (mm) was converted to

ash-free dry biomass (g m^{-2}) using the allometric equations of Hale *et al.* (2004) to facilitate comparison with previously published studies. This unit conversion was repeated for all survey sites (described below).

2.2.2. pH measurements

Humus ($N = 9$; $n = 74$) and mineral soil ($N = 4$; $n = 52$) pH were measured using a Fisher Scientific Accumet Basic AB15 pH meter in 1:1 mixtures of humus/soil: DI water (i.e. 10 g soil shaken in 10 mL DI water) unless otherwise specified in Table 1. For most samples (excluding the Padjelanta cultural soils), pH was also measured in 0.02 M $CaCl_2$ following determination in water (Table 1).

3. Results and discussion

Our earthworm surveys from primary succession gradients along the Gulf of Bothnia (Figure 1.2) and Sami cultural soils (milking grounds) in Padjelanta (Figure 1.3a, 1.3e) revealed only the epigeic earthworm species *Dendrobaena octaedra* (and on some occasions *Dendrodrilus rubidus* in the primary succession gradients); hence, our findings support hypotheses 1 and 2. The most parsimonious explanation for the absence of *Lumbricus* and *Aporrectodea* sp. in the indigenous cultural meadows is that geoengineering species did not migrate along with the traditional Sami cultures. We cannot fully exclude the possibility that geoengineering species were once present in the Sami milking grounds, but dissipated due to natural soil acidification processes following cessation of the reindeer milking culture (late ninetenth century). However, we find this scenario very unlikely as: (1) current soil pH around 4.3 (in KCl) is above the critical pH of 2.5 noted for *L. rubellus* (Hæggström and Terhivuo, 1979) and is comparable to other

sites where geoengineering species are present (Table 1.1); and, (2) *Lumbricus* and *Aporrectodea* sp. were present only in the acidic (pH_{CaCl_2} = 3.3) anthropogenic primary succession gradients (Figure 1.2c–2e) and not in naturally formed primary succession soils (Figure 1.2b), suggesting that the absence of geoengineering earthworms is more likely a result of their inability to be dispersed by indigenous cultural practices rather than by soil acidity.

Findings of *D. octaedra* in the Padjelanta alpine soils (milking grounds and control sites) and on about 68% of the surveyed tundra and alpine birch forest sites (Table 1.2) is consistent with North American studies implicating this litter dwelling species as the prime colonizer of pristine soils (e.g. Gundale *et al.,* 2005). Results from the primary succession gradients (Figure 1.2b) provide a mechanistic explanation for their early arrival to the Fennoscandian landscape, as these surveys indicate that *D. octaedra* and *D. rubidus* are effectively dispersed by brackish waters (i.e. hydrochory): a mechanism previously suggested for these species (Terhivuo, 1988; Terhivuo and Saura, 2006). We note that the driftwood zone within these successional gradients appears to be the main habitat for these earthworms, and possibly also the main sources of cocoons.

The likelihood of *L. rubellus* establishing via hydrochory in the post-glacial Fennoscandian landscape seems more improbable given that this species reproduces only biparentally (Muldal, 1952). That is, the probability that viable *L. rubellus* cocoons from continental Europe traversed the brackish Baltic water *and* were deposited adjacent to each other on post-glacial Fennoscandian shorelines seems very low. The same holds true for *Lumbricus terrestris* and most of the *Aporrectodea* sp., although *Aporrectodea rosea and Aporrectodea trapezoides* are believed to be parthenogenetic (Jaenike and Selander,

1979) and therefore may be exceptions. Nonetheless, based on this reasoning, and on the absence of geoengineering earthworm species in Sami cultural soils (Figure 1.3e) and primary succession coastal gradients not strongly affected by human disturbance (Figure 1.2b), we argue that geoengineering *Lumbricus* and *Aporrectodea* sp. are unlikely to have entered the Fennoscandian arctic biome by non-human mediated migration transport processes or with early native human cultures. Their modern presence in the arctic is likely the result of human introductions in recent centuries.

In all of the arctic gradients studied in detail, composts, fishing sites, and historic farmlands are the apparent sources of geoengineering earthworms, and their biomasses decrease significantly with increasing distance from the anthropogenic point sources into the surrounding sub-arctic birch forests (Figure 1.3). The invasive character of these anthropochorous geoengineering earthworms is also apparent in these gradients, as they become far more abundant than the native epigeic macrofauna, namely *D. octaedra*. In the arctic birch forest near the abandoned farms of Jierpen and Kopparåsen, we found a diverse geoengineering earthworm species assemblage including *L. rubellus* (epi-endogeic) and various endogeic *Aporrectodea* sp. including *Aporrectodea calignosa complex*, *Aporrectodea rosea*, and *Aporrectodea trapezoides*. At Jierpen, the control gradient showed none of these species as long as the two gradients were separated by a stream, further stressing that dispersal from the farmland is the best explanation for the observed spatial trends.

Similarly diverse communities were identified in modern compost from the Sami village of Staloluokta in the heart of Padjelanta national park. Local Sami residents informed us that earthworms were absent until their introduction by fishermen at the end

of the 1970s (Sven-Ingvar Blind, personal comm.), further supporting our interpretation of a non-native origin. Interestingly, *Lumbricus terrestris*, which is thought to have more strict environmental constraints with respect to climate and soil quality, was found in low densities within the compost at Staloluokta, making this one of the few reported occurrences of this species above the Arctic Circle in Fennoscandia (Terhivuo, 1988; Nieminen *et al.,* 2011).

The between-site difference in the length of the geoengineering earthworm migration front seems to largely reflect differences in anthropogenic introduction, i.e. late 1970s in Padjelanta, ca. 1900s at Kopparåsen (timing of railroad construction from Kiruna, Sweden to Narvik, Norway), and ca 1850s at Jierpen when agriculture first arrived to the interior of northern Sweden (Andersson *et al.,* 2005). We also note that the estimated dispersal rates at these sites, inferred using our estimated arrival times, are directly comparable to North American analogues were migration rates have been estimated to be on the order of ~ 5–10 m per year (e.g. Hale *et al.,* 2005). The importance of man-made biotopes as the primary sources of geoengineering earthworms was further supported by our more general survey indicating multiple lawns, gardens and abandoned farms as sources of geoengineering earthworm species across the Scandes (Table 2).

4. Conclusion

Our exploratory surveys stress that *Lumbricus* and *Aporrectodea* sp. are likely earthworm species that should be treated as non-native and invasive in the Fennoscandian arctic biome. In contrast to some other arctic countries where European earthworms are considered invasive (i.e. USA and Canada), the Nordic countries have no strategy

regarding the dispersal of these earthworm species to sensitive environments. We call for immediate attention to the potential invasiveness of this species assemblage and list four main reasons for our concern. First, the observed geoengineering earthworm species are known to be drivers of dramatic environmental changes in other formerly glaciated environments, including negative effects on native plants and preferential selection for non-native plants and graminoids (Roth *et al.,* 2015; Craven *et al.,* 2017), increased greenhouse gas emissions (Lubbers *et al.,* 2013) and depletion of key nutrients in surface soils (Resner *et al.,* 2015). We also note that the earthworm-driven modifications to soil morphologies appears to largely resemble observations from North American forests (Figure 1.4), wherein thick organic soil horizons (O horizon) diminish after the establishment of geoengineering earthworms while the underlying organic rich mineral soil (A horizon) expands (Lyttle *et al.,* 2015). Second, measured earthworm biomasses in Fennoscandian arctic birch forests adjacent to anthropogenic source areas are comparable to biomasses in North American temperate and boreal forests where invasive earthworms are recognized as a potent threat (e.g. Hale *et al.,* 2006; Eisenhauer *et al.,* 2007; Resner *et al.,* 2015). Third, we know from previous studies that earthworms are almost impossible to eradicate once they have invaded a system. Finally, the limited historical impact from humans on the Fennoscandian alpine environment makes this area one of the few remaining northern European biomes where anthropogenic spreading of earthworms is likely still limited. Thus, there is an urgent need for further assessment of this on-going earthworm invasion that can aid decision-making as to whether measures should be taken to restrict the spread of geoengineering earthworm species to the Fennoscandian arctic, before they have become fully established.

5. References

Alban DH, Berry EC (1994) Effects of earthworm invasion on morphology, carbon and nitrogen of a forest soil. *Applied Soil Ecology*, **1**, 243–249.

Andersson R, Ostlund L, Tornlund E (2005) The last European landscape to be colonized: a case study of land-use change in the far north of Sweden 1850–1930. *Environment and History*, **11**, 293–318

Cameron EK, Bayne EM, Clapperton MJ (2007) Human-facilitated invasion of exotic earthworms into northern boreal forests. *Ecoscience*, **14**, 482–490.

Costello DM, Tiegs SD, Lamberti GA (2011) Do non-native earthworms in Southeast Alaska use streams as invasional corridors in watersheds harvested for timber? *Biological Invasions*, **13**, 177–187.

Craven D, Thakur MP, Cameron EK *et al.* (2017) The unseen invaders: introduced earthworms as drivers of change in plant communities in North American forests (a meta- analysis). *Global Change Biology*, **23**, 1065–1074.

Egelkraut D, Aronsson KÅ, Allard A, Åkerholm M, Stark S, Olofsson J (2018a) Multiple feedbacks contribute to a centennial legacy of reindeer on tundra vegetation. Ecosystems, 1–19.

Egelkraut D, Kardol P, De Long JR, Olofsson J (2018b) The role of plant-soil feedbacks in stabilizing a reindeer-induced vegetation shift in subarctic tundra. *Functional Ecology*, **32**, 1959–1971.

Eisenhauer N, Partsch S, Parkinson D, Scheu S (2007) Invasion of a deciduous forest by earthworms: changes in soil chemistry, microflora, microarthropods and vegetation. *Soil Biology and Biochemistry*, **39**, 1099–1110.

Gates GE (1982) Farewell to North American megadriles. *Megadrilogica*, **4**, 12–77.

Gundale MJ, Jolly WM, Deluca TH (2005) Susceptibility of a northern hardwood forest to exotic earthworm invasion. *Conservation Biology*, **19**, 1075–1083.

Gunn A (1992) The use of mustard to estimate earthworm populations. *Pedobiologia*, **36**, 65–67.

Hæggström CA, Terhivuo J (1979) The Lumbricidae (Oligochaeta) in the archipelago of Åland, SW Finland. *Memoranda Societatis pro Fauna et Flora Fennica*, **55**, 17–31.

Hale CM, Reich PB, Frelich LE (2004) Allometric equations for estimation of ash-free dry mass from length measurements for selected European earthworm species

(Lumbricidae) in the western Great Lakes region. *American Midland Naturalist*, **151**, 179–185.

Hale CM, Frelich LE, Reich PB, Pastor J (2005) Effects of European earthworm invasion on soil characteristics in northern hardwood forests of Minnesota, USA. *Ecosystems*, **8**, 911–927.

Hale CM, Frelich LE, Reich PB (2006) Changes in hardwood forest understory plant communities in response to European earthworm invasions. *Ecology*, **87**, 1637–1649.

Hale CM (2007) Earthworms of the Great Lakes Region. Kollath & Stensaas Publishing. 36 pages.

Hendrix PF, Callaham Jr. MA, Drake JM, Huang C, James SW, Snyder BA, Zhang W (2008) Pandora's box contained bait: the global problem of introduced earthworms. *Annual Review of Ecology, Evolution, and Systematics*, **39**, 593–613.

Jaenike J, Selander RK (1979) Evolution and ecology of parthenogenesis in earthworms. *American Zoologist*, **19**, 729–737.

Lubbers IM, van Groenigen KJ, Fonte SJ, Six J, Brussaard L, van Groenigen JW (2013) Greenhouse-gas emissions from soils increased by earthworms. *Nature Climate Change*, **3**, 187–194.

Lyttle A, Yoo K, Hale CM, Aufdenkampe A, Sebestyen SD, Resner K, Blum A (2015) Impact of exotic earthworms on organic carbon sorption on mineral surfaces and soil carbon inventories in a northern hardwood forest. *Ecosystems*, **18**, 16–29.

Muldal S (1952) The chromosomes of the earthworms I. The evolution of polyploidy. *Heredity*, **6**, 55–76.

Nieminen M, Ketoja E, Mikola J, Terhivuo J, Sirén T, Nuutinen V (2011) Local land use effects and regional environmental limits on earthworm communities in Finnish arable landscapes. *Ecological Applications*, **21**, 3162–3177.

Pleasant J (2011) The paradox of plows and productivity: an agronomic comparison of cereal grain production under Iroquois hoe culture and European plow culture in the seventeenth and eighteenth centuries. *Agricultural History*, **85**, 460–492.

Resner K, Yoo K, Sebestyen S, Aufdenkampe A, Hale CM, Lyttle A, Blum A (2015) Invasive earthworms deplete key soil inorganic nutrients (Ca, Mg, K, and P) in a northern hardwood forest. *Ecosystems*, **18**, 89–102.

Roth AM, Whitfeld TJS, Lodge AG, Eisenhauer N, Frelich LE, Reich PB (2015) Invasive earthworms interact with abiotic conditions to influence the invasion of common buckthorn (*Rhamnus cathartica*). *Oecologia*, **178**, 219–230.

Sims RW, Gerard BM (1999) Earthworms. In: *Keys and notes for the identification and study of the species* (ed./eds Barnes RSK, Crothers JH). 171 pp. FSC publications, London, United Kingdom.

Skoglund P, Malmström H, Raghavan M, Storå J, Hall P, Willerslev EM, Gilbert TP, Götherström A, Jakobsson M (2012) Origins and genetic legacy of neolithic farmers and hunter-gatherers in Europe. *Science*, **336**, 466–469.

Svensson JS, Jeglum JK (2003) Spatio-temporal properties of tree-species belts during primary succession on rising Gulf of Bothnia coastlines. *Annales Botanici Fennici*, **40**, 265–282.

Terhivuo J (1988) The Finnish Lumbricidae (Oligochaeta) fauna and its formation. *Annales Zoologici Fennici*, **25**, 229–247.

Terhivuo J, Saura A (2006) Dispersal and clonal diversity of North-European parthenogenetic earthworms. *Biological Invasions*, **8**, 1205–1218.

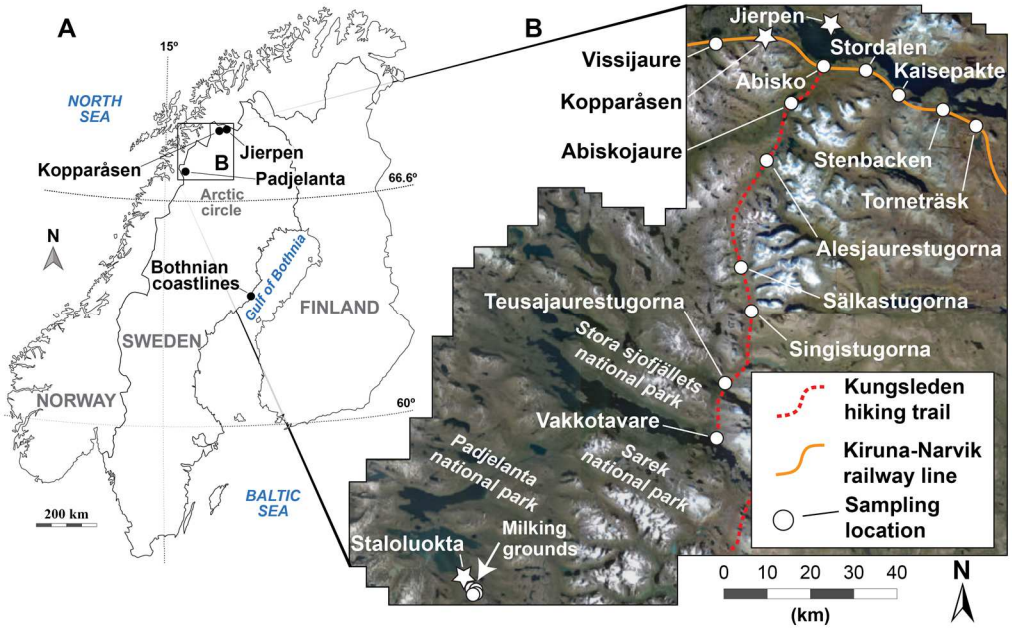

Figure 1.1. (a) Regional map of Fennoscandia showing the main earthworm sampling locations mentioned in the text. **(b)** Aerial photo of the studied alpine biome showing locations (white circles) of the arctic earthworm survey sites. Starred symbols indicate the three gradients studied with high spatial resolution (Jierpen, Kopparåsen, and Staloluokta). An arrow indicates the locations of the Sami cultural soils (reindeer milking grounds) within Padjelanta national park. Also shown are the survey points along the popular Kungsleden hiking trail and Kiruna-Narvik railway line.

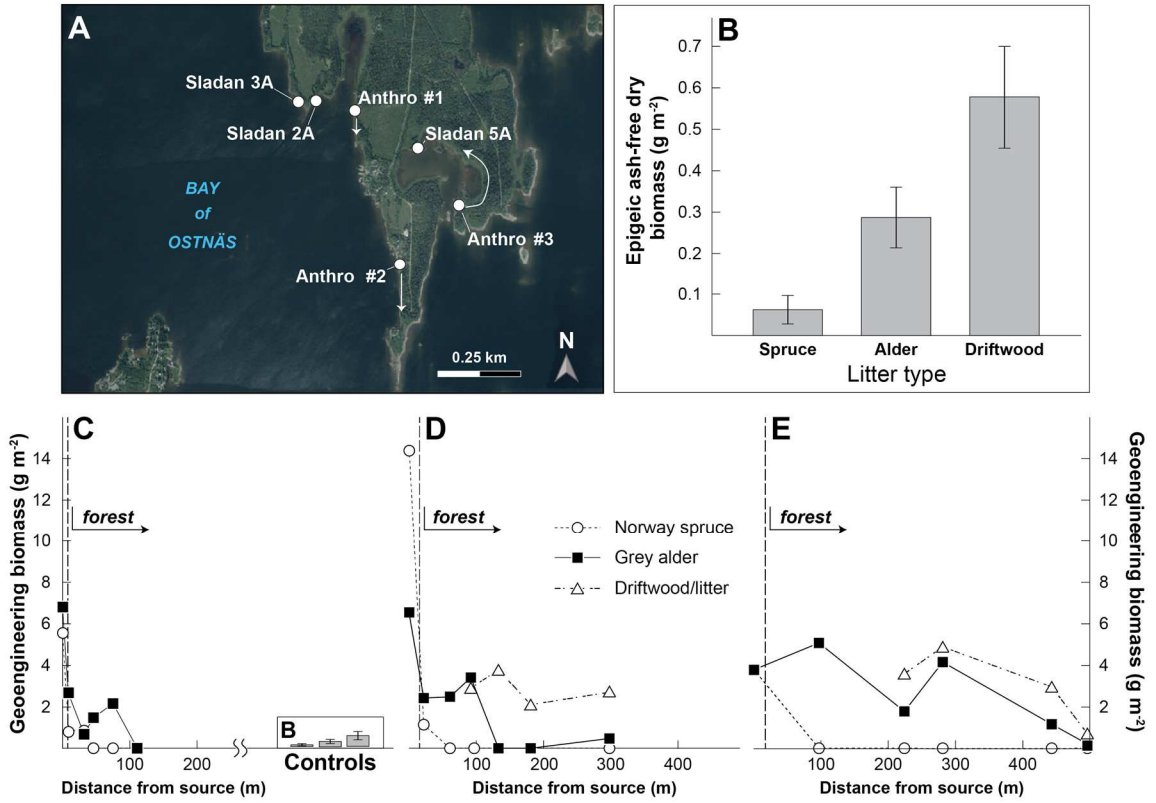

Figure 1.2. (a) Aerial map of earthworm sampling gradients along rising Bothnian coastlines within the Bay of Ostnäs, including gradients not obviously disturbed by human activities (Svensson and Jeglum, 2003), i.e. Sladan 2A, 3A, 5A and gradients affected by modern human disturbances (lawns and gardens, Anthro #1–3). **(b)** Epigeic earthworm (*D. octaedra* and *D. rubidus*) biomass in distinct temporal vegetation zones at the natural gradients of Svensson and Jeglum (2003) where biomass values represent an average from individual sub-plots ($n = 3$) sampled within each vegetation zone at the three ($N = 3$) natural gradients (i.e. total $n = 9$ for each vegetation type). Note that no geoengineering species were found (i.e. geoengineering biomass = 0) and thus the biomass units are different from other panels. **(c–e)** Geoengineering earthworm biomasses plotted versus distance from presumed source (lawn, garden or compost) at anthropogenic sites #1 **(c)**, #2 **(d)** and #3 **(e)**. The epigeic earthworm biomasses from the natural gradients (controls) are shown as an inset in panel **(c)** for comparison.

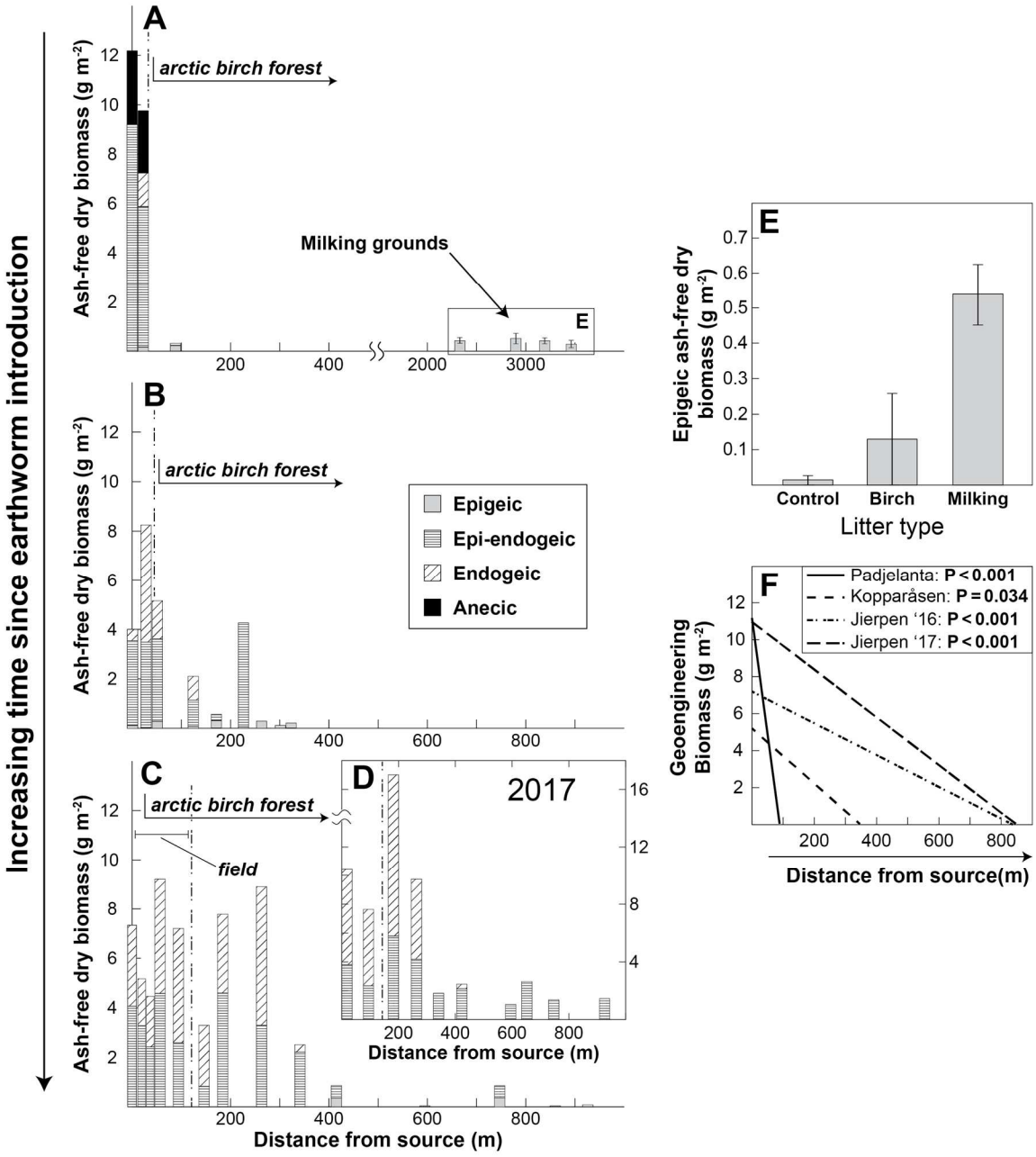

Figure 1.3. Total earthworm biomass (converted to ash free biomass, see methods) broken down by functional type (Hale, 2007) plotted versus distance from source (abandoned farm or compost) at the three detailed arctic gradients in **(a)** Staloluokta, Padjelanta, **(b)** Kopparåsen, **(c)** Jierpen (2016) and **(d)** Jierpen (2017). Biomass values shown represent an averaged of within-site replicates (n = 1–3). The border between the anthropogenic source area and surrounding birch forest is indicated with a dashed line. Note that all *Lumbricus* juveniles are classified as epi-endogeic given the absence of anecic *Lumbricus terrestris* adults at the Kopparåsen and Jierpen sites. Lumbricus juveniles were also classified as epi-endogeic in the Padjelanta gradient for consistency. **(e)** Epigeic (*D. octaedra*) biomass with vegetation type in Padjelanta national park.

Dendrobaena biomasses are significantly higher ($P < 0.05$) within the old Sami milking grounds ($N = 4$) than in the control plots ($N = 4$). Note that no geonengineering species were observed here and thus, y-axis units are different than in **(a–d)**. The milking ground biomasses are also shown as an inset in panel **(a)** for comparison. **(f)** Regression lines between distance from the anthropogenic sources and total biomass of geoengineering earthworms at Staloluokta ($F_{1,7} = 48.922$, $r^2 = 0.87$; $P < 0.001$), Kopparåsen ($F_{1,9} = 6.213$, $r^2 = 0.41$; $P < 0.034$), Jierpen 2016 ($F_{1,24} = 34.946$, $r^2 = 0.59$; $P < 0.001$) and Jierpen 2017 ($F_{1,31} = 26.106$, $r^2 = 0.46$; $P < 0.001$) supporting hypothesis 3. Note that the milking grounds were not included in the calculation of biomass versus distance for the Padjelanta gradient, since the milking grounds did not include any geoengineering earthworms.

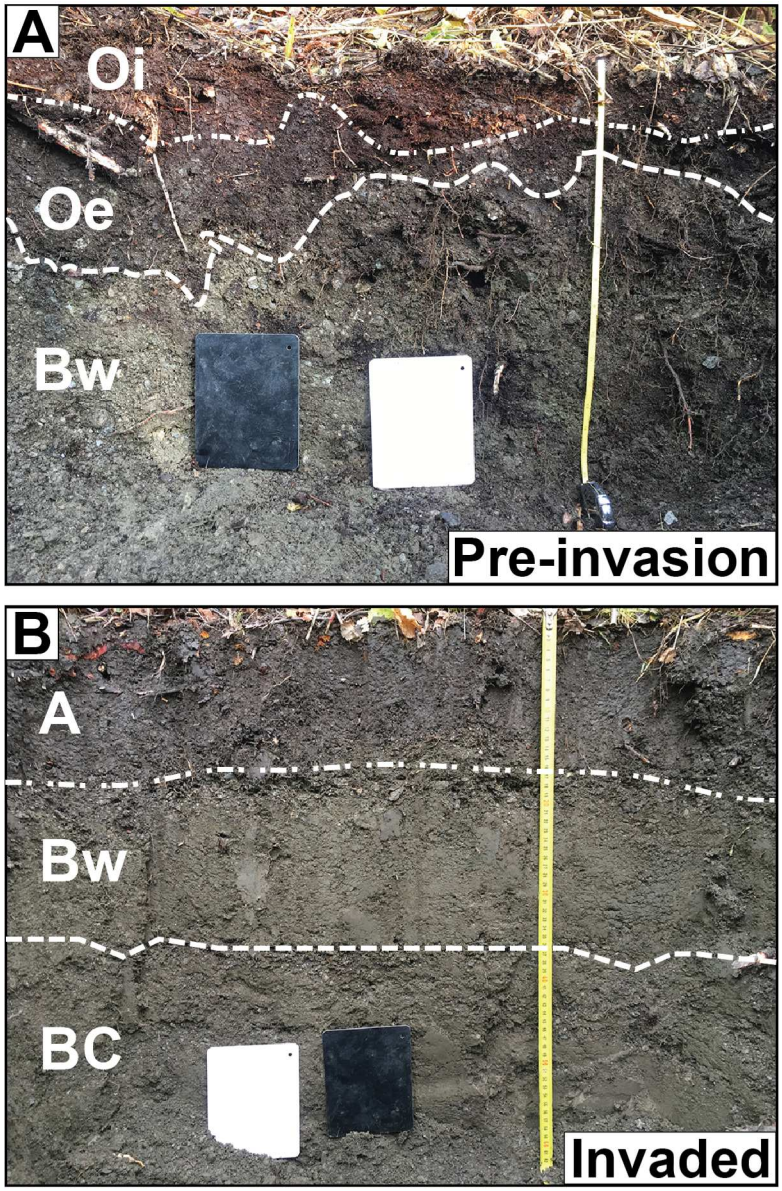

Figure 1.4 (a) Soil pit (51 cm depth) from the Jierpen gradient (Figure **3c**–**3d**) showing genetic soil horizons in sub-alpine arctic birch forests developing in the absence of geoengineering earthworms. **(b)** Soil pit (63 cm depth) from Jierpen showing soil horizons in sub-alpine arctic birch forests following decades of geoengineering by non-native earthworms. Letters indicate genetic soil horizons. Black and white color cards are shown to illustrate color differences between photos. Note that the organic surface horizons (Oi and Oe) have been completely mixed into the mineral subsoil, resulting in a thick (~ 20 cm) A-horizon in heavily invaded arctic forests.

Table 1.1. pH values of humus and mineral soil for Fennoscandian boreal (Bothnian coastlines) and arctic environments surveyed for earthworms in this study

Site type (Invasion status)	**Vegetation type** (*Distance from source*)	**Sample matrix** (*n*)	**Sample pH** [a] (H_2O,$CaCl_2$)[b]
		Bothnian coastlines	
Successional gradients	Spruce - *Picea abies*	Humus (*n*=14) [c]	(3.9,3.3)
	Alder - *Alnus incana*	Humus (*n*=17)	(5.0,4.5)
	Driftwood (thick litter)	Litter/Humus (*n*=9)	(5.8,5.5)
		Padjelanta national park	
Sami cultural soils	Milking ground	Humus	(4.3) [d]
	Control	Humus	(3.8)
		Arctic invasion gradients (near Abisko)	
Jierpen (Pre-invasion)	Birch forest (> *341 m from source*)	Humus (*n*=20) [e]	(5.2,4.6)
		Mineral soil (*n*=18) [f]	(5.5,4.7)
Jierpen [g] (Invaded)	Field/Birch forest (< *341 m from source*)	Humus (*n*=4)	(5.1,4.8)
		Mineral soil (*n*=20)	(6.4,5.5)
Kopparåsen (Pre-invasion)	Birch forest (> *171 m from source*)	Humus (*n*=8)	(4.8,4.4)
		Mineral soil (*n*=6)	(5.4,4.1)
Kopparåsen (Invaded)	Field/Birch forest (< *171 m from source*)	Humus (*n*=2)	(5.2,4.9)
		Mineral soil (*n*=8)	(5.6,5.1)

[a] Standard error (σ) for all sites and matrix types was in the range of $\pm$ 0.1 – 0.4

[b] pH was measured in 0.02 M $CaCl_2$ following pH determination in water

[c] Humus was sampled in bulk to 20 cm depth. When humus thickness <20 cm, the entire depth profile was collected.

[d] pH values for Padjelanta cultural soils were collected during a study by Egelkraut et al. by extracting 2 g fresh soil in 50 ml 1M KCl solution. The samples were shaken for 2 hours and left to settle overnight before measuring pH.

[e] At the arctic sites, humus was sampled to 10 cm depth (when present). If humus thickness <10 cm, the entire depth profile was collected.

[f] The upper 10 cm of the mineral soil profile was collected, either beginning at the base of the humus layer or at the ground surface in the absence of an organic horizon.

[g] We defined (*Invaded*) as the stage along our invasion gradients where the forest floor displays a (relatively) continuous humus layer. Fields and birch forests with diverse, well-established geoengineering earthworm communities are typically devoid of an organic horizon.

Table 1.2. Results from the site selective surveys of earthworm communities in proximity to anthropogenic sources across the Fennoscandian arctic alpine region (the Scandes)

	Native epigeic (litter) species		***Geoengineering species***		
Site name	*Dendro. octaedra*	*Dendrodrilus rubidus*	*Aporrectodea sp.*	*Lumbricus rubellus* [a]	*Lumbricus terrestris*
Jierpen	B	B	**B**, F	**B**, F	
Kopparåsen	B	B	**B**, F	**B**, F	
Staloluokta	B, C, L	B, L	L	**B**, C, L	C, L
Milking ground	A, F				
Abiskojaure	A				
Alesjaure					
Sälkastugorna					
Singistugorna					
Teusajaure	B, L		**B**, L	**B**, L	
Vakkotavare	B	B, L	L	**B**, L	
Vissijaure	G, L	L		G, L	
Stordalen	L			L	
Kaisepakte	B, F, L		**B**, L	**B**, F, L	
Stenbacken			**B**, L	**B**, L	
Torneträsk	G, L		G, L	G, L	
Abisko village	B, G, L	C, L		**B**, G[b], L	

Distributions of earthworm species argued to be native (*Dendrobeana octaedra* and *Dendrodrilus rubidus*) as well as those that are non-native and invasive in the arctic biome (*Aporrectodea sp*., *L. rubellus* and *L. terrestris*) are shown with respect to the environments in which they occur across the region. Letters indicate source areas and adjacent environments where specific earthworm species were identified (or were absent) at all survey locations shown in Figure 1. Locations where geoengineering earthworms have migrated beyond the boundary of man-made biotopes and thus occur in the alpine birch forest stands adjacent to their source areas are highlighted in bold.

Key: A – acidic tundra; **B – Sub-arctic alpine birch forest**; C – modern compost; F – abandoned farm field; G – modern garden; L – modern lawn

[a] *Lumbricus* juveniles cannot be distinguished between *rubellus* and *terrestris*

[b] Includes greenhouses and gardens used by researchers at the Abisko Scientific Research Station

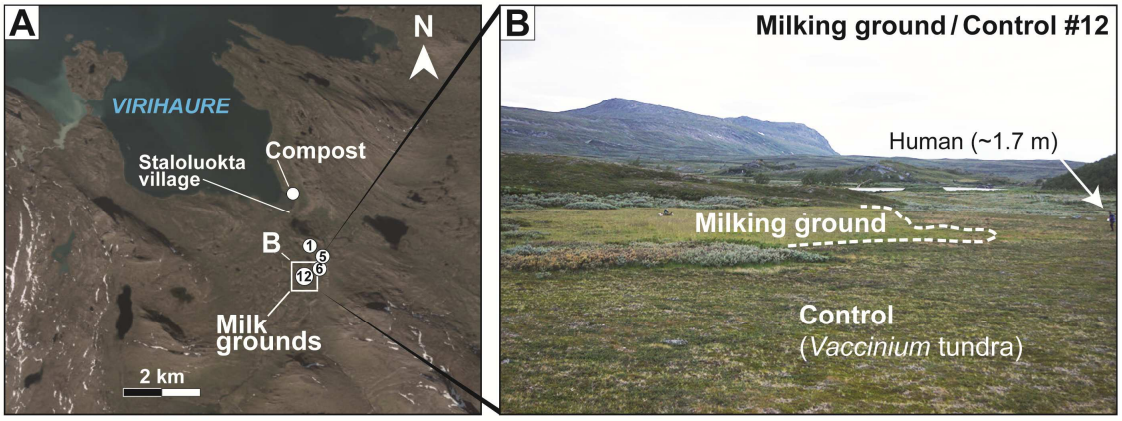

Figure S1.1. (a) Aerial photo of Padjelanta national park. Locations of the historical milking grounds and compost in modern village (Staloluokta) are marked with numbered circles that correspond to site numbers in Egelkraut *et al.* (2018a, 2018b). **(b)** Photo of milking ground-control site #12. Note the vegetation contrast marked by the dashed line.

Chapter 2

Arctic w‘o’rming: Human-facilitated earthworm invasion transforms soil organic matter budgets and pools across high latitude biomes

“The plough is one of the most ancient and most valuable of mans inventions; but long before he existed the land was in fact regularly ploughed, and still continues to be thus ploughed by earthworms.”

The formation of vegetable mould, through the actions of worms:
With observations on their habits

– Charles Darwin, 1881

Chapter Overview

The fate of soil organic carbon (SOC) stored in boreal and arctic ecosystems has been in the scientific spotlight due to their possible impacts on the climate system. However, none of these projections have considered that an important future driver of high-latitude SOC fluxes might be the anthropogenic spreading of ecosystem engineers such as European earthworms (*Lumbricidae*). Here we present the first empirical model that reconciles seemingly contrasting findings about how earthworms affect SOC fluxes at different timescales, i.e. 'the earthworm dilemma'. We then couple this empirical model with geospatial analyses that identify areas in the northern hemisphere historically lacking bioturbation (limited mixing zone, or LMZ) and derive an estimate of future SOC fluxes that may arise as geoengineering earthworm species become established across the LMZ. Our results show that increasing geoengineering earthworm biomass facilitates exponential depletion of SOC in organic surface horizons and linear growth of the mineral-associated SOC pool. The initial O-horizon depletion stage is marked by a short-lived (1–10 year) period of SOC loss, followed later by a longer (10 – >100 year) recovery phase wherein earthworms facilitate the transition of fresh litter inputs into the mineral-associated pool. These transformations strengthen mineral controls on SOC storage and likely alter the persistence of SOC in earthworm-affected soils. Even under a relatively conservative scenario of earthworms populating ~10% of earth's formerly glaciated forests, their dispersal from human biotopes may stimulate SOC losses approaching ~56 Tg of SOC yr^{-1} during the initial invasion and subsequent sequestration of ~12 Tg SOC yr^{-1} during the recovery: the latter alone representing an SOC flux exceeding all arctic rivers combined and almost twenty times greater than the annual

global CO_2 drawdown from silicate weathering. Our results suggest that with the help of humans, future releases of previously absent ecosystem engineers such as non-native earthworms will substantially perturb high-latitude SOC budgets and pools in the coming decades to centuries.

1. Introduction

High latitude soils are a massive reservoir of soil organic carbon (SOC) that has been a central focus of many carbon-climate feedback models and reviews (e.g. Davidson and Janssens, 2006; Schuur *et al.,* 2008, 2015; Koven *et al.,* 2011, 2015; MacDougall *et al.,* 2012; Bradford *et al.,* 2016; Crowther *et al.,* 2016). Estimates suggest boreal forests (including permafrost-affected soils) contain roughly 623 Pg (or ~27.4%) of global SOC stocks within 0-2 m depth (Hugelius *et al.,* 2014; Batjes, 2016; Jackson *et al.,* 2017). More than a quarter of this (~165 Pg) SOC is stored within the upper 30 cm of the soil profile, where it intimately interacts with atmospheric forcings, biota and the soil food web (Wall *et al.,* 2008; Jackson *et al.,* 2017). Studies have indicated that the rate at which this surface SOC is transported to depth in these soils will exert a strong control on deep carbon stability (Fontaine *et al.,* 2007) and its response to climate change (e.g. Koven *et al.,* 2011), but the size and rate of this transport vector represents the largest uncertainty in current models of the future soil carbon-climate system (Balesdent *et al.,* 2018). Furthermore, the formation of persistent mineral-organo associations (MOAs; after Kleber *et al.,* 2015) during mixing and downward translocation seems crucial for attenuating SOC temperature sensitivity (e.g. Gillabel *et al.,* 2010; Gentsch *et al.,* 2018; Moinet *et al.,* 2018; Williams *et al.,* 2018) and facilitating SOC accumulation over millennial-timescales (Torn *et al.,* 1997; Trumbore and Czimczik, 2008; Schmidt *et al.,* 2011).

The primary historical drivers of soil organic matter (SOM) translocation to depth in high latitude soils are considered to be cryoturbation (the physical churning of organic matter resulting from freeze-thaw cycles) and podzolation (the vertical transport of SOM

to depth with percolating soil water and soil roots; Lundström *et al.,* 2000 for review). Meanwhile, pedogenic mixing by soil fauna (bioturbation) has received little to no scientific attention in boreal and arctic regions despite being recognized as the primary mode of soil mixing in temperate regions (e.g. Taylor *et al.,* 2018) – presumably because the majority of soil macrofauna such as earthworms were eradicated from most northern environments during the last glacial maximum (LGM; Gates, 1977, 1982; Reynolds, 1994, 1995; James, 1998). In contrast, in temperate and tropical ecosystems, the critical role of earthworms in physically mixing otherwise stratified layers of organic and mineral soil has been routinely recognized in the scientific literature (Hoogerkamp *et al.,* 1983; Lee, 1985; Lavelle and Martin, 1992; Lavelle *et al.,* 1998, 2004) since the pioneering work of Darwin (1881), who showed that earthworms can bury soil through their castings at rates exceeding ~0.6 cm yr^{-1} (Darwin, 1881; Feller *et al.,* 2003 for review). These mixing rates are an order of magnitude higher than burial rates assumed for cryoturbation in global SOC models (e.g. Koven *et al.,* 2011), and multiple orders of magnitude faster than background mixing rates in non-cryoturbated podzolic soils of the boreal forest, where burrowing soil macrofauna is largely absent and physical perturbations of the soil profile are paced by low-frequency tree throw events (e.g. Schaetzl *et al.,* 1989; Bormann *et al.,* 1995; Ulanova, 2000; Gabet *et al.,* 2003 for review).

Although widely recognized as key soil ecosystem engineers (e.g. Lavelle *et al.,* 1997, 2006; Brown *et al.,* 2000; Jouquet *et al.,* 2006) that influence SOC cycling through multiple pathways (Lavelle *et al.,* 1998, 2004; Filsner *et al.,* 2016 for review), it remains unclear how earthworms modulate SOC storage across a range of spatial and temporal scales. The uncertainty surrounding earthworm impacts on SOC dynamics is best

captured by the 'earthworm dilemma' of Lubbers *et al.* (2013). This paradox considers the capacity of earthworms to enhance decomposition and stimulate microbial activity (e.g. Guggenberger *et al.,* 1995; Brown *et al.,* 2000; Marhan and Scheu, 2006; Lubbers *et al.,* 2013, 2017), while simultaneously facilitating SOC preservation (Zhang *et al.,* 2013) through SOC occlusion within aggregates/casts (Marashi and Scullion, 2003; Six *et al.,* 2004; Bossuyt *et al.,* 2005, 2006; Knowles *et al.,* 2016) and sorption onto reactive mineral surfaces (Lyttle *et al.,* 2015).

The 'earthworm dilemma' paradox is also apparent from studies of SOC dynamics following earthworm invasion into formerly glaciated temperate forests of N. America, as evidenced by the seemingly contradictory reports that earthworm invasion decreases (Bohlen *et al.,* 2004a, 2004b; Hale *et al.,* 2005a; Eisenhauer *et al.,* 2007; Groffman *et al.,* 2015), increases (Wironen and Moore, 2006), or has no significant effect (Fisk *et al.,* 2004; Crumsey *et al.,* 2013) on SOC stocks. This ongoing knowledge gap makes it difficult to forecast the likely effects of geoengineering (i.e. species that can cause significant perturbation of the SOC pool through their borrowing and feeding activities; see Table 2.1) earthworm invasions on long-term SOC dynamics in northern biomes: should they continue to be introduced through human activities (Hendrix and Bohlen, 2002). Indeed, recent findings of European earthworms (*Lumbricidae*) across the Fennoscandian (Terhivuo, 1988; Räty, 2004; Räty and Huhta, 2004; Wackett *et al.,* 2018), Alaskan (Saltmarsh *et al.,* 2016; Booysen *et al.,* 2018), Canadian (e.g. Cameron *et al.,* 2007; Addison, 2009 for review; Reynolds *et al.,* 2015), and Russian (Tiunov *et al.,* 2006; Meshcheryakova and Berman, 2014) boreal and arctic biomes suggest that widespread earthworm absence from most formerly glaciated boreal and arctic regions is

an artifact of limited anthropogenic development at high latitudes, coupled with slow passive dispersal rates (~5-10 m yr^{-1}, e.g. Marinissen and Van den Bosch 1992; James, 1998; Hale *et al.,* 2005b) from glacial refugia following deglaciation. In this light, the recent increase in documented non-native *Lumbricidae* earthworm sightings at high latitudes likely reflects the expansion of global commerce and accelerating recreational and industrial growth across the boreal and arctic zones.

Here, we outline a novel conceptual framework – based on empirical observations from multiple boreal and arctic earthworm invasion gradients – that resolves the earthworm dilemma. We couple this empirical framework with a simplified invasion model to explore how geoengineering earthworms are likely to affect SOC and MOA dynamics through time as they arrive (with humans) into boreal and arctic areas. We hypothesize that the consequent impacts of earthworm invasion into formerly glaciated boreal and arctic regions, assuming relevant dispersion scenarios, can impose significant perturbations of high latitude SOC pools with magnitudes of global importance.

2. Methods

2.1. Field methods and site descriptions

Earthworm surveys and soil profile samples/descriptions were collected from forested plots spanning a range of soil forming state factors including climate, vegetation, and soil parent material across the formerly glaciated world, with a specific emphasis on Fennoscandia and Minnesota, USA. For the Fennoscandian study sites, we report complete soil series descriptions including their morphological characteristics and basic physiochemical data following USDA taxonomic standards (NRCS Soil Survey Staff,

2014) in Appendix B (Tables AB.1 – AB.18). For additional details on the vegetation, soil morphology, or other site characteristics at the Otter Tail site in northern Minnesota, USA refer to Hale *et al.* (2005a, 2005b, 2006), Lyttle *et al.* (2015), or Resner *et al.* (2015).

Basic climatic and geographic data for all of the detailed soil profiles accompanying earthworm survey locations are reported in Table 2.2. All sampling sites were restricted to upland geomorphic positions to reduce variations in local hydrology across the sites. Our Fennoscandian survey sites span almost the entire range of climatic and vegetation zones found on the Fennoscandian peninsula (Figure 2.1a–c), as well as a wide range of soil orders and glacial-derived soil forming parent materials (Figure 2.1d–h). Detailed descriptions of earthworm (Appendix A) and soil (Appendix B) sampling methods and raw earthworm biomass/soil profile data are available in Appendices A and B, respectively.

The timing of earthworm introductions to the Swedish arctic and Minnesota temperate study sites had been previously dated using human land use records (Wackett *et al.,* 2018) and dendrochronology (Larson *et al.,* 2010), respectively. Since all of our Finnish boreal sites are situated in actively forested stands, we consulted the national Finnish Forestry inventory to determine forest stand age and used this metric to infer the maximum age of geoengineering earthworm invasion, assuming that earthworm communities would have dispersed following a stand-clearing harvest (see Appendix C for method details).

2.2 Laboratory analysis

2.2.1 Soil organic carbon and nitrogen contents

Splits of the fine earth (<2 mm) fraction from all soil samples were hand-homogenized and dried at 60 ºC for 48 hours. Carbon and nitrogen contents were determined on an elemental analyzer in the department of Forest Resources at the University of Helsinki. Additional method details and the complete C and N dataset for all profiles are available in Appendix F.

2.2.2 Mineral specific surface area measurements

Mineral specific surface area (SSA) was measured on fine-earth (<2 mm) soil fraction splits by N_2 gas adsorption using a TriStar 3020 Surface Area and Porosity Analyzer in the Department of Soil, Water and Climate at the University of Minnesota-Twin Cities. Samples were degassed at 423 K in a flow of He for at least 6 hours to purge adsorbed water from mineral surfaces prior to analysis. Surface area contents (m^2 g^{-1}) were calculated from the Brunauer-Emmett-Teller (BET) equation using 11 measurements made at different relative pressure points (P_o/P max = 0.3) under cryogenic temperatures (77 K). After processing, adsorption isotherms were monitored for their shape (e.g. Brunauer *et al.,* 1940) and only the linear portions of the isotherm were utilized as suggested by Heister *et al.* (2014).

Mineral SSA measurements were made prior to and after removal of organic matter by muffling. Soils were placed in ceramic crucibles and heated in a Lindberg/Blue 1100 °C box furnace (model BF51800) at 623 K for 12 hours to expose mineral surfaces previously occluded by organic matter. Following muffling, we repeated degassing at 423

K in a flow of He before measuring samples following the same procedure. The SSA covered by sorbed organic matter ($SSA_{occluded}$) and the surface area free of organic coatings was calculated using previously outlined methods (Mayer and Xing, 2001; Wagai *et al.,* 2009) described further in the calculations section below. See Appendix D for additional discussion pertaining to our correction and (re-) presentation of erroneous SSA data published by Lyttle *et al.* (2011, 2015).

2.3 Calculations

2.3.1. Mineral specific surface area (SSA) pools

In general, mineral SSA can be subdivided according to the expression below:

$$SSA_{total} = SSA_{occluded} + SSA_{exposed} \quad \text{(Eq. 1)}$$

where SSA_{total} represents the total amount ($m^2\ g^{-1}$) of specific surface area on mineral surfaces, $SSA_{occluded}$ refers to the area ($m^2\ g^{-1}$) covered by sorbed organic matter, and $SSA_{exposed}$ ($m^2\ g^{-1}$) constitutes the additional surface area free of organic coatings prior to heat treatment.

From an operational standpoint, SSA_{total} simply represents the amount of surface area measured following removal organic matter removal, while $SSA_{occluded}$ represents the difference in SSA values prior to and following removal of organic matter by muffling as described above. We also quantified the proportion of mineral surfaces coated by organic matter (Mayer and Xing, 2001; Wagai *et al.,* 2009) as:

$$\%SSA_{occluded} = \left[(SSA_{total} - SSA_{exposed}) \,/\, SSA_{total}\right] \times 100 \quad \text{(Eq. 2)}$$

In both equations 1 and 2 above, we assume that the BET surface area contributed by mineral-free organic matter to be negligible based on numerous previous studies reporting insignificant SSA values determined for pure, mineral-free organic material such as leaf litter or humus using a gas sorption approach (e.g. Chiou *et al.,* 1990). Our own observations of extremely low, non-viable BET surface area values (analyses must contain >1 m^2 of total surface area in the measured sample to be considered valid) for untreated (i.e. $SSA_{exposed}$) samples from organic surface layers further supports this assumption.

2.3.2. SOC and mineral SSA inventories

We calculated inventories of SOC and $SSA_{occluded}$ (derived from Eq. 1) for the total (0-25 cm) soil profile as well as individual soil horizons, including organic topsoil (O-horizons), mineral topsoil (A-horizons), and mineral subsoil (E- and/or B-horizons). We focused exclusively on the upper (0-25 cm) soil profile in calculating total and horizon-based inventories of SOC and mineral SSA. This depth was selected because it facilitated comparison with previous studies assessing earthworm invasion impacts on soils in N. America (e.g. Langmaid, 1964; Alban and Berry, 1994; Bohlen *et al.,* 2004a; Hale *et al.,* 2005a; Wironen and Moore, 2006; Frelich *et al.,* 2006 for review) and because earthworms (and other soil fauna) predominantly affect the upper (0-25 cm) soil profile (Jackson *et al.,* 2017). We explicitly accounted for the coarse (>2 mm) soil fraction – which often constitutes a significant portion of the soil volume in Fennoscandian soils (e.g. Stendahl *et al.,* 2009) – in our inventory calculations using the expression below:

$$SOC_{inventory} = \sum_{n=1}^{N} C_{n,fine} \times \rho_{n,total} \times (1 - cf_n) \times h_n$$

(Eq. 3)

where $SOC_{\text{inventory}}$ is the profile or horizon integrated soil organic carbon inventory (kg C m^{-2}), $C_{n,fine}$ is the mass fraction of organic carbon measured on fine fraction (<2 mm) soil splits from the n^{th} layer (unitless, or g g^{-1}), $\rho_{n,total}$ is the bulk density of the bulk sample from the n^{th} layer (g m^{-3}), cf_n is the mass fraction of coarse (>2 mm) in the n*th* layer such that it is determined by dividing the mass of coarse fraction by the mass of bulk soil (unitless, or g g^{-1}), h_n is the thickness of the nth soil layer (m), and N is the total number of sampled soil layers or horizons.

Mineral SSA inventories can be used to quantify the total size of mineral surface area available in the soil column at a certain point in space. They were also calculated to explicitly account for the coarse (>2 mm) soil fraction using the expression below:

$$SSA_{occluded,inventory} = \sum_{n=1}^{N} SSA_{n,fine} \times \rho_{n,total} \times (1 - cf_n) \times h_n \quad \text{(Eq. 4)}$$

where $SSA_{occluded,inventory}$ is the profile integrated mineral SSA_{occluded} inventory (m^2 m^{-2}), $SSA_{occluded,n,fine}$ is the amount of occluded surface area (determined by rearranging Eq. 1) measured on splits of the fine earth (<2 mm) soil fraction from the n^{th} layer (m^2 g^{-1}), $\rho_{n,total}$ is the bulk density measured for the bulk sample from the n^{th} layer (g m^{-3}), f_n is the mass fraction of coarse (>2 mm) in the n^{th} layer (unitless, g g^{-1}), h_n is the thickness of the nth soil layer (m), and N is the total number of sampled soil layers or horizons. We calculated the SSA inventory only for *mineral* soils (we did not quantify SSA_{occluded} for samples from organic horizons; see Appendix D for additional discussion).

2.4. Statistical analyses

To estimate the effects of earthworm biomass on stocks of SOC and occluded SSA across all our field sites, we conducted two complementary sets of analyses in the R statistical environment (R Core Team 2018). First, we estimated mean SOC and $SSA_{occluded}$ storages for each horizon within each site and modeled those storages as a function of site-level mean earthworm biomass. After initial data visualization and evaluation of model residuals, we chose to model site-level mean storages in the mineral horizons as simple linear functions of biomass, whereas we found that a two-parameter exponential decay model (storage = $Ce^{-k\ biomass}$) better represented the effect of biomass on SOC in organic horizons.

Next, we conducted a Monte Carlo analysis to assess whether our inferences are robust to the within-site variability in soil attributes and worm biomass that is disregarded by modeling site-level means. The Monte Carlo procedure entailed: 1) randomly selecting a single observation from each of the earthworm biomass, SOC, and $SSA_{occluded}$ datasets for each site (with replacement of observations in subsequent re-samplings), 2) fitting the same simple linear regressions and exponential decay models as applied to the site-level means, 3) reiterating the resampling and model fitting steps 2000 times, and 4) summarizing the distributions of parameter estimates and model fit. We employed this resampling-based approach (rather than a more formal hierarchical statistical framework, e.g., a mixed-effects model) because the multiple soil observations within each site were not explicitly paired with replicate earthworm sampling subplots.

2.5 Geospatial analyses

To get an estimate on the magnitude of change to high latitude ecosystems if earthworm invasions were to proceed to greater extents, we combined published global datasets for land cover (ESA GlobCover 2009), topographic roughness index (TRI; Gruber, 2012) and permafrost zonation index (PZI; Gruber, 2012) to construct a qualitative map of contemporary soil mixing modes (Figure S2.1). For details regarding map construction and the criteria used to assign grid cells to specific pedoturbation modes see Appendix E and Table S2.1, respectively. Based on the well-established concept that Pleistocene glaciations eradicated earthworms (e.g. Gates, 1982; James, 1998), we assumed the complete absence of geoengineering earthworms across northern forests in this analysis. We excluded formerly glaciated regions with continuous permafrost from the 'limited mixing zone' (LMZ), since soils in these areas experience more frequent mixing and organo-mineral interactions due to cryoturbation (e.g. Ping *et al.,* 2015).

To estimate how much of the SOC contained within the LMZ might be susceptible to earthworm invasion(s), we combined our pedoturbation mapping products (Figure S2.1) with recent estimates of global croplands (Ramankutty *et al.,* 2008) and projected population density (NASA Socioeconomic Data and Applications Center, 2017) for the year 2020. Additional details of this map construction and cell assignment criterion are available in Appendix E and Table S2.1, respectively.

Informed by our geospatial analyses and representative population/household densities (i.e. considering each household as a potential earthworm source) in high-

latitude regions, we set up a series of simple analytical solutions to model the outward expansion of earthworms from variable epicenter densities assuming an idealized, homogeneous 1-km^2 stretch of northern forest and uniform epicenter density. We also explored a range of earthworm dispersal rates between 2.5-10 m yr^{-1} in our analyses, informed by previously published values for the dispersal of established *Lumbricidae* populations (e.g. Marinissen and Van den Bosch 1992; Dymond *et al.,* 1997; Hale *et al.,* 2005a; Frelich *et al.,* 2006; Wackett *et al.,* 2018). To investigate how these idealized invasion scenarios would interact with high latitude C cycles, we coupled our earthworm expansion modeling outputs with the time-based empirical framework of earthworm-induced SOC dynamics to estimate area-normalized SOC fluxes through time for each of the modeled invasion scenarios.

3. Results

3.1. Earthworm effects on SOC pools

The data used for deriving a solution to the 'earthworm dilemma' are shown in Figures 2.2–2.7. A short description of the results follows below, but deductive interpretation and development of the empirical framework are presented in the discussion.

Where geoengineering earthworms are absent, SOC contents in surface soils (0-6 cm) average 325 ± 24 g kg^{-1} (N = 10, n = 31; open symbols Figure 2.2). Following earthworm invasion, organic horizons (O-horizons) are depleted (Figure 2.1d–h) and SOC contents in newly formed mineral topsoil (A-horizons) occupying the same depths (0-6 cm) decrease to 107 ± 11 g kg^{-1} (N = 13; n = 48; filled symbols Figure 2.2). The

earthworm-mediated reduction of topsoil SOC contents is consistent across all biomes (Figure 2.2). Most SOC depth profiles converge at >12 cm depth regardless of geoengineering earthworm presence and/or abundance (Figure 2.2).

Across all sites and biomes, the amount of SOC stored within O-horizons of geoengineering earthworm-free soils ranges greatly from 0.7±0.3 to 16±3 kg of SOC m^{-2}, but most sites fall within the range of ~2.5-7.5 kg C m^{-2} (Figure 2.3a). This suggests that 23-100% of the SOC in the upper profile is contained within organic surface layers. There is often ~0 kg of SOC m^{-2} remaining in organic horizons of soils infested with ≥ 5 g m^{-2} of earthworms (Figure 2.3a).

In contrast, geoengineering earthworm invaded soil pairings with ≥5 g m^{-2} of earthworm biomass typically contain only ~2-4.5 kg of C m^{-2} in mineral topsoil (Figure 2.3b): considerably less than the ~2.5-7.5 kg of C m^{-2} previously stored within organic surface layers (Figure 2.3a). In this new soil environment, the fraction of total SOC stored in O-horizons is reduced to 0% in many cases (but can remain as high as ~62 %) while the fraction in mineral topsoil climbs from near 0% to 33-91% (Figure 2.3b). Growth of the SOC pool in this newly formed mineral topsoil (i.e. A-horizon) is linearly coupled ($P < 0.0001$) to increasing earthworm biomass (Figure 2.3b). There is no correlation ($P = 0.28$) between earthworm biomass and SOC storage in mineral subsoil (E-/B-) horizons (Figure S2.2a), in line with the convergence of geoengineering earthworm-free and invaded SOC profiles at depth (Figure 2.2). Fixed-width distributions of the adjusted R^2 values for all 2000 Monte Carlo model fits (thin red lines in Figure 2.3) are shown in Figure S2.3.

3.2 Earthworm effects on mineral SSA pools

The area of mineral surfaces covered (i.e. occluded) by sorbed organic matter is significantly and linearly correlated with earthworm biomass for both the total upper (0-25 cm) mineral soil profile (P = <0.0001; Figure 2.4a) and especially within mineral topsoil (P = <0.0001; Figure 2.4b). Fixed-width distributions of the adjusted R^2 values for all 2000 Monte Carlo model fits (thin black lines in Fig. 2.4a and red lines in Figure 2.4b) are shown in Figure S2.4. There is no significant earthworm effect (P = 0.21) on the occlusion of mineral SSA in mineral subsoil horizons (Figure S2.2b). Regardless of geoengineering earthworm presence and abundance, SOC mass content is linearly correlated ($F_{1, 131}$ = 163.31; r^2 = 0.551, P = < 0.0001) with the amount of $SSA_{occluded}$ in mineral soil horizons across all sites and biomes (Figure 2.5).

3.3. Earthworm invasions and SOC/mineral SSA pools through time

By selecting study sites where we could estimate timing since the original earthworm introduction event (Table 2.2; see Appendix C for method details), we can monitor changes in total soil/horizon-integrated SOC and SSA pools across different invasion timescales. This replacement of geoengineering earthworm biomass (Figures 2.3 –2.4) by time since the invasion onset reveals the negative exponential nature of earthworm-induced SOC losses from organic horizons (Figure 2.6a). We derive an average SOC loss rate of 200 g of C m^{-2} yr^{-1} for invasion years 1-10 from the steep negative slope between years 1-10, which levels off after t = >10 years of invasion as the O-horizon SOC storages approach 0 kg of SOC m^{-2} (Figure 2.6a).

We observe consistent, steady linear growth of SOC inventories in the mineral topsoil (A-horizon) across the entire range of invasion durations explored here (Figure 2.6b). From the slope of this regression, we derive an annual earthworm-mediated 'sequestration' rate of 29±5 g of C m^{-2} yr^{-1} (Figure 2.6b). The inventories of total (P = <0.0001) and mineral topsoil (P = <0.0001) $SSA_{occluded}$ also increase significantly and linearly with increasing time since initial invasion, and their slopes yield occlusion rates of 4.4±0.5 km^2 m^{-2} (total mineral upper profile) and 5.0±0.3 km^2 m^{-2} (A-horizon only), respectively (Figure 2.7). We display a dashed line with several possible trajectories in panels (a–b) of Figures 2.6 and 2.7 to emphasize the uncertainty of these empirical relationships beyond >150 years of earthworm invasion.

3.4. The 'limited mixing zone' and invasion probability map

We present a simplified version of our qualitative map of pedoturbation modes in Figure 2.8a to highlight the areal extent of the 'limited mixing zone' (or LMZ). We presume these expansive stretches of temperate, boreal and (sub-) arctic forested ecosystems covering much of Canada, Fennoscandia, the northern United States (including southern Alaska), and parts of the Kamchatka peninsula have historically evolved without major soil bioturbators such as earthworms since the LGM. From this analysis, we calculate a total land area of approximately ~4.2 × 10^6 km^2 for formerly glaciated forests within the LMZ that have historically experienced a lack of soil mixing, excluding forested areas underlain by continuous (or semi-continuous) permafrost (Figure 2.8a).

We also find that significant portions of the boreal and arctic landscape already fall within our 'intermediate' (< 25% cropland; 0.25 ≤ household density < 5.25 per km^2; yellow shading in Figure 2.8b) or 'high' (≥ 25% cropland; household density ≥ 5.25 per km^2; red shading in Figure 2.8b) earthworm probability classes, which indicate the susceptibility of a given landscape area to current and/or future earthworm invasion (Figure 2.8b). For example, potential earthworm invaded areas cover almost 75% of the deglaciated landscape in Fennoscandia (Figure 2.8b). Much of the northern United States (specifically the Great Lakes and northeastern regions) is also already within these classes.

3.5. Modeling earthworm invasions

Assuming an idealized, homogeneous landscape unit (i.e. 1-km^2 box) with uniform epicenter distribution and a constant dispersal velocity, we find that the time required for earthworm invasion to permeate across the entire landscape is dependent on the epicenter density (d) and dispersal rate (v) (Figure 2.9). This outward expansion (following introduction and establishment) can be modeled by the expression:

$$t = \frac{\sqrt{\frac{1}{d}} \times \frac{1}{v}}{2} \qquad \text{(Eq. 5)}$$

where t is the time to invade the entire area (years), d is the epicenter density (# per m^2), and v is the earthworm passive dispersal rate (in m yr^{-1}).

4. Discussion

4.1. An empirical framework to resolve the 'earthworm dilemma'

If earthworm invasion facilitated a direct transfer (without net losses) of SOC from organic to mineral soil horizons, then the build-up of SOC in the A-horizon would follow a positive exponential trend (i.e. reciprocal of the exponential decay of O-horizon SOC as in Figure 2.3a): but that is not the case (Figure 2.3b). Instead, the SOC stock in mineral soil increases linearly with increasing earthworm biomass across all of our observed biomass ranges (0.048 – 13±3 g m^{-2}; Figure 2.3b). Our review of the literature indicates that exponential loss of SOC in the organic layer and linear increase in A-horizon SOC storage has also occurred at other earthworm invaded sites in N. America (e.g. Hale *et al.,* 2005a; Wironen and Moore, 2006), suggesting that this offset between exponential organic layer SOC loss and linear mineral topsoil gain is likely a universal phenomenon following non-native earthworm introductions into previously earthworm-free soils.

Our substitution of time (Figures 2.6–2.7) for biomass (Figure 2.3) also indicates rapid exponential depletion of O-horizon SOC (Figure 2.6a) and linear growth of the mineral-associated SOC pool following earthworm arrival (Figure 2.6b). How to best explain the rapid (1-10 years) exponential depletion of SOC in organic surface layers with the small presence of geoengineering earthworms (< 5 g m^{-2})? We posit that by fragmenting and decomposing litter and humus, geoengineering earthworms accelerate the decomposition of SOC contained within previously earthworm-free organic surface layers (e.g. van Geffen *et al.,* 2011): stimulating SOC losses that exceed the rate of vertical transfer and burial within the mineral soil reservoir. We note that this trend

matches the observed accelerated respiration losses during the initial period (<200 days) following earthworm establishment, as previously emphasized in studies addressing the 'earthworm dilemma' (e.g. Lubbers *et al.,* 2013; Zhang *et al.,* 2013).

This conceptual framework also predicts that the initial earthworm-induced priming of respiration rates should cease over time. Importantly, the presence of such an 'aging-effect' has so far been based largely on deductive reasoning due to a lack of significant respiration effects in mesocosms and field studies lasting longer than 200 days (Lubbers *et al.,* 2013), although recent studies have found significant earthworm-induced increases in cumulative respiration persisting up to ~2 years (Lubbers *et al.,* 2015, 2017). Studies across earthworm invasion fronts also routinely report insignificant effects on soil respiration rates in soils where the earthworm invasion is relatively old (e.g. Eisenhauer *et al.,* 2011; Xia *et al.,* 2011; Crumsey *et al.,* 2013), corroborating results from a unique long-term monitoring experiment that found no lasting effect of earthworm invasion on soil respiration and SOC storage (Fisk *et al.,* 2004). Thus, although there is ample (indirect) evidence to support an earthworm 'aging-effect' – particularly following earthworm introductions into previously earthworm-free soils – empirical data that validate this phenomenon remain lacking.

Our data provide the first empirical evidence to suggest a rapid depletion of the O-horizon and concomitant C loss during the first ~10 years of earthworm invasion (Figure 2.6a), followed by a later (i.e. 10-150 years) invasion stage where net losses are slowed and eventually reversed through the persistent (linear; $P = < 0.0001$) incorporation of SOC into the mineral topsoil (Figure 2.6b). At least over the invasion timescales considered here (0-150 years), SOC stocks in mineral subsoils remain largely

unaffected by geoengineering earthworm invasion (Figure S2.3a). The increasing stock of mineral surfaces occluded by sorbed organic matter with increasing biomass (Figure 2.4) and invasion duration (Figure 2.7) indicates that the growing SOC stocks in mineral topsoil include substantial amounts of organic carbon (OC) that is now closely associated with minerals surfaces.

We tentatively suggest that this earthworm-induced increase in $SSA_{occluded}$ inventories is one likely mechanism responsible for growing topsoil (A-horizon) SOC stocks during the later (10-150 years) stages of earthworm invasion. This inference is in line with the emerging knowledge that MOAs increase the persistence of organic matter (Kleber *et al.,* 2015; Lehmann and Kleber, 2015) and thereby influence SOC storage (e.g. Torn *et al.,* 1997; Mikutta *et al.,* 2006). It is also consistent with our own observation of a strong mineral control on SOC contents in mineral soil layers across all sites (Figure 2.5). Physical protection of SOC through the earthworm-mediated formation of macro- and micro-aggregates is another likely SOC sequestration mechanism (e.g. Six *et al.,* 2004; Bossuyt *et al.,* 2005; Zhang *et al.,* 2013; Knowles *et al.,* 2016) during later invasion stages, but we did not attempt to quantify earthworm contributions to aggregate size, strength, and/or structure here. A schematic diagram that highlights our empirically-based conceptual framework in the context of non-native geoengineering earthworm introductions into previously earthworm-free soils within the LMZ is presented in Figure 2.10.

These results highlight the growing recognition of SOM as an ecosystem property (Schmidt *et al.,* 2011) and lend support to recent works that emphasize the role of soil fauna and other bioturbators as key regulators of many ecosystem processes that govern

SOM persistence (e.g. Wall *et al.,* 2008; Filsner *et al.,* 2016). Our findings also indicate that previously earthworm-free ecosystems across the LMZ are ideal natural laboratories to isolate earthworm impacts on SOC dynamics across a wide range of spatial and temporal scales, as long as the timing of earthworm introduction can be roughly constrained. Finally, they suggest that future releases of non-native earthworms into the 'limited mixing zone' (Figure 2.8) are likely to pace the rate of bioturbation (Taylor *et al.,* 2018), formation of organo-mineral complexes, and delivery of C inputs to depth across these important high-latitude SOC reservoirs.

4.2 Future earthworm invasions into high latitude biomes

We combined our invasion model (Eq. 5; Figure 2.9) with our empirical time-dependent 'C loss' (Figure 2.6a) and 'C sequestration' (Figure 2.6b) rates to explore the magnitude to which future northward expansions of geoengineering earthworms might alter the C balance of northern forests within the LMZ (Figure 2.8a). A conceptual diagram illustrating how we these results were combined in time and space is shown in Figure 2.11. Our calculated land area for the LMZ equates to roughly ~20% of earth's northern boreal forest (Brandt *et al.,* 2013), which contain ~45 Pg of SOC to 30 cm depth in non-cryoturbated, mineral upland soils (Hugelius *et al.,* 2014; Batjes, 2016; Jackson *et al.,* 2017). On this basis, we estimate that northern forests within the LMZ contain roughly ~9 Pg of SOC – or ~1.2% of global SOC stocks – within the upper 30 cm: the majority of which is stored in organic surface horizons (e.g. Callesen *et al.,* 2003). We posit that this sizeable SOC pool contained in organic surface layers has evolved in the absence of earthworms since deglaciation.

Through our geospatial mapping exercises, we found that significant portions of the boreal and arctic regions will have population densities between 0.5 and 10.5 people km^{-2} in the year 2020 (Figure 2.8b). Informed by these analyses, we selected these values (1- and 10- epicenters per km^2) for use in our invasion models to represent earthworm source densities that might be expected across the LMZ, assuming all households (or human-inhabited areas) constitute geoengineering earthworm source areas (Figure 2.11). Our models assume passive dispersal radiating outward from the source to be on the order of ~5-10 m yr^{-1}, based on previously published dispersal rates for a range of *Lumbricidae* (e.g. Marinissen and Van den Bosch 1992; Dymond *et al.,* 1997; Hale *et al.,* 2005b; Frelich *et al.,* 2006; Wackett *et al.,* 2018). We note, however, that most of these previously published rates have been derived from the Netherlands (Marinissen and Van den Bosch 1992) or more southern formerly glaciated regions of North America (e.g. Dymond *et al.,* 1997; Hale *et al.,* 2005b), and they also tend to occur in more favorable litter types such as aspen or sugar maple. The notable exception to this is Wackett *et al.* (2018), who found that non-native earthworms are radiating outwards from anthropogenic point sources into birch forests of the Swedish arctic alpine zone at rates between ~2.5-5 m yr^{-1}. Slower rates on the order of ~2.5 m yr^{-1} may be more typical across the northernmost stretches of the LMZ, where extremely short growing seasons and less palatable (acidic) litter may restrict earthworm activity and population expansion.

The results of this modeling exercise demonstrate how scarce epicenter densities can lead to nearly ubiquitous landscape coverage in a matter of decades (Figure 2.11), especially when faster (~10 m yr^{-1}) dispersal rates and/or greater epicenter (10 per km^2)

densities are considered (Figure 2.11b). When these outputs are coupled with our empirically-derived C loss (~200 g of C m^{-2} yr^{-1}; Figure 2.6a) and sequestration (29±5 g of C m^{-2} yr^{-1}; Figure 2.6b) rates, the results are even more striking (Figure 2.12): especially once these area-normalized C fluxes are placed in the context of the LMZ (Figure 2.8a). For example, even under a conservative scenario with low epicenter density (1 source per km^2), slow earthworm dispersal (2.5 m yr^{-1}), and invasion into only 10% of the LMZ, we find that earthworm invaded soils would release ~11 Tg of C over the next three decades (Table 2.3). Although seemingly small, the average annual flux over this time (~0.37 Tg of C yr^{-1}) equates to approximately half of the global annual CO_2 drawdown from silicate weathering (Gaillardet *et al.,* 1999). If faster (~10 m yr^{-1}) dispersal rates and higher epicenter densities (10 per km^2) are assumed, the net C loss grows to 0.645 Pg of C (or 645 Tg) over this same time period (Table 2.3). This equates to an average annual C loss of ~21 Tg of C yr^{-1}, or roughly half of the estimated global petrogenic particulate organic carbon (POC) flux (~43 Tg of C yr^{-1}) from rivers to oceans (e.g. Galy *et al.,* 2015). Thus, our modeling scenarios suggest that the potential SOC fluxes generated by human-facilitated introductions of geoengineering soil fauna are of a magnitude of global importance; hence, our main hypothesis appears valid.

Although our model is admittedly simplistic and is based on modeled household densities density per km^2 (which we expect to be lower than population density), we emphasize that any landscape unit impacted by human activities represents a potential earthworm epicenter. Thus, even if permanent settlements at high latitudes remain sparse, we predict that the total number and density of earthworm epicenters will intensify as natural resource exploitation (e.g. logging) and recreational activities (e.g. fishing,

vacation homes with gardens, etc.) increasingly penetrate high-latitude biomes. For example, studies have shown that non-native *Lumbricidae* can be present in up to 54% of the landscape adjacent to roads and boat launches in the boreal forest of northern Alberta, Canada (Cameron *et al.,* 2007), despite having population densities <<0.5 people km^{-2} (green in Figure 2.8b). The successful colonization and outward expansion of earthworms from human biotopes into formerly earthworm-free will also only be further amplified by the warmer winter temperatures, longer growing seasons, and increasing cover of deciduous tree species (due to both direct human disturbance, fire, and climate change) expected in high-latitude environments (e.g. Bonan, 2008; Johnstone *et al.,* 2010; Hansen *et al.,* 2013).

4.3. Earthworm invasion and the temperature dependence of SOM decomposition

As organic matter in O-horizons is transformed into mineral-associated forms within A-horizons, these ecosystems may go through drastic changes in the temperature sensitivity of organic matter decomposition. There is a growing consensus that physical and chemical protection of SOM attenuates decomposition and dampens its temperature sensitivity, presumably by limiting microbial accessibility to reactive sites (Davidson and Janssens, 2006; Gillabel *et al.,* 2010; Schmidt *et al.,* 2011; Wagai *et al.,* 2013; Gentsch *et al.,* 2018; Moinet *et al.,* 2018). However, in the boreal and arctic, studies investigating the role of mineral protection in regulating SOC turnover had to sample and focus on subsoil materials (e.g. Gentsch *et al.,* 2018), since organic surface horizons (and mineral-free SOC) are nearly ubiquitous in earthworm-free landscapes. Considering that the amount of mineral SSA occluded by SOM is positively correlated with earthworm

biomass (Figure 2.4) and the duration of earthworm invasion (Figure 2.7), and that mineral soil SOC contents are positively and linearly correlated with OM-occluded mineral surface area (Figure 2.5), we tentatively propose that high-latitude SOC pools entering the later stages of earthworm invasion may turn over at longer time scales and be less sensitive to temperature increases than in earthworm-free forests.

In addition, we expect that earthworm-mediated removal of organic surface horizons during the initial (1-10 years) invasion stages (Figure 2.6a) will significantly modify the thermal and hydrologic regime of these soils, placing an important feedback loop on the temperature-dependent decomposition of SOC in post-invaded soils. For example, a recent study in the Alaskan arctic showed that loss of organic surface horizons due to surface slumping increased ground temperatures in peak growing season by a staggering 8.4 ± 1.5 °C (Baughman *et al.,* 2015), resulting in a positive feedback that accelerated subsequent permafrost thaw. Others have found similar effects on temperature as well as major reductions in mineral soil moisture conditions following O-horizon reduction due to fire in the Alaskan boreal (e.g. Kasischke and Johnstone, 2005; Harden *et al.,* 2006). However, unlike fire and/or slumping, where surface organic layers can return following disturbance, the removal of organic horizons by geoengineering earthworms represents a permanent state-shift in the soil environment.

Our data indicate that the apparent biomass of earthworms required to cross this 'threshold' and cultivate an irreversible state-shift is only ~5 g m^{-2} (Figure 2.3a), which is equivalent to only ~2-3 individual adult endogeic earthworms such as *Aporrectodea sp.*, or even a single *Lumbricus terrestris* adult. In this light, the long-term impacts of earthworm invasion on high-latitude soil climates may be comparable or even greater

than the effects of fire and/or permafrost thaw: two key processes thought to govern SOC persistence in soils (e.g. Schmidt *et al.,* 2011). Unlike these other processes, the extent to which earthworm invasion will alter the C balance of these important high-latitude SOC reservoirs – and thereby potentially influence the global C cycle – is tightly coupled to human activities and their capacity to disperse novel geoengineering organisms such as non-native earthworms.

5. Conclusion

Global models of soil organic matter dynamics and carbon-climate feedbacks are becoming increasingly complex but still generally do not include soil animals and organisms (Wall *et al.,* 2008; Filsner *et al.,* 2016). We demonstrate that the human-facilitated introduction of non-native geoengineering earthworms profoundly alters the size and form of SOC stocks in temperate, boreal, and arctic forests across the formerly glaciated world. We show that a human-facilitated introduction of these previously absent ecosystem engineers into the LMZ perturbs the pre-existing ecological equilibrium as vertically stratified organic and mineral soil layers become thoroughly mixed. We estimate SOC losses of ~200 g of C m^{-2} yr^{-1} during the initial decade of earthworm invasion, followed by an earthworm-mediated downward SOC flux or 'sequestration' rate of 29±5 g of C m^{-2} yr^{-1} that persists for decades to centuries. These novel bioturbation rates greatly outpace the historical modes of SOC burial (cryoturbation and podzolization) in these landscapes and cultivate a new steady-state soil system wherein the majority of high latitude surface (0-25 cm) SOC stocks are associated with mineral surfaces in mineral topsoil, rather than stored in mineral-free organic surface layers.

Thus, the apparent 'earthworm dilemma' can be resolved by more explicitly considering the temporal (and spatial) scales of earthworm activities, which highlights the importance of considering invasion stages in assessing the biogeochemical impacts of earthworm invasion. Lastly, despite the slow passive dispersal of lumbricid earthworms, the time period required for earthworms to invade large areas of formerly glaciated forests with the help of humans can be remarkably short: suggesting that expansive stretches of northern boreal and arctic forests are likely to come under the influence of the 'unseen invaders' (Craven *et al.,* 2017) in the coming decades to centuries. As larger portions of the LMZ come under the influence of earthworms, the magnitude of earthworm-induced perturbations to high latitude C cycles will become a flux of increasing global importance. These results collaboratively highlight the urgency to understand earthworms' ecological effects – together with their human-mediated dispersal vectors – as they occur through time and space. Harnessing a better understanding of these coupled processes and their feedbacks is integral to accurately predict future SOC dynamics across earth's high latitude biomes.

6. References

Addison JA (2009) Distribution and impacts of invasive earthworms in Canadian forest ecosystems. *Biological Invasions*, **11**, 59–79.

Alban DH, Berry EC (1994) Effects of earthworm invasion on morphology, carbon and nitrogen of a forest soil. *Applied Soil Ecology*, **1**, 243–249.

Arino O, Perez R, Julio J, Kalogirou V, Bontemps S, Defourny P, van Bogaert E (2012) Global land cover map for 2009 (GlobCover 2009). European Space Agency, PANGAEA, doi:10.1594/PANGAEA.787668.

Balesdent J, Basile-Doelsch I, Chadoeuf J, Cornu S, Derrien D, Fekiakova Z, Hatté C (2018) Atmosphere-soil carbon transfer as a function of soil depth. *Nature*, **559**, 599–602.

Batjes NH (2016) Harmonized soil property values for broad-scale modelling (WISE30sec) with estimates of global soil carbon stocks, *Geoderma*, **269**, 61–68.

Baughman CA, Mann DH, Verbyla DL, Kunz ML (2015) Soil surface organic layers in arctic Alaska: Spatial distribution, rates of formation, and microclimatic effects. Journal of Geophysical Research: *Biogeosciences*, **120**, 1150–1164.

Bohlen PJ, Pelletier DM, Groffman PM, Fahey TJ, Fisk MC 2004a. Influence of earthworm invasion on redistribution and retention of soil carbon and nitrogen in northern temperate forests. *Ecosystems*, **7**, 13–27.

Bohlen PJ, Scheu S, Hale CM, McLean MA, Migge S, Groffman PM, Parkinson D (2004b) Non-native invasive earthworms as agents of change in northern temperate forests. *Frontiers in Ecology and the Environment*, **2**, 427–435.

Bonan GB (2008) Forests and climate change: Forcings, feedbacks, and the climate benefits of forests. *Science*, **320**, 1444–1449.

Booysen M, Sikes D, Bowser ML, Andrews R (2018) Earthworms (Oligochaeta: Lumbricidae) of Interior Alaska. *Biodiversity Data Journal*, **6**, e27427.

Bormann BT, Spaltenstein H, McClellan MH, Ugolini FC, Cromack Jr K, Nay SM (1995) Rapid soil development after windthrow disturbance in pristine forests. *Journal of Ecology*, **83**, 747–757.

Bossuyt H, Six J, Hendrix PF (2005) Protection of soil carbon by macroaggregates within earthworm casts. *Soil Biology and Biochemistry*, **37**, 251–258.

Bossuyt H, Six J, Hendrix PF (2006) Interactive effects of functionally different earthworm species on aggregation and incorporation and decomposition of newly

added residue carbon. *Geoderma*, **130**, 14–25.

Bradford MA, Wieder WR, Bonan GB, Fierer N, Raymond PA, Crowther TW (2016) Managing uncertainty in soil carbon feedbacks to climate change. *Nature Climate Change*, **6**, 751–758.

Brandt JP, Flannigan MD, Maynard DG, Thompson ID, Volney WJA (2013) An introduction to Canada's boreal zone: ecosystem processes, health, sustainability, and environmental issues. *Environmental Reviews*, **21**, 207–226.

Brown GG, Barois I, Lavelle P (2000) Regulation of soil organic matter dynamics and microbial activity in the drilosphere and the role of interactions with other functional domains. *European Journal of Soil Biology*, **36**, 177–198.

Brunauer S, Deming LS, Deming WE, Teller E (1940) On a theory of the van der Waals adsorption of gases. *Journal of the American Chemical Society*, **62**, 1723–1732.

Callesen I, Liski J, Raulund-Rasmussen K, Olsson MT, Tau-Strand L, Vesterdal L, Westman CJ (2003) Soil carbon stores in Nordic well-drained forest soils — relationships with climate and texture class. *Global Change Biology*, **9**, 358–370.

Cameron EK, Bayne EM, Clapperton MJ (2007) Human-facilitated invasion of exotic earthworms into northern boreal forests. *Ecoscience*, **14**, 482–490.

Center for International Earth Science Information Network – CIESIN – Columbia University (2017) Gridded population of the world, version 4 (GPWv4): Population density, revision 10. NASA Socioeconomic Data and Application Center (SEDAC), Palisades, NY. https://doi.org/10.7927/H4DZ068D.

Chiou CT, Lee J-F, Boyd SA (1990) The surface area of soil organic matter. *Environmental Science and Technology*, **24**, 1164–1166.

Craven D, Thakur MP, Cameron EK *et al.* (2017) The unseen invaders: introduced earthworms as drivers of change in plant communities in North American forests (a meta- analysis). *Global Change Biology*, **23**, 1065–1074.

Crumsey JM, Le Moine JM, Capowiez Y, Goodsitt MM, Larson SC, Kling GW, Nadelhoffer KJ (2013) Community-specific impacts of exotic earthworm invasions on soil carbon dynamics in a sandy temperate forest. *Ecology*, **94**, 2827–2837.

Crowther TW, Todd-Brown KEO, Rowe CW *et al*. (2016) Quantifying global soil carbon losses in response to warming. *Nature*, **540**, 104 –108.

Csuzdi C, Chang C-H, Pavlícek T, Szederjesi T, Esopi D, Szlávecz K (2017) Molecular phylogeny and systematics of native North American lumbricid earthworms (Clitellata: Megadrili). *PLoS ONE*, **12**, e0181504.

Davidson EA, Janssens IA (2006) Temperature sensitivity of soil carbon decomposition and feedbacks to climate change. *Nature*, **440**, 165–173.

Darwin C (1881) The formation of vegetable mould, through the action of worms, with observations on their habits. 326 pp. Murray Publishing, London, United Kingdom.

Dymond P, Scheu S, Parkinson D (1997) Density and distribution of *Dendrobaena octaedra* (Lumbricidae) in aspen and pine forests in the Canadian Rocky Mountains (Alberta). *Soil Biology and Biochemistry*, **29**, 265–273.

Ehlers J, Gibbard PL, Hughes PD (2011) Quaternary glaciations – extent and chronology. Elsevier, Amsterdam, the Netherlands. 1126 p.

Eisenhauer N, Partsch S, Parkinson D, Scheu S (2007) Invasion of a deciduous forest by earthworms: changes in soil chemistry, microflora, microarthropods and vegetation. *Soil Biology and Biochemistry*, **39**, 1099–1110.

Eisenhauer N, Schlaghamersky J, Reich PB, Frelich LE (2011) The wave towards a new steady state: effects of earthworm invasion on soil microbial functions. *Biological Invasions*, **13**, 2191–2196.

Feller C, Brown GG, Blanchart E, Deleporte P, Chernyanskii SS (2003) Charles Darwin, earthworms, and the natural sciences: various lessons from past to future. *Agriculture, Ecosystems and Environment*, **99**, 29–49.

Filsner J, Faber JH, Tiunov AV *et al.* (2016) Soil fauna: key to new carbon models. *Soil*, **2**, 565–582.

Fisk MC, Fahey TJ, Groffman PM, Bohlen PJ (2004) Earthworm invasion, fine root distribution and soil respiration in hardwood forests. *Ecosystems*, **7**, 55–62.

Fontaine S, Barot S, Barré P, Bdioui N, Mary B, Rumpel C (2007) Stability of organic carbon in deep soil layers controlled by fresh carbon supply. *Nature*, **450**, 277–280.

Frelich LE, Hale CM, Scheu S, Holdsworth AR, Heneghan L, Bohlen PJ, Reich PB (2006) Earthworm invasion into previously earthworm-free temperate and boreal forests. *Biological Invasions*, **8**, 1235–1245.

Gabet EJ, Reichman OJ, Seabloom EW (2003) The effects of bioturbation on soil processes and sediment transport. *Annual Review of Earth and Planetary Sciences*, **31**, 249–273.

Gaillardet J, Dupré B, Louvat P, Allegre CA (1999) Global silicate weathering and CO_2 consumption rates deduced from the chemistry of large rivers. *Chemical Geology*, **159**, 3–30.

Galy V, Peucker-Ehrenbrink B, Eglinton T (2015) Global carbon export from the terrestrial biosphere controlled by erosion. *Nature*, **521**, 204–207.

Gates GE (1977) More on the earthworm genus *Diplocardia*. *Megadrilogica*, **3**, 1–48.

Gates GE (1982) Farewell to North American megadriles. *Megadrilogica*, **4**, 12–77.

Gentsch N, Wild B, Mikutta R, Čapek P, Diáková K, Schrumpf M *et al.* (2018) Temperature response of permafrost soil carbon is attenuated by mineral protection. *Global Change Biology*, **24**, 3401–3415.

Gillabel J, Cebrian–Lopez B, Six J, Merckx R (2010) Experimental evidence for the attenuating effect of SOM protection on temperature sensitivity of SOM decomposition. *Global Change Biology*, **16**, 2789–2798.

Groffman PM, Fahey TJ, Fisk MC, Yavitt JB, Sherman RE, Bohlen PJ, Maerz JC (2015) Earthworms increase soil microbial carrying capacity and nitrogen retention in northern hardwood forests. *Soil Biology and Biochemistry*, **87**, 51–58.

Gruber S (2012) Derivation and analysis of a high-resolution estimate of global permafrost zonation. *The Cryosphere*, **6**, 221–233.

Guggenberger G, Zech W, Thomas RJ (1995) Lignin and carbohydrate alteration in particle size separates of an oxisol under tropical pastures following native savanna. *Soil Biology and Biochemistry*, **27**, 1629–1638.

Hale CM, Reich PB, Frelich LE (2004) Allometric equations for estimation of ash-free dry mass from length measurements for selected European earthworm species (Lumbricidae) in the western Great Lakes region. *American Midland Naturalist*, **151**, 179–185.

Hale CM, Frelich LE, Reich PB (2005a) Effects of European earthworm invasion on soil characteristics in northern hardwood forests of Minnesota. *Ecosystems*, **8**, 911–927.

Hale CM, Frelich LE, Reich PB (2005b) Exotic European earthworm invasion dynamics in northern hardwood forests of Minnesota, USA. *Ecological Applications*, **15**, 848–860.

Hale CM, Frelich LE, Reich PB (2006) Changes in hardwood forest understory plant communities in response to European earthworm invasions, *Ecology*, **87**, 1637–1649.

Hale CM (2007) Earthworms of the Great Lakes Region. Kollath & Stensaas Publishing. 36 pp.

Hansen MC, Potapov PV, Moore R *et al.* (2013) High-resolution global maps of 21st century forest cover change. *Science*, **342**, 850–853.

Harden JW, Manies KL, Turetsky MR, Neff JC (2006) Effects of wildfire and permafrost on soil organic matter and soil climate in interior Alaska. *Global Change Biology*, **12**, 2391–2403.

Heister K (2014) The measurement of the specific surface area of soils by gas and polar liquid adsorption methods — limitations and potentials. *Geoderma*, **216**, 75–87.

Hendrix PF, Bohlen PJ (2002) Exotic earthworm invasions in North America: ecological and policy implications. *BioScience*, **52**, 801–811.

Hoogerkamp M, Roogar H, Eijsackers HJP (1983) Effect of earthworms on grassland on recently reclaimed polder soils in the Netherlands. In: *Earthworm Ecology: From Darwin to Vermiculture* (ed./eds Satchell JE), pp. 85–105. Springer, Dordrecht, the Netherlands.

Hugelius G, Strauss J, Zubrzycki S *et al*. (2014) Estimated stocks of circumpolar permafrost carbon with quantified uncertainty ranges and identified data gaps. *Biogeosciences*, **11**, 6573–6593.

Jackson RB, Lajtha K, Crow SE, Hugelius G, Kramer MG, Piñiero G (2017) The ecology of soil carbon: pools, vulnerabilities, and biotic and abiotic controls. *Annual Review of Ecology, Evolution, and Systematics*, **48**, 419–445.

James SW (1998) Earthworms and earth history. In: *Earthworm ecology* (ed. Edwards CA) pp. 3–14. CRC Press, Boca Raton, Florida, USA.

Johnstone JF, Hollingsworth TN, Chapin III FS, Mack MC (2010) Changes in fire regime break the legacy lock on successional trajectories in Alaskan boreal forest. *Global Change Biology*, **16**, 1281–1295.

Jouquet P, Dauber J, Lagerlöf J, Lavelle P, Lepage M (2006) Soil invertebrates as ecosystem engineers: Intended and accidental effects on soil and feedback loops. *Applied Soil Ecology*, **32**, 153–164.

Kasischke ES, Johnstone JF (2005) Variation in postfire organic layer thickness in a black spruce forest complex in interior Alaska and its effects on soil temperature and moisture. *Canadian Journal of Forest Research*, **35**, 2164–2177.

Kleber M, Eusterhues K, Keiluweit M, Mikutta C, Mikutta R, Nico PS (2015) Mineral-organic associations: formation, properties, and relevance in soil environments. *Advances in Agronomy*, **130**, 1–140.

Knowles ME, Ross DS, Görres JH (2016) Effect of the endogeic earthworm Aporrectodea tuberculata on aggregation and carbon redistribution in uninvaded forest soil columns. *Soil Biology and Biochemistry*, **100**, 192–200.

Koven CD, Ringeval B, Friedlingstein P *et al.* (2011) Permafrost carbon-climate feedbacks accelerate global warming. *Proceedings of the National Academy of Sciences*, **108**, 14769–14774.

Koven CD, Lawrence DM, Riley WJ (2015) Permafrost carbon-climate feedback is sensitive to deep soil carbon decomposability but not deep soil nitrogen dynamics. *Proceedings of the National Academy of Sciences*, **112**, 3752–3757.

Langmaid KK (1964) Some effects of earthworm invasion in virgin podzols. *Canadian Journal of Soil Science*, **44**, 34–37.

Larson ER, Kipfmueller KF, Hale CM, Frelich LE, Reich PB (2010) Tree rings detect earthworm invasions and their effects in northern hardwood forests. *Biological Invasions*, **12**, 1053–1066.

Lavelle P, Martin A (1992) Small-scale and large-scale effects of endogeic earthworms on soil organic matter dynamics in soils of the humid tropics. *Soil Biology and Biochemistry*, **24**, 1491–1498.

Lavelle P, Bignell D, Lepage M, Wolters V, Roger P, Ineson P, Heal OW, Dhillion S (1997) Soil function in a changing world: the role of invertebrate ecosystem engineers. *European Journal of Soil Biology*, **33**, 159–193.

Lavelle P, Pashanasi B, Charpentier F, Gilot C, Rossi J-P, Derouard L, André J, Ponge J-F, Bernier N (1998) Large-scale effects of earthworms on soil organic matter and nutrient dynamics. In: *Earthworm Ecology* (ed./eds Edwards CA). pp. 103–122. St. Lucies Press, Boca Raton, Florida, USA.

Lavelle P, Charpentier F, Villenave C, Rossi J-P, Derouard L, Pashanasi B, André J, Ponge J-F, Bernier N (2004) Effects of earthworms on soil organic matter and nutrient dynamics at a landscape scale over decades. In: *Earthworm Ecology* (ed./eds Edwards CA). pp. 145–160. CRC Press, Boca Raton, Florida, USA.

Lavelle P, Decaëns T, Aubert M, Barot S, Blouin M, Bureau F, Margerie P, Mora P, Rossi J-P (2006) Soil invertebrates and ecosystem services. *European Journal of Soil Biology*, **42**, S3–S15.

Lee KE (1985) Earthworms – Their ecology and relationships with soils and land use. Academic Press, Sydney, Australia.

Lehmann J, Kleber M (2015) The contentious nature of soil organic matter. *Nature*, **528**, 60–68.

Lubbers IM, van Groenigen KJ, Fonte SJ, Six J, Brussaard L, van Groenigen JW (2013) Greenhouse-gas emissions from soils increased by earthworms. *Nature Climate Change*, **3**, 187–194.

Lubbers IM, van Groenigen KJ, Brussaard L, van Groenigen JW (2015) Reduced greenhouse gas mitigation potential of no-tillage soils through earthworm activity. *Scientific Reports*, **5**, 13787.

Lubbers IM, Pulleman MM, van Groenigen JW (2017) Can earthworms simultaneously enhance decomposition and stabilization of plant residue carbon? *Soil Biology and Biochemistry*, **105**, 12–24.

Lundström US, van Breemen N, Bain DC *et al.* (2000) Advances in understanding the podzolization process resulting from a multidisciplinary study of three coniferous forest soils in the Nordic countries. *Geoderma*, **94**, 335–353.

Lyttle A, Yoo K, Hale CM, Aufdenkampe A, Sebestyen S (2011) Carbon-mineral interactions along an earthworm invasion gradient at a sugar maple forest in northern Minnesota. *Applied Geochemistry*, **26**, S85–S88.

Lyttle AM (2013) Carbon-mineral interactions and bioturbation: an earthworm invasion chronosequence in a sugar maple forest in Northern Minnesota, MS thesis, Department of Soil, Water, and Climate, University of Minnesota, St. Paul, Minnesota, United States.

Lyttle A, Yoo K, Hale CM, Aufdenkampe A, Sebestyen SD, Resner K, Blum A (2015) Impact of exotic earthworms on organic carbon sorption on mineral surfaces and soil carbon inventories in a northern hardwood forest. *Ecosystems*, **18**, 16–29.

MacDougall AH, Avis CA, Weaver AJ (2012) Significant contributions to climate warming from the permafrost carbon feedback. *Nature Geoscience*, **5**, 719–721.

Marashi ARA, Scullion J (2003) Earthworm casts form stable aggregates in physically degraded soils. *Biology and Fertility of Soils*, **37**, 375–380.

Marhan M, Scheu S (2006) Mixing of different mineral soil layers by endogeic earthworms affects carbon and nitrogen mineralization. *Biology and Fertility of Soils*, **32**, 308–314.

Marinissen JCY, Van den Bosch F (1992) Colonization of new habitats by earthworms. *Oecologia*, **91**, 371–376.

Mayer LM, Xing B (2001) Organic matter–surface area relationships in acid soils. *Soil Science Society of America Journal*, **65**, 250–258.

Mescheryakova EN, Berman DI (2014) Cold hardiness and geographic distribution of earthworms (Oligochaeta, Lumbricidae, Moniligastridae). *Entomological Review*, **94**, 486–497.

Mikutta R, Kleber M, Torn MS, Jahn R (2006). Stabilization of soil organic matter: Association with minerals or chemical recalcitrance? *Biogeochemistry*, **77**, 25–56.

Moinet GYK, Hunt JE, Kirschbaum MUF, Morcom CP, Midwood AJ, Millard P (2018) The temperature sensitivity of soil organic matter decomposition is constrained by microbial access to substrates. *Soil Biology and Biochemistry*, **116**, 333–339.

Ping CL, Jastrow JD, Jorgenson MT, Michaelson GJ, Shur YL (2015) Permafrost soils and carbon cycling. *Soil*, **1**, 147–171.

R Core Team (2018) R: A language and environment for statistical computing. R Foundation for Statistical Computing, Vienna, Austria.

Ramankutty N, Evan AT, Monfreda C, Foley JA (2008) Farming the planet: 1. Geographic distribution of global agricultural lands in the year 2000. *Global Biogeochemical Cycles*, **22**, GB1003.

Räty M (2004) Growth of *Lumbricus terrestris* and *Aporrectodea calignosa* in an acid forest soil, and their effects on enchytraeid populations and soil properties. *Pedobiologia*, **48**, 321–328.

Räty M, Huhta V (2004) Earthworm communities in birch stands with different origin in central Finland. *Pedobiologia*, **48**, 283–291.

Resner K, Yoo K, Hale CM, Aufdenkampe A, Sebestyen S (2011) Elemental and mineralogical changes in soils due to bioturbation along an earthworm invasion chronosequence in northern Minnesota. *Applied Geochemistry*, **26**, S127–S131.

Resner K, Yoo K, Sebestyen S, Aufdenkampe A, Hale C, Lyttle A, Blum A (2015) Invasive earthworms deplete key soil inorganic nutrients (Ca, Mg, K, and P) in a northern hardwood forest. *Ecosystems*, **18**, 89–102.

Reynolds JW (1994) The distribution of the earthworms (Oligochaeta) of Indiana: a case for the post-Quaternary introduction theory for megadrile migration in North America. *Megadrilogica*, **5**, 13–35.

Reynolds JW (1995) The distribution of earthworms (Annelida: Oligochaeta) in North America. In: *Advances in ecology and environmental sciences* (eds. Mishra PC, Behera N, Senapati BK, Guru BC), pp. 133–153. Ashish Publishing House, New Delhi, India.

Reynolds JW (2015) A checklist of earthworms (Oligochaeta: Lumbricidae and Megascolecidae) in western and northern Canada. *Megadrilogica*, **17**, 141–156.

Saltmarsh DM, Bowser ML, Morton JM, Lang S, Shain D, Dial R (2016) Distribution and abundance of exotic earthworms within a boreal forest system in southcentral Alaska. *NeoBiota*, **28**, 67–86.

Schaetzl R.J., Johnson, D.L., Burns, S.F., and Small, T.W. (1989), Tree uprooting: review of terminology, process, and environmental implications. Can. J. For. Res, 19, 1–11.

Schmidt MWI, Torn MS, Abiven S *et al.* (2011) Persistence of soil organic matter as an ecosystem property. *Nature*, **478**, 49–56.

Schuur EAG, Bockheim J, Canadell JG *et al*. (2008) Vulnerability of permafrost carbon to climate change: Implications for the global carbon cycle. *BioScience*, **58**, 701–714.

Schuur EAG, McGuire AD, Schädel C *et al*. (2015) Climate change and the permafrost carbon feedback. *Nature*, **520**, 171–179.

Six J, Bossuyt, H, Degryze, S, Denef, K, (2004) A history on the link between (micro)aggregates, soil biota, and soil organic matter dynamics. *Soil Tillage Research*, **79**, 7–31.

Soil Survey Staff, (2014) Keys to Soil Taxonomy. 12th ed. USDA – Natural Resource Conservation Service, Washington, D.C.

Stendahl J, Lundin L, Nilsson T (2009) The stone and boulder content of Swedish forest soils. *Catena*, **77**, 285–291.

Taylor AR, Lenoir L, Vegerfors B, Persson T (2018) Ant and earthworm bioturbation in cold-temperate ecosystems. *Ecosystems*, doi:10.1007/s10021-018-0317-2.

Terhivuo J (1988) The Finnish Lumbricidae (Oligochaeta) fauna and its formation. *Annales Zoologici Fennici*, **25**, 229–247.

Tiunov AV, Hale CM, Holdsworth AR, Vsevolodova-Perel TS (2006) Invasion patterns of Lumbricidae into the previously earthworm-free areas of northeastern Europe

and the western Great Lakes region of North America. *Biological Invasions*, **8**, 1223–1234.

Torn MS, Trumbore SE, Chadwick OA, Vitousek PM, Hendricks DM (1997) Mineral control of soil organic carbon storage and turnover. *Nature*, **389**, 170–173.

Trumbore SE, Czimczik CI (2008) An uncertain future for soil carbon. *Science*, **321**, 1455–1456.

Ulanova NG (2000) The effects of windthrow on forests at different spatial scales: a review. *Forest Ecology and Management*, **135**, 155–167.

van Geffen KG, Berg MP, Aerts R (2011) Potential macro-detritivore range expansion into the subarctic stimulates litter decomposition: a new positive feedback mechanism to climate change? *Oecologia*, **167**, 1163–1775.

Wackett AA, Yoo K, Olofsson J, Klaminder J (2018) Human-mediated introduction of geoengineering earthworms in the Fennoscandian arctic. *Biological Invasions*, **20**, 1377–1386.

Wagai R, Mayer LM, Kitayama K (2009) Nature and extent of organic coverage of soil mineral surfaces assessed by a gas sorption approach. *Geoderma*, **149**, 152–160.

Wagai R, Kishimoto-Mo AW, Yonemura S, Shirato Y, Hiradate S, Yagasaki Y (2013) Linking temperature sensitivity of soil organic matter decomposition to its molecular structure, accessibility, and microbial physiology. *Global Change Biology*, **19**, 1114–1125.

Wall DH, Bradford MA, St. John MG *et al.* (2008) Global decomposition experiment shows soil animal impacts on decomposition are climate-dependent. *Global Change Biology*, **14**, 2661–2677.

Williams EK, Fogel ML, Berhe AA, Plante AF (2018) Distinct bioenergetic signatures in particulate versus mineral-associated soil organic matter. *Geoderma*, **330**, 107–116.

Wironen M, Moore TR (2006) Exotic earthworm invasion increases soil carbon and nitrogen in an old-growth forest in southern Quebec. *Canadian Journal of Forest Research*, **36**, 845–854.

Xia L, Szlavecz K, Swan CM, Burgess JL (2011) Inter- and intra-specific interactions of *Lumbricus rubellus* (Hoffmeister, 1843) and *Octolasion lacteum* (Orley, 1881) (Lumbricidae) and the implication for C cycling. *Soil Biology and Biochemistry*, **43**, 1584–1590.

Zhang W, Hendrix PF, Dame LE, Burke RA, Wu J, Neher DA, Li J, Shao Y, Fu S (2013) Earthworms facilitate carbon sequestration through unequal amplification of carbon stabilization compared with mineralization. *Nature Communications*, **4**, 2576.

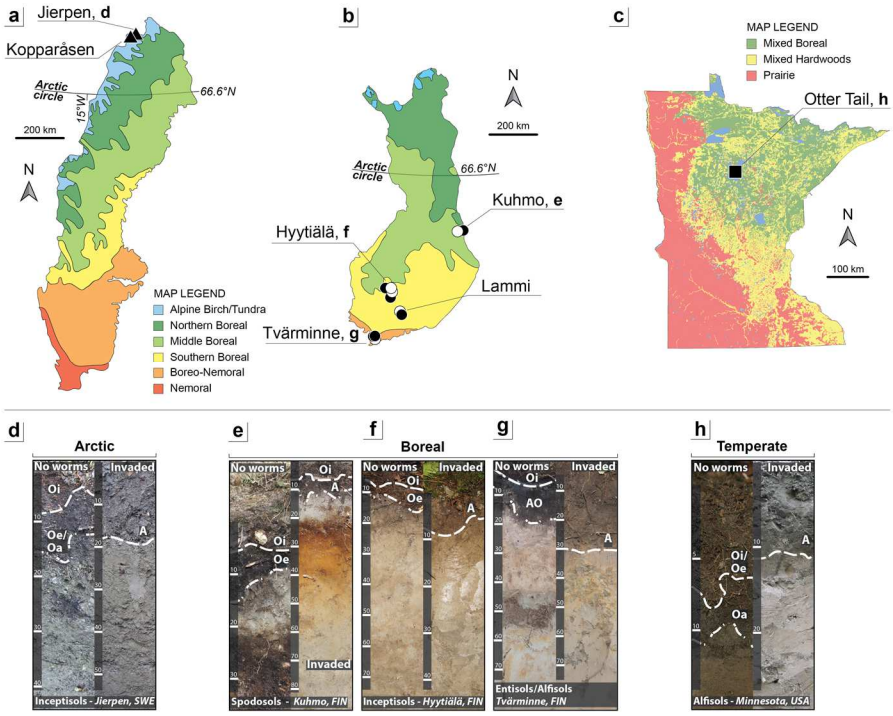

Figure 2.1. (Top) Maps of dominant vegetation zones for **(a)** Sweden, **(b)** Finland, and **(c)** Minnesota, USA. Vegetation maps for **(a)** Sweden and **(b)** Finland are modified from Hagen *et al.* (2013). The map for **(c)** Minnesota is constructed from the Marschner pre-settlement vegetation map (available at https://gisdata.mn.gov/dataset/biota-marschner-presettle-veg). (Bottom) Morphological characteristics of geoengineering earthworm-free and earthworm invaded soils across the formerly glaciated worlds. Representative earthworm-invaded and earthworm-free soil profile pairings from (north to south) **(d)** Inceptisols at Jierpen, Abisko, Sweden; **(e)** Spodosols near Kuhmo, Finland; **(f)** Inceptisols in Hyytiälä, Finland; **(g)** Entisols and Alfisols near Tvärminne, Finland; **(h)** Alfisols (Warba series) near Grand Rapids, Minnesota, USA.

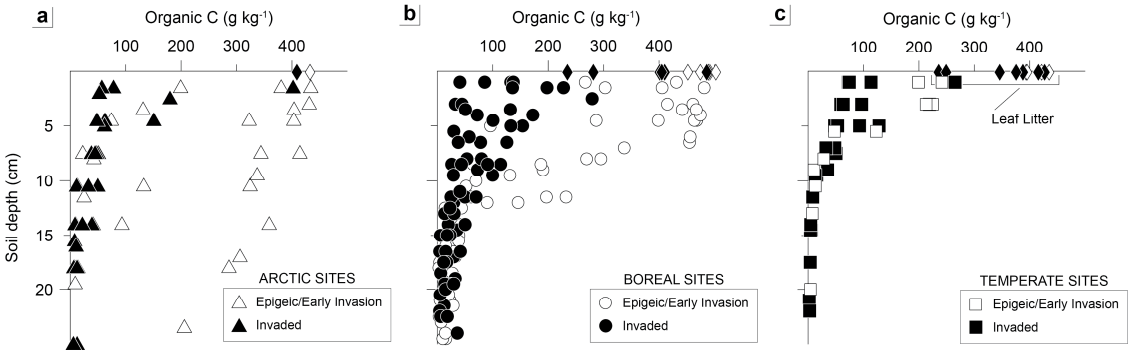

Figure 2.2. Depth profiles of soil organic carbon for horizon and depth interval samples collected from (left to right) **(a)** Swedish arctic, **(b)** Finnish boreal and **(c)** Minnesotan temperate sites. Diamonds indicate surface leaf litter samples as shown in panel **(c)**.

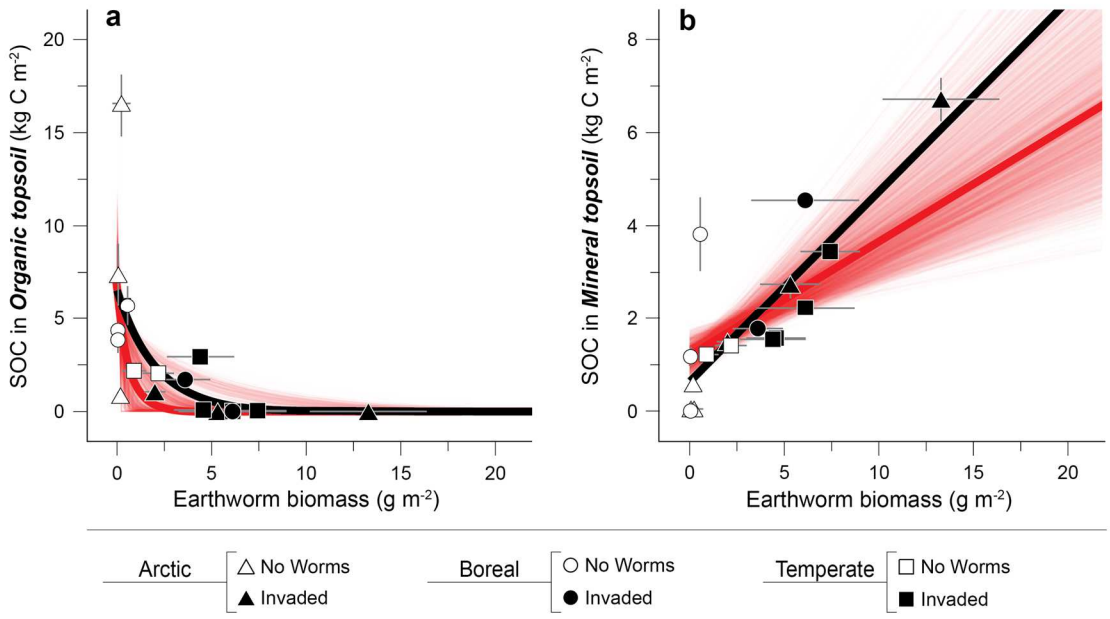

Figure 2.3. Earthworm invasion alters SOC pools in topsoils of arctic, boreal, and temperate forests. **(a)** Soil organic carbon (SOC) stored in organic surface layers (O horizon) exponentially declines (N = 17; $r^2_{average}$ = 0.33; P = 0.014) whereas **(b)** SOC stored in mineral surface soils (A horizon) increases linearly with increasing earthworm biomass (N = 17; $r^2_{average}$ = 0.695; P = <0.0001). Thin red lines represent regression outputs of individual Monte Carlo simulations on horizon inventories and the thick red line depicts the median result of the 2000 re-samplings. The solid black line represents the best-fit exponential **(a)** or linear **(b)** regression for averaged SOC and biomass values. Horizontal error bars represent variation (± SE) in earthworm sub-plot replicates (n = 3–6 for deciduous and arctic zones; n = 9–11 for boreal). Vertical error bars (± SE) are propagated from replicates of bulk density (n = 3) when available.

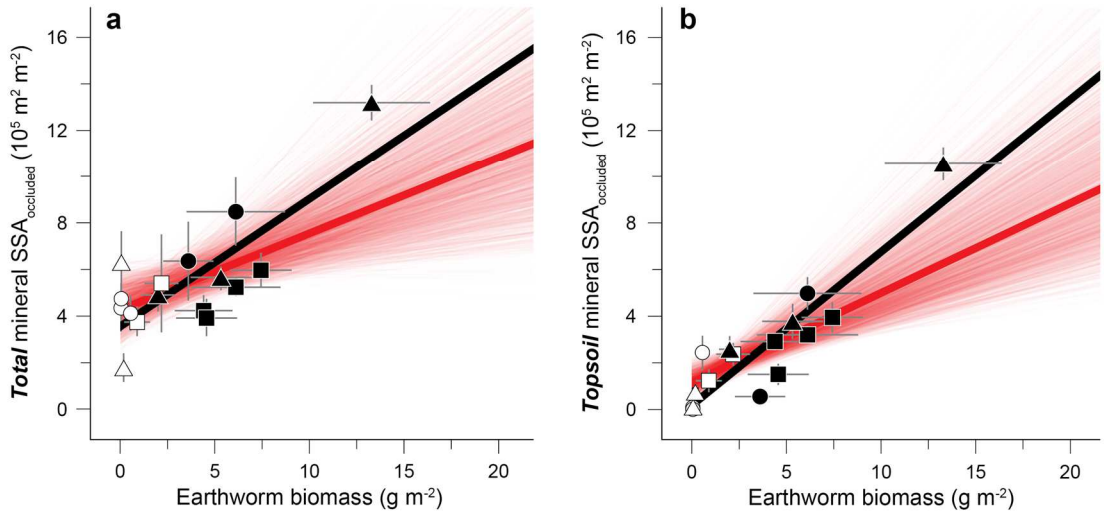

Figure 2.4. Earthworm invasion facilitates organo-mineral associations in topsoils of arctic, boreal, and temperate forests. **(a)** *Total* upper profile (0–25 cm) and **(b)** *Topsoil* (A-horizon) inventories of mineral $SSA_{occluded}$ from arctic, boreal, and temperate forest soils are positively correlated with earthworm biomass (**a** – N = 16, r^2 = 0.543; P = <0.0001; **b** – N = 16, r^2 = 0.744; P = <0.0001). Thin red lines represent regression outputs of individual Monte Carlo simulations on horizon inventories and the thick red line shows the median for the 2000 re-samplings. The thick black lines show best-fit linear regressions for site-level averaged SOC and biomass values. Horizontal error bars represent variation (± SE) in earthworm sub-plot replicates (n = 3–6 for deciduous and arctic zones; n = 9–11 for boreal). Vertical error bars (± SE) are propagated from replicates of mineral $SSA_{occluded}$ (n = 2–5) and bulk density (n = 3) when available.

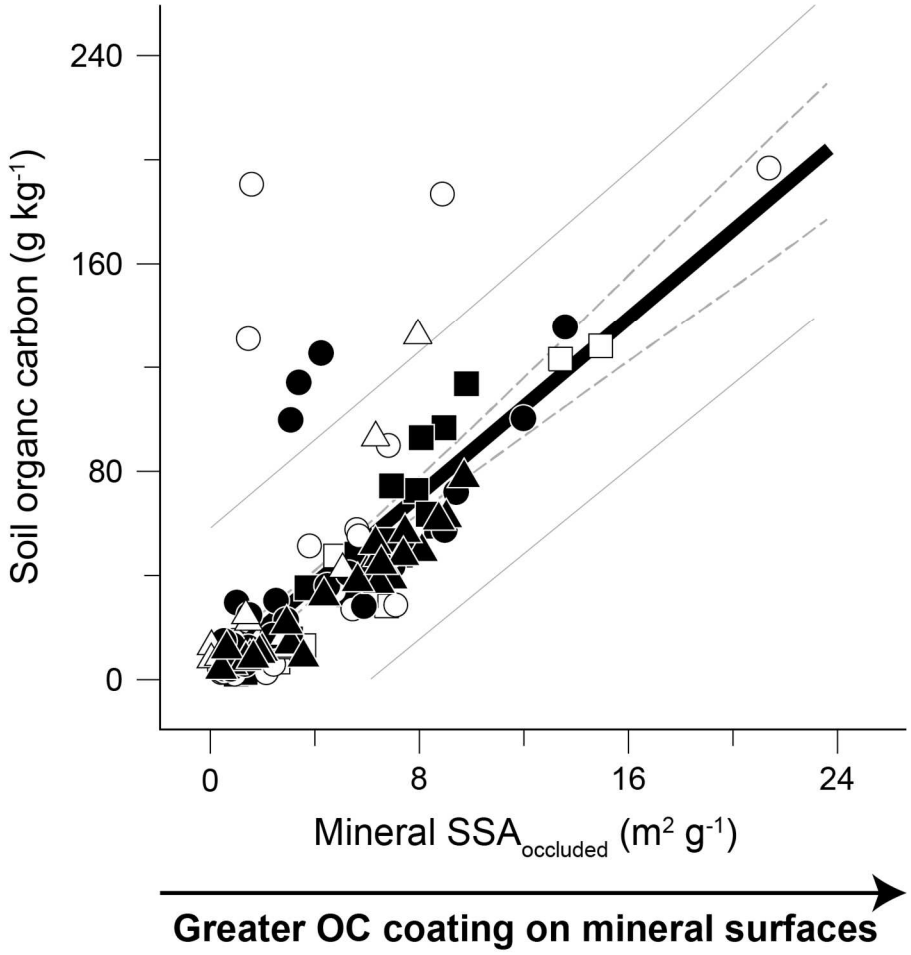

Figure 2.5. Evidence for mineral control of SOC storages in temperate, boreal, and arctic forest soils of the formerly glaciated world. SOC contents of mineral soils are significantly (N = 16, n = 133, r^2 = 0.55; P = <0.0001) and positively correlated with the amount of occluded mineral SSA regardless of geoengineering earthworm presence and abundance. Thin dashed lines represent the 95% confidence interval for the fitted regression.

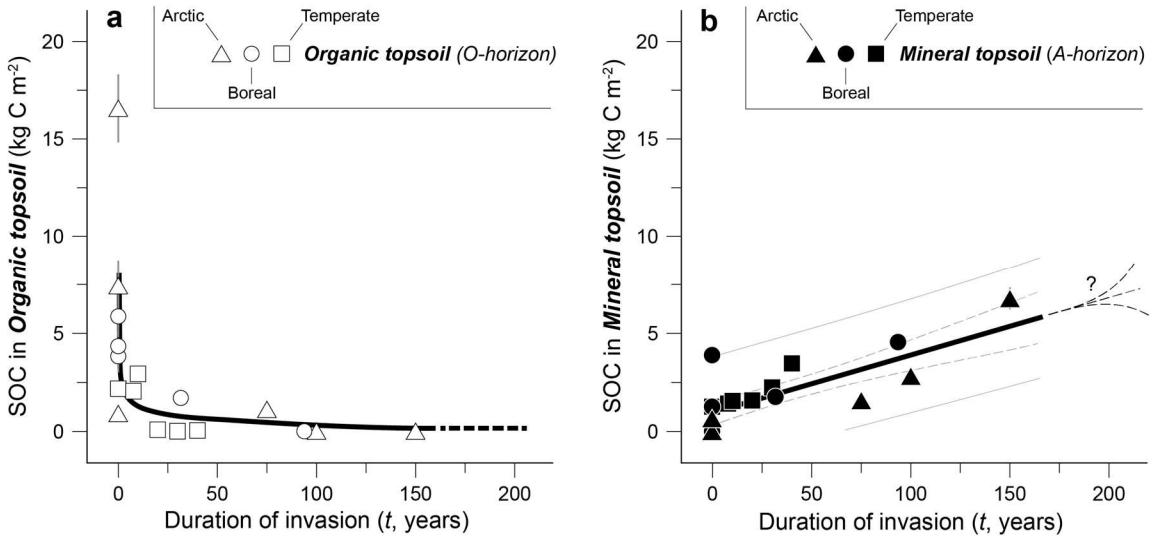

Figure 2.6. Effects of the duration of earthworm invasion on SOC storage in the **(a)** organic (O-horizon, open symbols) and **(b)** mineral topsoil (A-horizon, black filled symbols) reservoirs. The slope of the exponential regression in **(a)** was used to estimate a C loss rate (~200 g of C m^{-2} yr^{-1} during years 1–10) and the slope of the linear regression (P = <0.0001) in **(b)** was used to derive an earthworm-mediated sequestration rate of 29±5 g of C m^{-2} yr^{-1}. Thin dashed lines represent the 95% confidence interval.

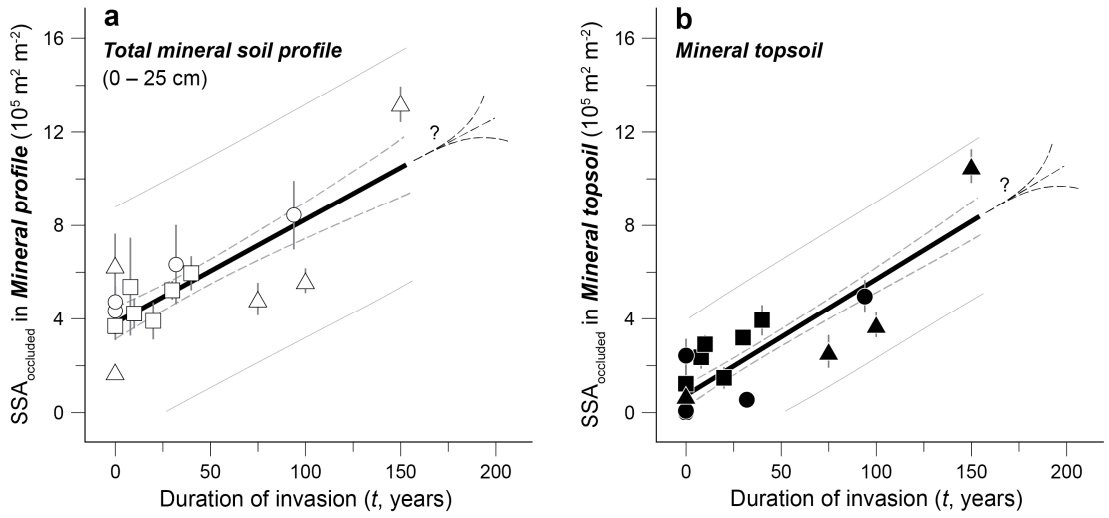

Figure 2.7. Effects of the duration of earthworm invasion on $SSA_{occluded}$ storages in the **(a)** total (0 – 25 cm, open symbols; P = <0.0001) and **(b)** mineral topsoil (A-horizon, black filled symbols; P = <0.0001) reservoirs. The slopes yield total and A-horizon occlusion rates of **(a)** 4.4 ± 0.5 km^2 m^{-2} and **(b)** 5.0 ± 0.3 km^2 m^{-2}, respectively. Thin dashed lines represent the 95% confidence interval for the fitted regression.

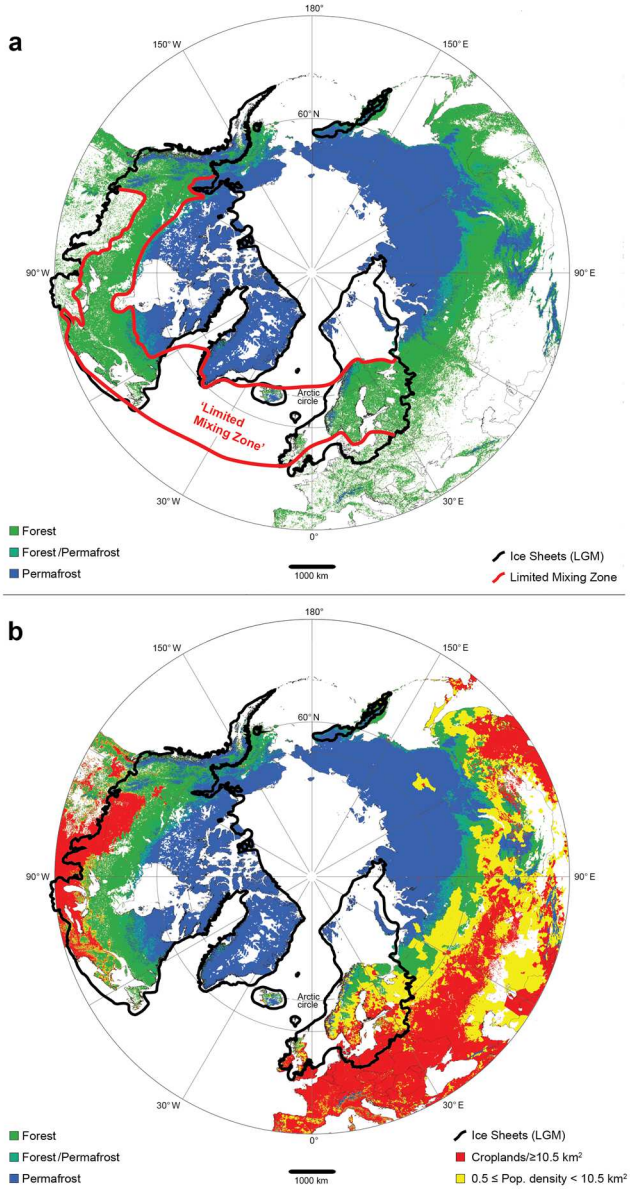

Figure 2.8. Circumpolar map of forest vegetation and continuous permafrost (PZI > 0.7) for the northern hemisphere (above 40 °N) constructed from global datasets of land cover (ESA GlobCover, 2009), topographic roughness and the permafrost zonation index (PZI; Gruber, 2012): see Table 2 and Appendix S5 for additional details. Continental ice sheets for N. America, Fennoscandia, N. Atlantic islands (Iceland, Faroe Islands, etc.), and Kamchatka after Ehlers *et al.* (2010) are outlined in black and the 'Limited mixing zone' utilized in areal estimates (including Kamchatka and the N. Atlantic Islands) is traced in red. **(b)** The same circumpolar Pedoturbation map is overlaid with global datasets for croplands (Ramankutty *et al.,* 2008) and population density estimates for the year 2020 (Center for International Earth Science Information Network, 2017, available at https://doi.org/10.7927/H4DZ068D) to emphasize likely areas of current (and future) earthworm invasion. Datum, WGS84: projection, Azimuthal Equidistant (N. Pole).

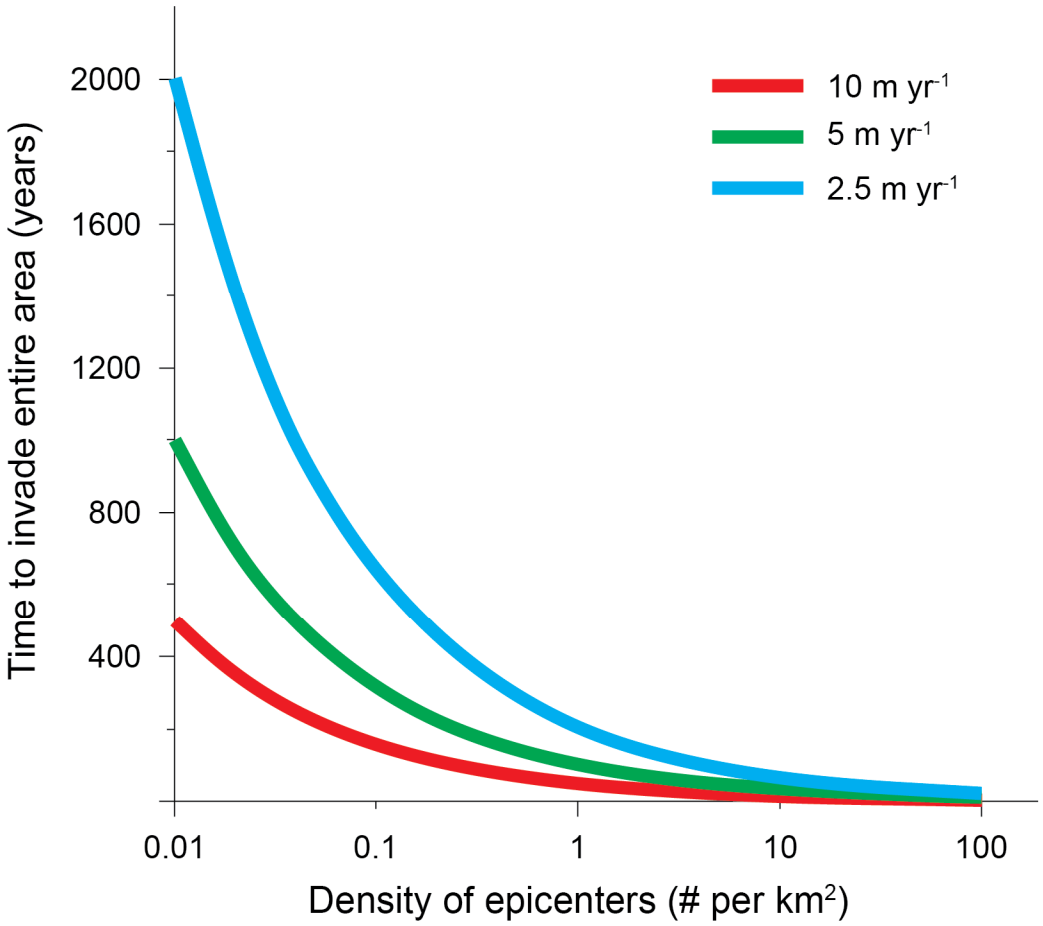

Figure 2.9. Model results estimating the time for introduced earthworms to invade a given area (i.e. 1-km^2 box) as a function of epicenter (i.e. earthworm source) density and earthworm dispersal rate (2.5-10 m yr^{-1}) assuming a uniform epicenter distribution.

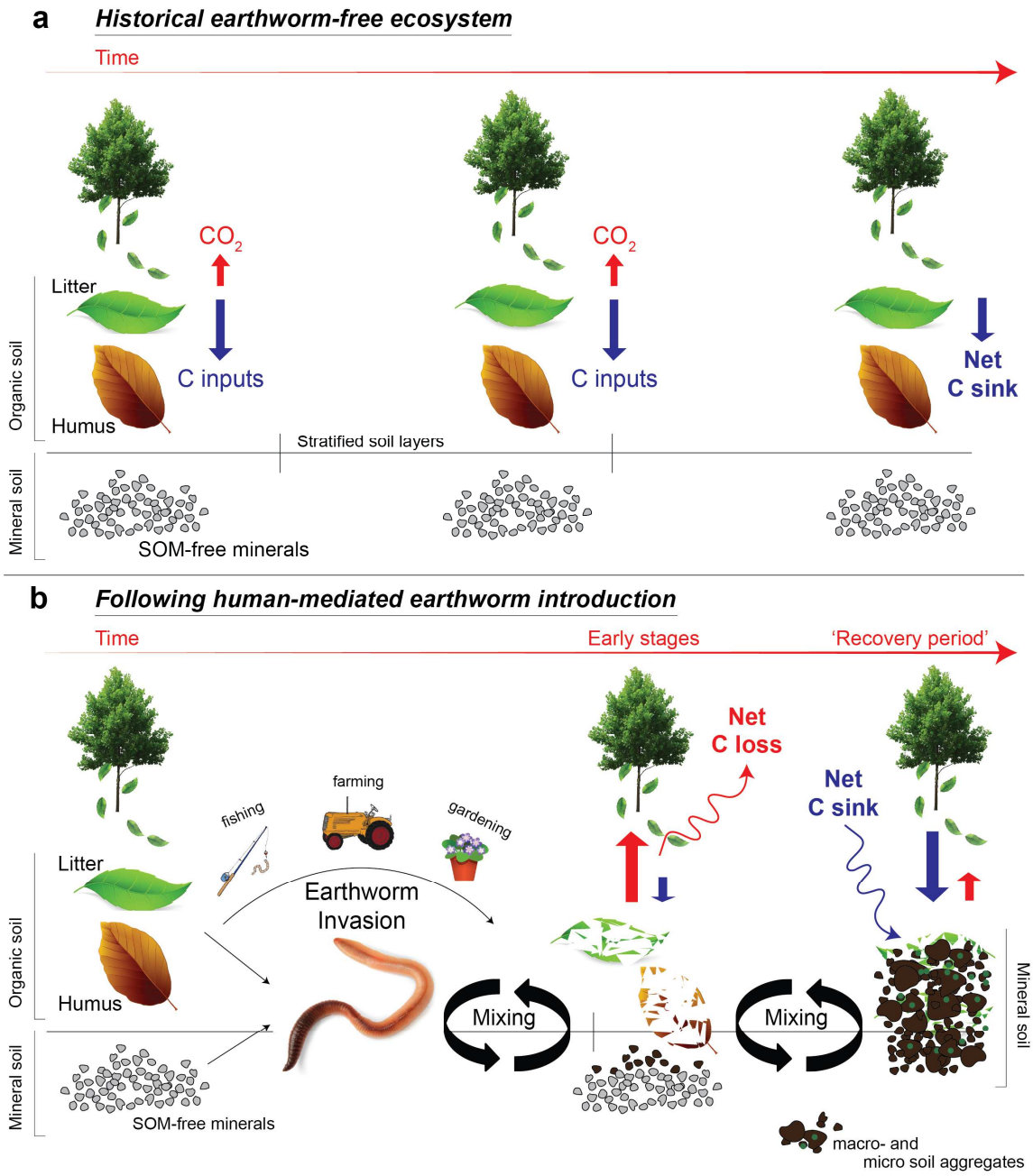

Figure 2.10. New conceptual view of high-latitude environmental change following human-facilitated introduction of geoengineering earthworms. **(a)** Baseline framework of pedogenesis and steady-state SOM balance (net C sink) in high-latitude environments through time in the absence of major bioturbators other than tree throw. **(b)** Human modes of earthworm dispersal (fishing, farming, and gardening) cultivate a regime shift in high-latitude soil processes. Earthworms and microbes stimulate rapid decomposition of litter and in particular humus, resulting in heightened CO_2 emissions and a net C loss following initial invasion (**b**, bottom center). As the invasion proceeds, annual litter fall (labile SOC) is stabilized via occlusion in macro- and micro-aggregates or sorption onto mineral surfaces (shown far right), transforming the system back into an SOC sink.

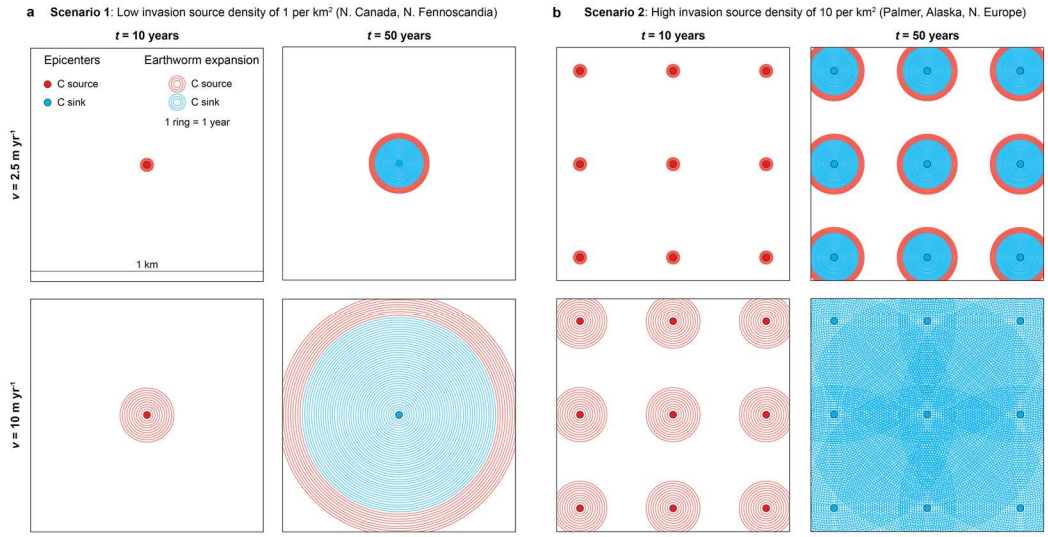

Figure 2.11. Modeling of the time required for non-native earthworms to invade a given land area (i.e. 1 km^2 area) following their introduction at **(a)** 1 epicenter per km^2 and **(b)** 10 epicenters per km^2 assuming various earthworm dispersal rates (top panel: v = 2.5 m yr^{-1}; bottom panel: v = 10 m yr^{-1}). Concentric circles represent the range of earthworm expansion (1 ring = 1 year). Red circles denote a recently (<10 years) invaded landscape in the C loss stage (C loss rate = 200 g of C m^{-2} yr^{-1} for years 1-10) and blue circles indicate later invasion stages where C sequestration dominates (C sequestration rate = 29±5 g of C m^{-2} yr^{-1} for years 10-150).

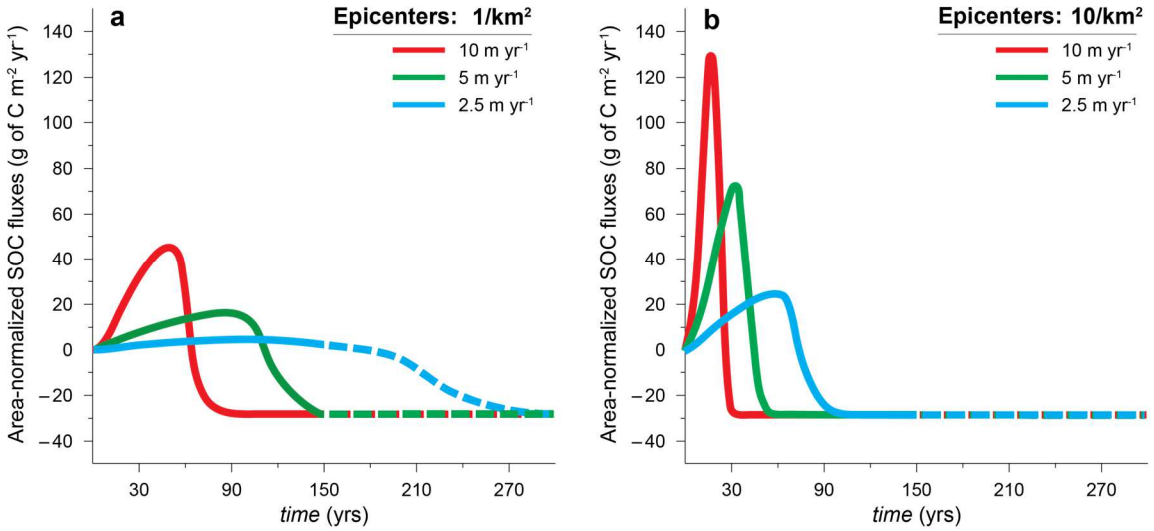

Figure 2.12. Modeling of the area-normalized net SOC fluxes through time assuming a given land area (i.e. 1 km^2) following the establishment and outward expansion of earthworms from source densities of **(a)** 1 epicenter per km^2 and **(b)** 10 epicenters per km^2 assuming a range (2.5-10 m yr^{-1}) of earthworm dispersal rates.

Table 2.1. Common non-native *Lumbricidae* earthworms across the 'limited mixing zone' and their associated ecological groups

Species	Ecological group
L. rubellus (adults)	epi-endogeic*
Dendrobaena octaedra	epigeic
Bimastos rubidus [a]	epigeic
Aporrectodea spp. (*A. caliginosa, A. rosea*)	endogeic*
L. terrestris (adults)	anecic*
Octolasion tyrtaeum	endogeic*
L. juveniles	epi-endogeic/anecic*

[a] Formerly *Dendrodrilus rubidus* (see Csuzdi *et al.,* 2017)
* Indicates geoengineering earthworm-type

Table 2.2. Earthworm invasion status/duration and geospatial data for soil profiles collected in this study

Profile	Earthworm Assemblage (age)	Latitude (°N)	Longitude (°E)	Age (yrs.)	MAT (°C)	MAP (mm)
		Arctic				
Jierpen Invaded	Invaded[a]	68.44908	18.85954	150	−0.7[d]	300−500[e]
Jierpen Intermediate	Invaded	68.44897	18.85626	75	−0.6	300−500
Jierpen Early Inv	Epigeic[b]	68.45232	18.86833	0	−1.7	300−500
Jierpen Shoreline	Epigeic	68.44703	18.86060	0	−0.5	300−500
Kopparåsen Invaded	Invaded	68.43075	18.61546	100	−1.3	500−700
Kopparåsen Early Inv	Epigeic	68.42871	18.61384	0	−1.4	500−700
		Boreal				
Kuhmo_176	Invaded	63.84763	30.15834	32[f]	1.3[f]	570−670[f]
Kuhmo_k02	Epigeic	63.83765	29.45825	0	1.4	570−670
Hyytiälä_1A	Invaded	61.62291	24.29813	94	3.8	550−650
Hyytiälä_H4	Invaded	61.87703	24.10126	33	3.4	550−650
Hyytiälä_4C	Epigeic	61.92270	24.35137	0	3.3	550−650
Hyytiälä_5C	Early Invasion[c]	61.72920	24.56165	5	3.7	550−650
Lammi_12	Invaded	61.03999	25.08480	77	3.9	600−700
Lammi_S02	Early Invasion	61.05502	25.05164	5	3.9	600−700
Tvärminne_61	Invaded	60.00135	23.17143	55	5.3	550−650
Tvärminne_34	Invaded	60.00246	23.17609	59	5.3	550−650
Tvärminne_8	Epigeic	59.98125	23.36439	0	5.4	550−650
		Temperate				
Otter tail Pit 8	Invaded	47.26690	–94.39629	40	8.5	500−600
Otter tail Pit 7	Invaded	47.26669	–94.39795	30	8.5	500−600
Otter tail Pit 6	Invaded	47.26670	–94.39739	20	8.5	500−600
Otter tail Pit 5	Invaded	47.26675	–94.39675	10	8.5	500−600
Otter tail Pit 4	Early Invasion	47.26670	–94.39659	8	8.5	500−600
Otter tail Pit 3	Epigeic	47.26672	–94.39629	0	8.5	500−600

[a] *Invaded* denotes consistent presence of at least one geoengineering earthworm *sp.* (*Aporrectodea sp.*, *Octolasion sp., Lumbricus rubellus*, *Lumbricus terrestris*)

[b] *Epigeic* signifies inconsistent earthworms and exclusive presence of epigeic *Dendrobaena octaedra* (Savigny, 1826) or *Bismastos rubidus* (Csuzdi *et al.,* 2017)

[c] *Early Invasion* signifies consistent presence of epigeic-type earthworms and discontinuous presence of geoengineering earthworm species (*Lumbricus rubellus*)

[d] Mean annual temperature (MAT) for all arctic profiles calculated from Alexanderson *et al.*, (1991) and corrected for differences in elevation (0.6 °C/100 m asl)

[e] Mean annual precipitation (MAP) for all arctic profiles from Alexanderson *et al.*, (1991) and Rapp (1960)

[f] MAT and MAP data for boreal profiles collected from the Land Survey of Finland GIS geodata portal (https://kartta.paikkatietoikkuna.fi/?lang=en)

Table 2.3. Estimated C fluxes from earthworm invaded soils of the 'limited mixing zone' (All fluxes reported in Pg or Gt of C)

	Density *1-km^{-2}*			Density *10/km^{-2}*		
Dispersal rate	*10 m yr^{-1}*	*5 m yr^{-1}*	*2.5 m yr^{-1}*	*10 m yr^{-1}*	*5 m yr^{-1}*	*2.5 m yr^{-1}*
Time (*years*)	***10 % invasion into 'limited mixing zone'***					
5	1.5E-03 [a]	3.6E-04	9.1E-05	0.01	3.6E-03	9.1E-04
10	0.01	2.5E-03	6.4E-04	0.10	0.03	6.3E-03
20	0.07	0.02	4.2E-03	0.57	0.16	0.04
30	0.18	0.04	0.01	0.65	0.41	0.09
50	0.51	0.13	0.03	0.40	0.64	0.26
75	0.60	0.27	0.07	0.10	0.34	0.45
100	0.30	0.43	0.11	-0.21	3.3E-02	0.23
150	-0.31[b]	0.16	0.17	-0.82	-0.58	-0.38
200	-0.92	-0.45	0.15	-1.4	-1.2	-0.99
300	-2.1	-1.7	-0.74	-2.7	-2.4	-2.2
Time (*years*)	***25 % invasion into 'limited mixing zone'***					
5	3.6E-03	9.1E-04	2.3E-04	0.04	0.01	2.3E-03
10	0.03	0.01	1.6E-03	0.25	0.06	0.02
20	0.17	0.04	0.01	1.4	0.40	0.09
30	0.44	0.11	0.03	1.6	1.0	0.23
50	1.3	0.32	0.08	1.0	1.6	0.65
75	1.5	0.68	0.17	0.24	0.84	1.1
100	0.75	1.1	0.27	-0.52	0.08	0.58
150	-0.77	0.39	0.41	-2.1	-1.4	-0.95
200	-2.3	-1.1	0.37	-3.6	-3.0	-2.5
300	-5.4	-4.2	-1.9	-6.6	-6.0	-5.5

[a] Positive values indicate net C loss (i.e. C flux out of soils)
[b] Negative values indicate net C sequestration (i.e. C flux into soils)

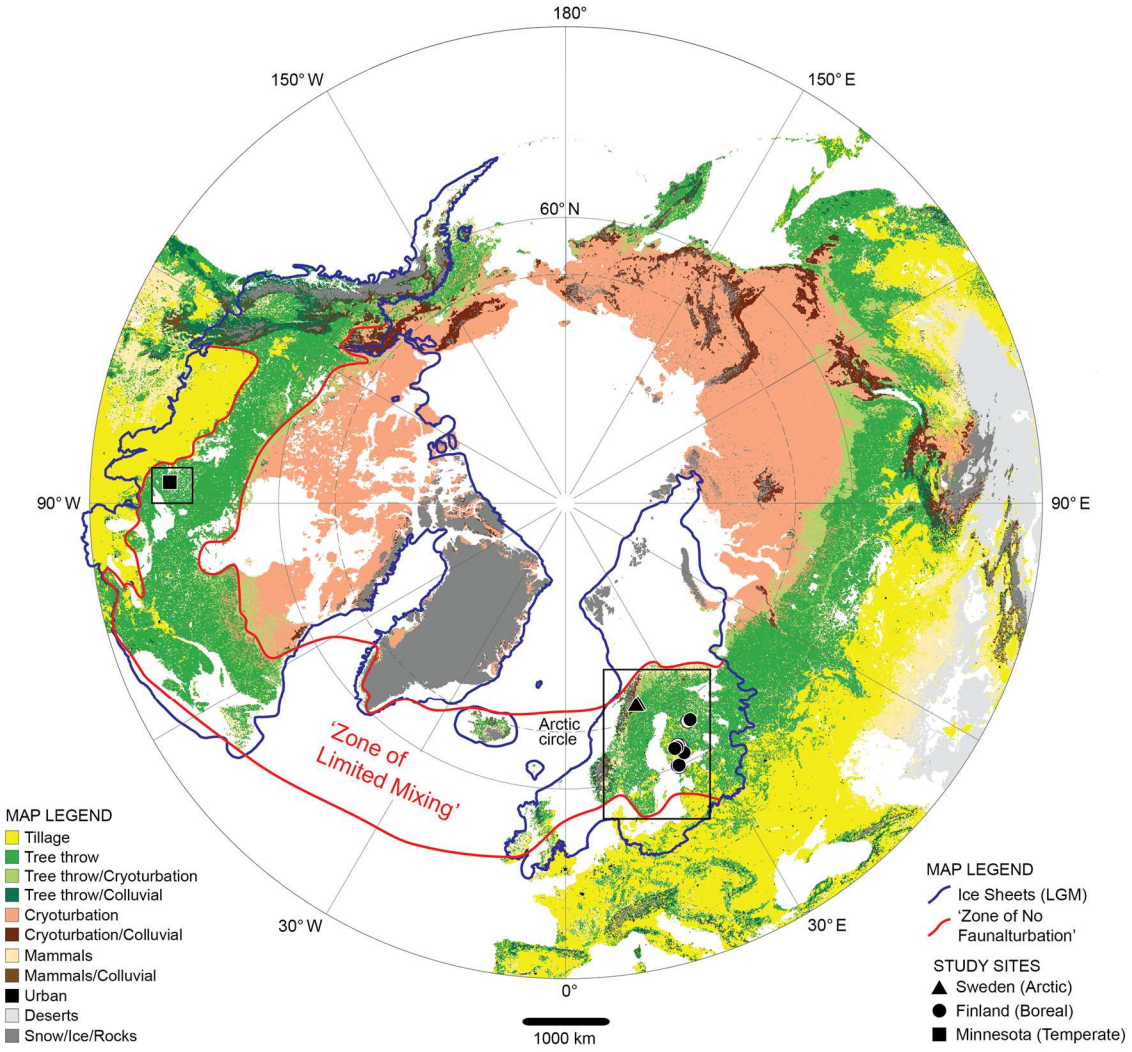

Figure S2.1. Biogeography of pedoturbation modes for the northern hemisphere (above 40 °N) constructed from global datasets of land cover (ESA GlobCover, 2009), topographic roughness and permafrost (Gruber, 2012) and croplands (Ramankutty *et al.,* 2008): see Table 1 for additional details. Continental ice sheets for N. America, Fennoscandia, and N. Atlantic islands (Iceland, Faroe Islands, etc.) after Ehlers *et al.* (2011) are outlined in blue and the 'limited mixing zone is traced in red. Boxes indicate areas of interest for this study and sampling sites from arctic (triangles), boreal (circles) and temperate (squares) biomes are shown. Exact site locations have been altered for display purposes; datum, WGS84: projection, Azimuthal Equidistant (N. Pole).

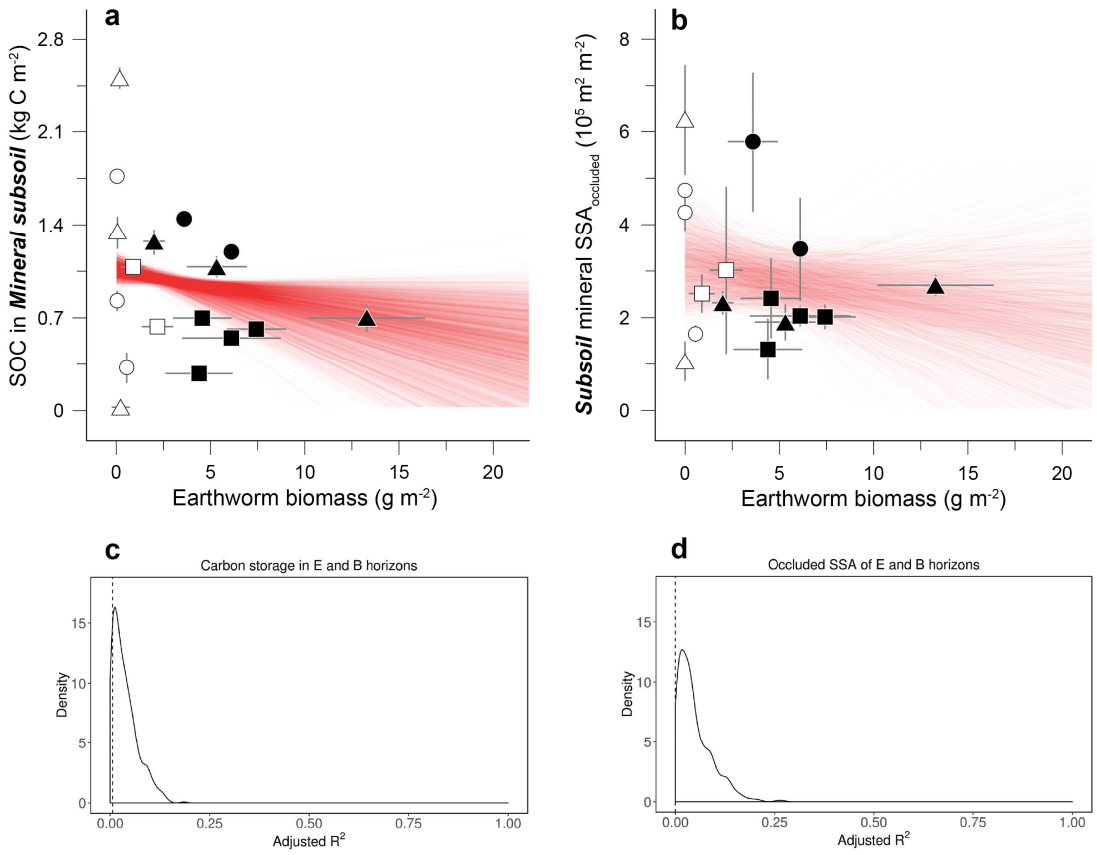

Figure S2.2. Earthworm invasion does not affect subsoil (E-/B-horizon) SOC budgets or organo-mineral associations in formerly glaciated arctic, boreal, and temperate forests. **(a)** Soil organic carbon (SOC) and **(b)** $SSA_{occluded}$ inventories in mineral subsoils (E- and/or B-horizons) do not respond to increasing earthworm biomass (**a**, $P = 0.28$; **b**, $P = 0.21$). Thin red lines represent regression outputs of individual Monte Carlo simulations for subsoil inventories. Horizontal error bars represent variation (± SE) in earthworm sub-plot replicates ($n = 3$–6 for deciduous and arctic zones; $n = 9$–11 for boreal). Vertical error bars (± SE) are propagated from replicates of bulk density ($n = 3$) and $SSA_{occluded}$ (**b**, $n = 2$–5) when available. **(c–d)** Adjusted r^2 distributions for the 2000 best-fit linear regressions generated through Monte Carlo resampling of **(c)** SOC and **(d)** $SSA_{occluded}$ inventories and site-level earthworm biomass (thin red lines in panels **(a)** and **(b)**, respectively).

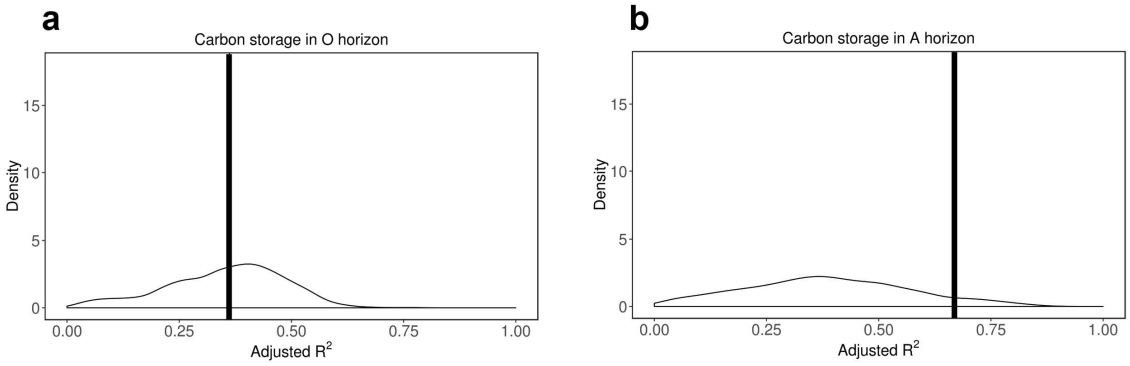

Figure S2.3. Adjusted r^2 distributions for the 2000 best-fit linear regressions generated through Monte Carlo resampling of the **(a)** O-horizon and **(b)** A-horizon SOC inventories and earthworm biomass (thin red lines in main text Figure 2.3, respectively). The thick black line corresponds to the best-fit regression obtained by assuming site-level averages for SOC and earthworm biomass (denoted by thick black line in main text Figure 2.3).

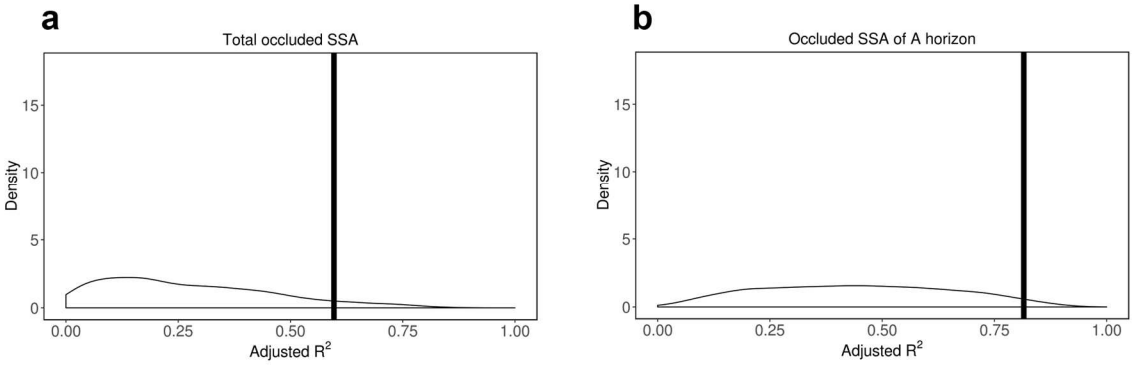

Figure S2.4. Adjusted r^2 distributions for the 2000 best-fit linear regressions generated through Monte Carlo resampling of the **(a)** total (0-25 cm) and **(b)** mineral topsoil (i.e. A-horizon) $SSA_{occluded}$ inventories and earthworm biomass (thin red lines in main text Figure 2.4, respectively). The thick black line corresponds to the best-fit regression obtained by assuming site-level averages for **(a)** total (0-25 cm) or **(b)** A-horizon $SSA_{occluded}$ and earthworm biomass (denoted by thick black line in main text Figure 2.4).

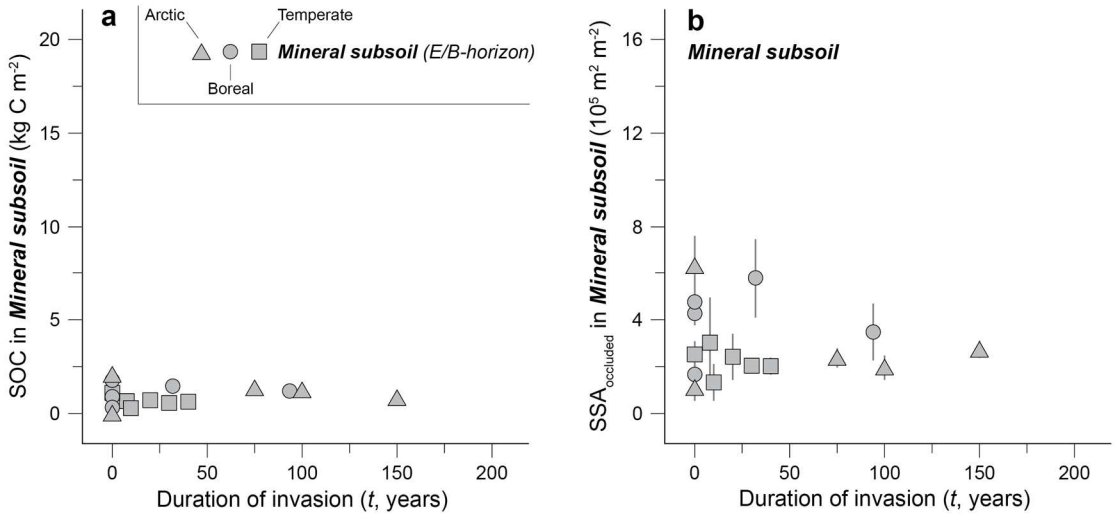

Figure S2.5. Earthworm invasion does not affect SOC budgets or organo-mineral associations in arctic, boreal, and temperate forest subsoils through time. **(a)** Soil organic carbon (SOC) and **(b)** $SSA_{occluded}$ inventories in mineral subsoils (E- and/or B-horizons) are not correlated ($P > 0.05$) with increasing duration of earthworm invasion. Vertical error bars (± SE) are propagated from replicates of bulk density ($n = 3$) and $SSA_{occluded}$ ($n = 2–5$) when available.

Table S2.1. Pedoturbation modes and criteria used to classify designations for the thematic map

Pedoturbation type	Criteria
Tillage	[b] Croplands ≥ 0.20 (20%)
Cryoturbation	PZI ≥ 0.70 (Forest); PZI ≥ 0.30 (Non-Forest); TRI < 0.35
Cryoturbation/Colluvial	PZI ≥ 0.70 (Forest); PZI ≥ 0.30 (Non-Forest); TRI ≥ 0.35
Cryoturbation/Tree Throw	[c] Forest; 0.70 < PZI ≥ 0.50, TRI < 0.35
Tree Throw	Forest; PZI < 0.50, TRI < 0.35
Tree Throw/Colluvial	Forest; PZI < 0.70, TRI ≥ 0.35
Mammals	[d] Non-Forest; PZI ≤ 0.30, TRI < 0.35
Mammals/Colluvial	Non-Forest; PZI ≤ 0.30, TRI < 0.35
Urban	Urban Land Cover
Snow/Rock/Ice	Bare Areas; Permanent Snow/Ice

[a] Tillage designation of ≥ 0.20 (or 20%) cropland coverage from Ramankutty *et al.* (2008) and/or the following land cover values (classes) from ESA GlobCover (2009): 11 – Post-flooding or irrigated croplands; 14 – Rainfed croplands; Mosaic cropland (50 – 70%)/Vegetation (20 – 50%)

[c] Forest land cover types include the following values (classes) sourced from the ESA GlobCover (2009) publication: 30 – Mosaic vegetation (50 – 70%)/Cropland (20 – 50%); 40 – Closed to open (>15%) broadleaved evergreen and/or semi-deciduous forest; 50 – Closed (> 40%) broadleaved deciduous forest; 60 – Open (15 – 40%) broadleaved deciduous forest; 70 – Closed (> 40%) needleleaved evergreen forest; 90 – Open (15 – 40%) needleleaved deciduous or evergreen forest; 100 – Closed to open (>15%) mixed broadleaved and needleleaved forest; 110 – Mosaic Forest/Shrubland (50 – 70%)/Grassland (20 – 50%); 160 – Closed (>40%) broadleaved forest regularly flooded – Fresh water.

[d] Non-Forest land cover types include the following values (classes) sourced from the ESA GlobCover (2009) publication: 120 – Mosaic Grassland (50 – 70%)/Forest/Shrubland (20 – 50%); 130 – Closed to open (>15%) shrubland; 150 – Closed to open (>15%) grassland; 160 – Sparse (>15%) vegetation (woody vegetation, shrubs, grassland).

Bibliography

Addison JA (2009) Distribution and impacts of invasive earthworms in Canadian forest ecosystems. *Biological Invasions*, **11**, 59–79.

Alban DH, Berry EC (1994) Effects of earthworm invasion on morphology, carbon and nitrogen of a forest soil. *Applied Soil Ecology*, **1**, 243–249.

Andersson R, Ostlund L, Tornlund E (2005) The last European landscape to be colonized: a case study of land-use change in the far north of Sweden 1850–1930. *Environment and History*, **11**, 293–318

Arino O, Perez R, Julio J, Kalogirou V, Bontemps S, Defourny P, van Bogaert E (2012) Global land cover map for 2009 (GlobCover 2009). European Space Agency, PANGAEA, doi:10.1594/PANGAEA.787668.

Balesdent J, Basile-Doelsch I, Chadoeuf J, Cornu S, Derrien D, Fekiakova Z, Hatté C (2018) Atmosphere-soil carbon transfer as a function of soil depth. *Nature*, **559**, 599–602.

Batjes NH (2016) Harmonized soil property values for broad-scale modelling (WISE30sec) with estimates of global soil carbon stocks, *Geoderma*, **269**, 61–68.

Baughman CA, Mann DH, Verbyla DL, Kunz ML (2015) Soil surface organic layers in arctic Alaska: Spatial distribution, rates of formation, and microclimatic effects. Journal of Geophysical Research: *Biogeosciences*, **120**, 1150–1164.

Bohlen PJ, Pelletier DM, Groffman PM, Fahey TJ, Fisk MC 2004a. Influence of earthworm invasion on redistribution and retention of soil carbon and nitrogen in northern temperate forests. *Ecosystems*, **7**, 13–27.

Bohlen PJ, Scheu S, Hale CM, McLean MA, Migge S, Groffman PM, Parkinson D (2004b) Non-native invasive earthworms as agents of change in northern temperate forests. *Frontiers in Ecology and the Environment*, **2**, 427–435.

Bonan GB (2008) Forests and climate change: Forcings, feedbacks, and the climate benefits of forests. *Science*, **320**, 1444–1449.

Booysen M, Sikes D, Bowser ML, Andrews R (2018) Earthworms (Oligochaeta: Lumbricidae) of Interior Alaska. *Biodiversity Data Journal*, **6**, e27427.

Bormann BT, Spaltenstein H, McClellan MH, Ugolini FC, Cromack Jr K, Nay SM (1995) Rapid soil development after windthrow disturbance in pristine forests. *Journal of Ecology*, **83**, 747–757.

Bossuyt H, Six J, Hendrix PF (2005) Protection of soil carbon by macroaggregates within

earthworm casts. *Soil Biology and Biochemistry*, **37**, 251–258.

Bossuyt H, Six J, Hendrix PF (2006) Interactive effects of functionally different earthworm species on aggregation and incorporation and decomposition of newly added residue carbon. *Geoderma*, **130**, 14–25.

Bradford MA, Wieder WR, Bonan GB, Fierer N, Raymond PA, Crowther TW (2016) Managing uncertainty in soil carbon feedbacks to climate change. *Nature Climate Change*, **6**, 751–758.

Brandt JP, Flannigan MD, Maynard DG, Thompson ID, Volney WJA (2013) An introduction to Canada's boreal zone: ecosystem processes, health, sustainability, and environmental issues. *Environmental Reviews*, **21**, 207–226.

Brown GG, Barois I, Lavelle P (2000) Regulation of soil organic matter dynamics and microbial activity in the drilosphere and the role of interactions with other functional domains. *European Journal of Soil Biology*, **36**, 177–198.

Brunauer S, Deming LS, Deming WE, Teller E (1940) On a theory of the van der Waals adsorption of gases. *Journal of the American Chemical Society*, **62**, 1723–1732.

Callesen I, Liski J, Raulund-Rasmussen K, Olsson MT, Tau-Strand L, Vesterdal L, Westman CJ (2003) Soil carbon stores in Nordic well-drained forest soils — relationships with climate and texture class. *Global Change Biology*, **9**, 358–370.

Cameron EK, Bayne EM, Clapperton MJ (2007) Human-facilitated invasion of exotic earthworms into northern boreal forests. *Ecoscience*, **14**, 482–490.

Center for International Earth Science Information Network – CIESIN – Columbia University (2017) Gridded population of the world, version 4 (GPWv4): Population density, revision 10. NASA Socioeconomic Data and Application Center (SEDAC), Palisades, NY. https://doi.org/10.7927/H4DZ068D.

Chiou CT, Lee J-F, Boyd SA (1990) The surface area of soil organic matter. *Environmental Science and Technology*, **24**, 1164–1166.

Costello DM, Tiegs SD, Lamberti GA (2011) Do non-native earthworms in Southeast Alaska use streams as invasional corridors in watersheds harvested for timber? *Biological Invasions*, **13**, 177–187.

Craven D, Thakur MP, Cameron EK *et al.* (2017) The unseen invaders: introduced earthworms as drivers of change in plant communities in North American forests (a meta- analysis). *Global Change Biology*, **23**, 1065–1074.

Crumsey JM, Le Moine JM, Capowiez Y, Goodsitt MM, Larson SC, Kling GW, Nadelhoffer KJ (2013) Community-specific impacts of exotic earthworm

invasions on soil carbon dynamics in a sandy temperate forest. *Ecology*, **94**, 2827–2837.

Crowther TW, Todd-Brown KEO, Rowe CW *et al*. (2016) Quantifying global soil carbon losses in response to warming. *Nature*, **540**, 104 –108.

Csuzdi C, Chang C-H, Pavlícek T, Szederjesi T, Esopi D, Szlávecz K (2017) Molecular phylogeny and systematics of native North American lumbricid earthworms (Clitellata: Megadrili). *PLoS ONE*, **12**, e0181504.

Davidson EA, Janssens IA (2006) Temperature sensitivity of soil carbon decomposition and feedbacks to climate change. *Nature*, **440**, 165–173.

Darwin C (1881) The formation of vegetable mould, through the action of worms, with observations on their habits. 326 pp. Murray Publishing, London, United Kingdom.

Dymond P, Scheu S, Parkinson D (1997) Density and distribution of *Dendrobaena octaedra* (Lumbricidae) in aspen and pine forests in the Canadian Rocky Mountains (Alberta). *Soil Biology and Biochemistry*, **29**, 265–273.

Egelkraut D, Aronsson KÅ, Allard A, Åkerholm M, Stark S, Olofsson J (2018a) Multiple feedbacks contribute to a centennial legacy of reindeer on tundra vegetation. Ecosystems, 1–19.

Egelkraut D, Kardol P, De Long JR, Olofsson J (2018b) The role of plant-soil feedbacks in stabilizing a reindeer-induced vegetation shift in subarctic tundra. *Functional Ecology*, **32**, 1959–1971.

Ehlers J, Gibbard PL, Hughes PD (2011) Quaternary glaciations – extent and chronology. Elsevier, Amsterdam, the Netherlands. 1126 p.

Eisenhauer N, Partsch S, Parkinson D, Scheu S (2007) Invasion of a deciduous forest by earthworms: changes in soil chemistry, microflora, microarthropods and vegetation. *Soil Biology and Biochemistry*, **39**, 1099–1110.

Eisenhauer N, Schlaghamersky J, Reich PB, Frelich LE (2011) The wave towards a new steady state: effects of earthworm invasion on soil microbial functions. *Biological Invasions*, **13**, 2191–2196.

Feller C, Brown GG, Blanchart E, Deleporte P, Chernyanskii SS (2003) Charles Darwin, earthworms, and the natural sciences: various lessons from past to future. *Agriculture, Ecosystems and Environment*, **99**, 29–49.

Filsner J, Faber JH, Tiunov AV *et al.* (2016) Soil fauna: key to new carbon models. *Soil*, **2**, 565–582.

Fisk MC, Fahey TJ, Groffman PM, Bohlen PJ (2004) Earthworm invasion, fine root distribution and soil respiration in hardwood forests. *Ecosystems*, **7**, 55–62.

Fontaine S, Barot S, Barré P, Bdioui N, Mary B, Rumpel C (2007) Stability of organic carbon in deep soil layers controlled by fresh carbon supply. *Nature*, **450**, 277–280.

Frelich LE, Hale CM, Scheu S, Holdsworth AR, Heneghan L, Bohlen PJ, Reich PB (2006) Earthworm invasion into previously earthworm-free temperate and boreal forests. *Biological Invasions*, **8**, 1235–1245.

Gabet EJ, Reichman OJ, Seabloom EW (2003) The effects of bioturbation on soil processes and sediment transport. *Annual Review of Earth and Planetary Sciences*, **31**, 249–273.

Gaillardet J, Dupré B, Louvat P, Allegre CA (1999) Global silicate weathering and CO_2 consumption rates deduced from the chemistry of large rivers. *Chemical Geology*, **159**, 3–30.

Galy V, Peucker-Ehrenbrink B, Eglinton T (2015) Global carbon export from the terrestrial biosphere controlled by erosion. *Nature*, **521**, 204–207.

Gates GE (1977) More on the earthworm genus *Diplocardia*. *Megadrilogica*, **3**, 1–48.

Gates GE (1982) Farewell to North American megadriles. *Megadrilogica*, **4**, 12–77.

Gentsch N, Wild B, Mikutta R, Čapek P, Diáková K, Schrumpf M *et al.* (2018) Temperature response of permafrost soil carbon is attenuated by mineral protection. *Global Change Biology*, **24**, 3401–3415.

Gillabel J, Cebrian–Lopez B, Six J, Merckx R (2010) Experimental evidence for the attenuating effect of SOM protection on temperature sensitivity of SOM decomposition. *Global Change Biology*, **16**, 2789–2798.

Groffman PM, Fahey TJ, Fisk MC, Yavitt JB, Sherman RE, Bohlen PJ, Maerz JC (2015) Earthworms increase soil microbial carrying capacity and nitrogen retention in northern hardwood forests. *Soil Biology and Biochemistry*, **87**, 51–58.

Gruber S (2012) Derivation and analysis of a high-resolution estimate of global permafrost zonation. *The Cryosphere*, **6**, 221–233.

Guggenberger G, Zech W, Thomas RJ (1995) Lignin and carbohydrate alteration in particle size separates of an oxisol under tropical pastures following native savanna. *Soil Biology and Biochemistry*, **27**, 1629–1638.

Gundale MJ, Jolly WM, Deluca TH (2005) Susceptibility of a northern hardwood forest to exotic earthworm invasion. *Conservation Biology*, **19**, 1075–1083.

Gunn A (1992) The use of mustard to estimate earthworm populations. *Pedobiologia*, **36**, 65–67.

Hæggström CA, Terhivuo J (1979) The Lumbricidae (Oligochaeta) in the archipelago of Åland, SW Finland. *Memoranda Societatis pro Fauna et Flora Fennica*, **55**, 17–31.

Hale CM, Reich PB, Frelich LE (2004) Allometric equations for estimation of ash-free dry mass from length measurements for selected European earthworm species (Lumbricidae) in the western Great Lakes region. *American Midland Naturalist*, **151**, 179–185.

Hale CM, Frelich LE, Reich PB (2005a) Effects of European earthworm invasion on soil characteristics in northern hardwood forests of Minnesota. *Ecosystems*, **8**, 911–927.

Hale CM, Frelich LE, Reich PB (2005b) Exotic European earthworm invasion dynamics in northern hardwood forests of Minnesota, USA. *Ecological Applications*, **15**, 848–860.

Hale CM, Frelich LE, Reich PB (2006) Changes in hardwood forest understory plant communities in response to European earthworm invasions, *Ecology*, **87**, 1637–1649.

Hale CM (2007) Earthworms of the Great Lakes Region. Kollath & Stensaas Publishing. 36 pp.

Hansen MC, Potapov PV, Moore R *et al.* (2013) High-resolution global maps of 21st century forest cover change. *Science*, **342**, 850–853.

Harden JW, Manies KL, Turetsky MR, Neff JC (2006) Effects of wildfire and permafrost on soil organic matter and soil climate in interior Alaska. *Global Change Biology*, **12**, 2391–2403.

Heister K (2014) The measurement of the specific surface area of soils by gas and polar liquid adsorption methods — limitations and potentials. *Geoderma*, **216**, 75–87.

Hendrix PF, Bohlen PJ (2002) Exotic earthworm invasions in North America: ecological and policy implications. *BioScience*, **52**, 801–811.

Hendrix PF, Callaham Jr. MA, Drake JM, Huang C, James SW, Snyder BA, Zhang W (2008) Pandora's box contained bait: the global problem of introduced earthworms. *Annual Review of Ecology, Evolution, and Systematics*, **39**, 593–613.

Hoogerkamp M, Roogar H, Eijsackers HJP (1983) Effect of earthworms on grassland on recently reclaimed polder soils in the Netherlands. In: *Earthworm Ecology: From Darwin to Vermiculture* (ed./eds Satchell JE), pp. 85–105. Springer, Dordrecht, the Netherlands.

Hugelius G, Strauss J, Zubrzycki S *et al*. (2014) Estimated stocks of circumpolar permafrost carbon with quantified uncertainty ranges and identified data gaps. *Biogeosciences*, **11**, 6573–6593.

Jackson RB, Lajtha K, Crow SE, Hugelius G, Kramer MG, Piñiero G (2017) The ecology of soil carbon: pools, vulnerabilities, and biotic and abiotic controls. *Annual Review of Ecology, Evolution, and Systematics*, **48**, 419–445.

Jaenike J, Selander RK (1979) Evolution and ecology of parthenogenesis in earthworms. *American Zoologist*, **19**, 729–737.

James SW (1998) Earthworms and earth history. In: *Earthworm ecology* (ed. Edwards CA) pp. 3–14. CRC Press, Boca Raton, Florida, USA.

Johnstone JF, Hollingsworth TN, Chapin III FS, Mack MC (2010) Changes in fire regime break the legacy lock on successional trajectories in Alaskan boreal forest. *Global Change Biology*, **16**, 1281–1295.

Jouquet P, Dauber J, Lagerlöf J, Lavelle P, Lepage M (2006) Soil invertebrates as ecosystem engineers: Intended and accidental effects on soil and feedback loops. *Applied Soil Ecology*, **32**, 153–164.

Kasischke ES, Johnstone JF (2005) Variation in postfire organic layer thickness in a black spruce forest complex in interior Alaska and its effects on soil temperature and moisture. *Canadian Journal of Forest Research*, **35**, 2164–2177.

Kleber M, Eusterhues K, Keiluweit M, Mikutta C, Mikutta R, Nico PS (2015) Mineral-organic associations: formation, properties, and relevance in soil environments. *Advances in Agronomy*, **130**, 1–140.

Knowles ME, Ross DS, Görres JH (2016) Effect of the endogeic earthworm Aporrectodea tuberculata on aggregation and carbon redistribution in uninvaded forest soil columns. *Soil Biology and Biochemistry*, **100**, 192–200.

Koven CD, Ringeval B, Friedlingstein P *et al.* (2011) Permafrost carbon-climate feedbacks accelerate global warming. *Proceedings of the National Academy of Sciences*, **108**, 14769–14774.

Koven CD, Lawrence DM, Riley WJ (2015) Permafrost carbon-climate feedback is sensitive to deep soil carbon decomposability but not deep soil nitrogen dynamics. *Proceedings of the National Academy of Sciences*, **112**, 3752–3757.

Langmaid KK (1964) Some effects of earthworm invasion in virgin podzols. *Canadian Journal of Soil Science*, **44**, 34–37.

Larson ER, Kipfmueller KF, Hale CM, Frelich LE, Reich PB (2010) Tree rings detect earthworm invasions and their effects in northern hardwood forests. *Biological Invasions*, **12**, 1053–1066.

Lavelle P, Martin A (1992) Small-scale and large-scale effects of endogeic earthworms on soil organic matter dynamics in soils of the humid tropics. *Soil Biology and Biochemistry*, **24**, 1491–1498.

Lavelle P, Bignell D, Lepage M, Wolters V, Roger P, Ineson P, Heal OW, Dhillion S (1997) Soil function in a changing world: the role of invertebrate ecosystem engineers. *European Journal of Soil Biology*, **33**, 159–193.

Lavelle P, Pashanasi B, Charpentier F, Gilot C, Rossi J-P, Derouard L, André J, Ponge J-F, Bernier N (1998) Large-scale effects of earthworms on soil organic matter and nutrient dynamics. In: *Earthworm Ecology* (ed./eds Edwards CA). pp. 103–122. St. Lucies Press, Boca Raton, Florida, USA.

Lavelle P, Charpentier F, Villenave C, Rossi J-P, Derouard L, Pashanasi B, André J, Ponge J-F, Bernier N (2004) Effects of earthworms on soil organic matter and nutrient dynamics at a landscape scale over decades. In: *Earthworm Ecology* (ed./eds Edwards CA). pp. 145–160. CRC Press, Boca Raton, Florida, USA.

Lavelle P, Decaëns T, Aubert M, Barot S, Blouin M, Bureau F, Margerie P, Mora P, Rossi J-P (2006) Soil invertebrates and ecosystem services. *European Journal of Soil Biology*, **42**, S3–S15.

Lee KE (1985) Earthworms – Their ecology and relationships with soils and land use. Academic Press, Sydney, Australia.

Lehmann J, Kleber M (2015) The contentious nature of soil organic matter. *Nature*, **528**, 60–68.

Lubbers IM, van Groenigen KJ, Fonte SJ, Six J, Brussaard L, van Groenigen JW (2013) Greenhouse-gas emissions from soils increased by earthworms. *Nature Climate Change*, **3**, 187–194.

Lubbers IM, van Groenigen KJ, Brussaard L, van Groenigen JW (2015) Reduced greenhouse gas mitigation potential of no-tillage soils through earthworm activity. *Scientific Reports*, **5**, 13787.

Lubbers IM, Pulleman MM, van Groenigen JW (2017) Can earthworms simultaneously enhance decomposition and stabilization of plant residue carbon? *Soil Biology and Biochemistry*, **105**, 12–24.

Lundström US, van Breemen N, Bain DC *et al.* (2000) Advances in understanding the podzolization process resulting from a multidisciplinary study of three coniferous forest soils in the Nordic countries. *Geoderma*, **94**, 335–353.

Lyttle A, Yoo K, Hale CM, Aufdenkampe A, Sebestyen S (2011) Carbon-mineral interactions along an earthworm invasion gradient at a sugar maple forest in northern Minnesota. *Applied Geochemistry*, **26**, S85–S88.

Lyttle AM (2013) Carbon-mineral interactions and bioturbation: an earthworm invasion chronosequence in a sugar maple forest in Northern Minnesota, MS thesis, Department of Soil, Water, and Climate, University of Minnesota, St. Paul, Minnesota, United States.

Lyttle A, Yoo K, Hale CM, Aufdenkampe A, Sebestyen SD, Resner K, Blum A (2015) Impact of exotic earthworms on organic carbon sorption on mineral surfaces and soil carbon inventories in a northern hardwood forest. *Ecosystems*, **18**, 16–29.

MacDougall AH, Avis CA, Weaver AJ (2012) Significant contributions to climate warming from the permafrost carbon feedback. *Nature Geoscience*, **5**, 719–721.

Marashi ARA, Scullion J (2003) Earthworm casts form stable aggregates in physically degraded soils. *Biology and Fertility of Soils*, **37**, 375–380.

Marhan M, Scheu S (2006) Mixing of different mineral soil layers by endogeic earthworms affects carbon and nitrogen mineralization. *Biology and Fertility of Soils*, **32**, 308–314.

Marinissen JCY, Van den Bosch F (1992) Colonization of new habitats by earthworms. *Oecologia*, **91**, 371–376.

Mayer LM, Xing B (2001) Organic matter–surface area relationships in acid soils. *Soil Science Society of America Journal*, **65**, 250–258.

Mescheryakova EN, Berman DI (2014) Cold hardiness and geographic distribution of earthworms (Oligochaeta, Lumbricidae, Moniligastridae). *Entomological Review*, **94**, 486–497.

Mikutta R, Kleber M, Torn MS, Jahn R (2006). Stabilization of soil organic matter: Association with minerals or chemical recalcitrance? *Biogeochemistry*, **77**, 25–56.

Moinet GYK, Hunt JE, Kirschbaum MUF, Morcom CP, Midwood AJ, Millard P (2018) The temperature sensitivity of soil organic matter decomposition is constrained by microbial access to substrates. *Soil Biology and Biochemistry*, **116**, 333–339.

Muldal S (1952) The chromosomes of the earthworms I. The evolution of polyploidy. *Heredity*, **6**, 55–76.

Nieminen M, Ketoja E, Mikola J, Terhivuo J, Sirén T, Nuutinen V (2011) Local land use effects and regional environmental limits on earthworm communities in Finnish arable landscapes. *Ecological Applications*, **21**, 3162–3177.

Ping CL, Jastrow JD, Jorgenson MT, Michaelson GJ, Shur YL (2015) Permafrost soils and carbon cycling. *Soil*, **1**, 147–171.

Pleasant J (2011) The paradox of plows and productivity: an agronomic comparison of cereal grain production under Iroquois hoe culture and European plow culture in the seventeenth and eighteenth centuries. *Agricultural History*, **85**, 460–492.

R Core Team (2018) R: A language and environment for statistical computing. R Foundation for Statistical Computing, Vienna, Austria.

Ramankutty N, Evan AT, Monfreda C, Foley JA (2008) Farming the planet: 1. Geographic distribution of global agricultural lands in the year 2000. *Global Biogeochemical Cycles*, **22**, GB1003.

Räty M (2004) Growth of *Lumbricus terrestris* and *Aporrectodea calignosa* in an acid forest soil, and their effects on enchytraeid populations and soil properties. *Pedobiologia*, **48**, 321–328.

Räty M, Huhta V (2004) Earthworm communities in birch stands with different origin in central Finland. *Pedobiologia*, **48**, 283–291.

Resner K, Yoo K, Hale CM, Aufdenkampe A, Sebestyen S (2011) Elemental and mineralogical changes in soils due to bioturbation along an earthworm invasion chronosequence in northern Minnesota. *Applied Geochemistry*, **26**, S127–S131.

Resner K, Yoo K, Sebestyen S, Aufdenkampe A, Hale C, Lyttle A, Blum A (2015) Invasive earthworms deplete key soil inorganic nutrients (Ca, Mg, K, and P) in a northern hardwood forest. *Ecosystems*, **18**, 89–102.

Reynolds JW (1994) The distribution of the earthworms (Oligochaeta) of Indiana: a case for the post-Quaternary introduction theory for megadrile migration in North America. *Megadrilogica*, **5**, 13–35.

Reynolds JW (1995) The distribution of earthworms (Annelida: Oligochaeta) in North America. In: *Advances in ecology and environmental sciences* (eds. Mishra PC,

Behera N, Senapati BK, Guru BC), pp. 133–153. Ashish Publishing House, New Delhi, India.

Reynolds JW (2015) A checklist of earthworms (Oligochaeta: Lumbricidae and Megascolecidae) in western and northern Canada. *Megadrilogica*, **17**, 141–156.

Roth AM, Whitfeld TJS, Lodge AG, Eisenhauer N, Frelich LE, Reich PB (2015) Invasive earthworms interact with abiotic conditions to influence the invasion of common buckthorn (*Rhamnus cathartica*). *Oecologia*, **178**, 219–230.

Saltmarsh DM, Bowser ML, Morton JM, Lang S, Shain D, Dial R (2016) Distribution and abundance of exotic earthworms within a boreal forest system in southcentral Alaska. *NeoBiota*, **28**, 67–86.

Schaetzl R.J., Johnson, D.L., Burns, S.F., and Small, T.W. (1989), Tree uprooting: review of terminology, process, and environmental implications. Can. J. For. Res, 19, 1–11.

Schmidt MWI, Torn MS, Abiven S *et al.* (2011) Persistence of soil organic matter as an ecosystem property. *Nature*, **478**, 49–56.

Schuur EAG, Bockheim J, Canadell JG *et al*. (2008) Vulnerability of permafrost carbon to climate change: Implications for the global carbon cycle. *BioScience*, **58**, 701–714.

Schuur EAG, McGuire AD, Schädel C *et al*. (2015) Climate change and the permafrost carbon feedback. *Nature*, **520**, 171–179.

Sims RW, Gerard BM (1999) Earthworms. In: *Keys and notes for the identification and study of the species* (ed./eds Barnes RSK, Crothers JH). 171 pp. FSC publications, London, United Kingdom.

Six J, Bossuyt, H, Degryze, S, Denef, K, (2004) A history on the link between (micro)aggregates, soil biota, and soil organic matter dynamics. *Soil Tillage Research*, **79**, 7–31.

Skoglund P, Malmström H, Raghavan M, Storå J, Hall P, Willerslev EM, Gilbert TP, Götherström A, Jakobsson M (2012) Origins and genetic legacy of neolithic farmers and hunter-gatherers in Europe. *Science*, **336**, 466–469.

Soil Survey Staff, (2014) Keys to Soil Taxonomy. 12th ed. USDA – Natural Resource Conservation Service, Washington, D.C.

Stendahl J, Lundin L, Nilsson T (2009) The stone and boulder content of Swedish forest soils. *Catena*, **77**, 285–291.

Svensson JS, Jeglum JK (2003) Spatio-temporal properties of tree-species belts during primary succession on rising Gulf of Bothnia coastlines. *Annales Botanici Fennici*, **40**, 265–282.

Taylor AR, Lenoir L, Vegerfors B, Persson T (2018) Ant and earthworm bioturbation in cold-temperate ecosystems. *Ecosystems*, doi:10.1007/s10021-018-0317-2.

Terhivuo J (1988) The Finnish Lumbricidae (Oligochaeta) fauna and its formation. *Annales Zoologici Fennici*, **25**, 229–247.

Terhivuo J, Saura A (2006) Dispersal and clonal diversity of North-European parthenogenetic earthworms. *Biological Invasions*, **8**, 1205–1218.

Tiunov AV, Hale CM, Holdsworth AR, Vsevolodova-Perel TS (2006) Invasion patterns of Lumbricidae into the previously earthworm-free areas of northeastern Europe and the western Great Lakes region of North America. *Biological Invasions*, **8**, 1223–1234.

Torn MS, Trumbore SE, Chadwick OA, Vitousek PM, Hendricks DM (1997) Mineral control of soil organic carbon storage and turnover. *Nature*, **389**, 170–173.

Trumbore SE, Czimczik CI (2008) An uncertain future for soil carbon. *Science*, **321**, 1455–1456.

Ulanova NG (2000) The effects of windthrow on forests at different spatial scales: a review. *Forest Ecology and Management*, **135**, 155–167.

van Geffen KG, Berg MP, Aerts R (2011) Potential macro-detritivore range expansion into the subarctic stimulates litter decomposition: a new positive feedback mechanism to climate change? *Oecologia*, **167**, 1163–1775.

Wackett AA, Yoo K, Olofsson J, Klaminder J (2018) Human-mediated introduction of geoengineering earthworms in the Fennoscandian arctic. *Biological Invasions*, **20**, 1377–1386.

Wagai R, Mayer LM, Kitayama K (2009) Nature and extent of organic coverage of soil mineral surfaces assessed by a gas sorption approach. *Geoderma*, **149**, 152–160.

Wagai R, Kishimoto-Mo AW, Yonemura S, Shirato Y, Hiradate S, Yagasaki Y (2013) Linking temperature sensitivity of soil organic matter decomposition to its molecular structure, accessibility, and microbial physiology. *Global Change Biology*, **19**, 1114–1125.

Wall DH, Bradford MA, St. John MG *et al.* (2008) Global decomposition experiment shows soil animal impacts on decomposition are climate-dependent. *Global Change Biology*, **14**, 2661–2677.

Williams EK, Fogel ML, Berhe AA, Plante AF (2018) Distinct bioenergetic signatures in particulate versus mineral-associated soil organic matter. *Geoderma*, **330**, 107–116.

Wironen M, Moore TR (2006) Exotic earthworm invasion increases soil carbon and nitrogen in an old-growth forest in southern Quebec. *Canadian Journal of Forest Research*, **36**, 845–854.

Xia L, Szlavecz K, Swan CM, Burgess JL (2011) Inter- and intra-specific interactions of *Lumbricus rubellus* (Hoffmeister, 1843) and *Octolasion lacteum* (Orley, 1881) (Lumbricidae) and the implication for C cycling. *Soil Biology and Biochemistry*, **43**, 1584–1590.

Zhang W, Hendrix PF, Dame LE, Burke RA, Wu J, Neher DA, Li J, Shao Y, Fu S (2013) Earthworms facilitate carbon sequestration through unequal amplification of carbon stabilization compared with mineralization. *Nature Communications*, **4**, 2576.

APPENDIX

Appendix A – Earthworm sampling and identification

Methods

Earthworm populations at the Ottertail site in northern Minnesota, USA were originally surveyed during four consecutive summers from 1998 – 2001 (Hale et al., 2005a, 2005b, 2006). The site was later revisited during the fall months (Sept–Oct) of 2010 – 2011 and earthworm samples were collected by liquid mustard extraction (Gunn, 1992) at the same points as the previous study (e.g. Hale *et al.,* 2005a, 2005b). Given that these surveys from 2010 – 2011 are more recent and also coincide with the soil sampling featured in this study, we only consider the 2010 – 2011 earthworm population data here. See Lyttle *et al.,* (2015) and/or Resner *et al.,* (2015) for detailed descriptions of the study site, transect design, and earthworm sampling procedure at Ottertail during the 2010 – 2011 field seasons.

We surveyed earthworm populations at a diverse array of forested plots ($N = 60$) dispersed throughout Finland during the summer (July-August) of 2015. Sites were selected on the basis of being free from recent (within ~20 years) forestry disturbance and on their proximity to the network of Finnish zoological stations. Unlike the Ottertail (see Hale *et al.,* 2005a, 2005b, 2006; Lyttle *et al.,* 2015; Resner *et al.,* 2015) and Swedish arctic (Jierpen and Kopparåsen) sites (see Wackett *et al.,* 2018), the survey sites in Finland did not target specific 'hotspots' with well-constrained land use histories where it's possible to identify and sample across the leading edge of an earthworm invasion front. Instead, they represent a random sampling across Finland that informs spatial patterns of non-native earthworm communities at the landscape scale.

At each selected Finnish survey site ($N = 60$), we excavated nine 25 x 25 x 25 cm^3 subplots ($n = 9$) in a line approximately 25 m from each other and hand-sorted the exposed organic and mineral soil to collect earthworms. We randomly selected three of the subplots for liquid mustard extraction to assess the presence of deep-burrowing anecic species, which are particularly sensitive to the mustard extraction approach (Gunn, 1992; Bartlett *et al.,* 2006). Following collection, earthworms were euthanized and stored in 70% ethanol. Species were identified by external morphology following the keys of Sims and Easton (1999) and Hale (2007). While returning for soil sampling at selected sites during summer 2016, we re-sampled earthworms in 25 x 25 cm sub-plots to check for consistency with the 2015 survey. At one of the sites (Kuhmo_k02, $n = 11$), we found earthworms that differed from the results of the 2015 survey during our re-sampling ($n = 2$), and elected to count these earthworm specimens in the total site biomass. At all other sites earthworm communities and biomass were similar to the 2015 sampling, so we chose not to quantify biomass in the additional 2016 sub-plots. Following species identification, earthworm specimens were measured and ash-free dried biomass (AFDB, g m^{-2}) was calculated using the species-specific logarithmic expressions of Hale *et al.,* (2004).

Earthworm sampling at the Jierpen and Kopparåsen sites in the Swedish arctic (Figure 2) was initially conducted during the fall (Sept) of 2016 and re-sampled during both the 2017 – 2018 summers. Both sites contain a leading earthworm invasion front, where non-native geoengineering earthworms are radiating out from a human-modified biotope (in both cases abandoned farms). Earthworms were collected from 0.07 m^2 sub-plots ($n = 1–3$) using the liquid mustard extraction (Gunn, 1992) during fall of 2016 and

by hand-sorting down to 30 cm coupled with liquid mustard extraction on 0.09 m^2 sub-plots (n = 3) during the 2017 – 2018 summer seasons. See Wackett *et al.,* (2018) for detailed descriptions of the Jierpen and Kopparåsen study sites and earthworm sampling and identification procedures.

Table AA.1. Earthworm sampling inventory recording number of sites (*N*) and replicates (*n*), GPS coordinates, and sampling dates for all (*N*=127, *n*=290) earthworm surveys conducted in 2016-2017.

Site	Vegetation type (***distance from source***)	Sub-plot replicates (n)	Latitude (°N)	Longitude (°E)	Sampling date (m/d/yy)
Natural successional gradients (Bothnian coastlines)					
Sladan 3A	Norway spruce	n=3	63.84527	20.70559	9/5/16
	Grey alder	n=3	63.84516	20.70556	9/5/16
	Litter/driftwood	n=3	63.84532	20.70545	9/5/16
Sladan 2A	Nprway spruce	n=3	63.84507	20.70598	9/7/16
	Grey alder	n=3	63.84504	20.70618	9/7/16
	Litter/driftwood	n=3	63.84486	20.70633	9/7/16
Sladan 5A	Norway spruce	n=3	63.84188	20.71898	9/27/16
	Grey alder	n=3	63.84183	20.71849	9/27/16
	Litter/driftwood	n=3	63.84190	20.71823	9/27/16
Anthropogenic successional gradients (Bothnian coastlines)					
Anthro #1	Lawn (***0 m***)	n=2	63.84427	20.71211	9/5/16
	Spruce (***9 m***)	n=2	63.84429	20.71195	9/5/16
	Spruce (***32 m***)	n=2	63.84399	20.71207	9/6/16
	Spruce (***46 m***)	n=2	63.84386	20.71205	9/6/16
	Spruce (***75 m***)	n=1	63.84361	20.71193	9/6/16
	Spruce (***111 m***)	n=1	63.84327	20.71202	9/6/16
Anthro #1	Lawn (***0 m***)	n=2	63.84427	20.71211	9/5/16
	Grey alder (***9 m***)	n=2	63.84429	20.71195	9/5/16
	Grey alder (***32 m***)	n=2	63.84399	20.71207	9/6/16
	Grey alder (***46 m***)	n=2	63.84386	20.71205	9/8/16
	Grey alder (***75 m***)	n=2	63.84361	20.71193	9/8/16
	Grey alder (***111 m***)	n=2	63.84327	20.71202	9/8/16
Anthro #2	Lawn (***0 m***)	n=2	63.83583	20.71586	9/27/16
	Spruce (***22 m***)	n=2	63.83564	20.71584	9/28/16
	Spruce (***61 m***)	n=2	63.83529	20.71576	9/28/16
	Spruce (***97 m***)	n=2	63.83497	20.71574	9/28/16
	Spruce (***133 m***)	n=1	63.83468	20.71547	9/29/16
	Spruce (***181 m***)	n=1	63.83422	20.71551	9/29/16
	Spruce (***298 m***)	n=1	63.83318	20.71529	9/29/16

Anthro #2	Lawn (***0 m***)	n=2	63.83583	20.71586	9/27/16
	Grey alder (***22 m***)	n=2	63.83564	20.71584	9/28/16
	Grey alder (***61 m***)	n=2	63.83529	20.71576	9/28/16
	Grey alder (***92 m***)	n=2	63.83502	20.71562	9/28/16
	Grey alder (***133 m***)	n=1	63.83468	20.71547	9/29/16
	Grey alder (***181 m***)	n=1	63.83422	20.71551	9/29/16
	Grey alder (***298 m***)	n=1	63.83318	20.71529	9/29/16
Anthro #2	Lawn (***0 m***)	n=2	63.83583	20.71586	9/27/17
	Driftwood (***92 m***)	n=2	63.83502	20.71562	9/29/16
	Driftwood (***133 m***)	n=1	63.83468	20.71547	9/30/16
	Driftwood (***181 m***)	n=1	63.83422	20.71551	9/30/16
	Driftwood (***298 m***)	n=1	63.83318	20.71529	9/30/16
Anthro #3	Garden (***0 m***)	n=2	63.83894	20.72381	10/4/16
	Spruce (***97 m***)	n=1	63.83888	20.72573	10/7/16
	Spruce (***224 m***)	n=1	63.83992	20.72634	10/7/16
	Spruce (***281 m***)	n=1	63.83404	20.72667	10/6/16
	Spruce (***443 m***)	n=1	63.84116	20.72451	10/6/16
	Spruce (***496 m***)	n=1	63.84158	20.72413	10/6/16
Anthro #3	Garden (***0 m***)	n=2	63.83894	20.72381	10/4/16
	Grey alder (***97 m***)	n=2	63.83888	20.72573	10/6/16
	Grey alder (***224 m***)	n=2	63.83992	20.72634	10/6/16
	Grey alder (***281 m***)	n=2	63.83404	20.72667	10/5/16
	Grey alder (***443 m***)	n=2	63.84116	20.72451	10/5/16
	Grey alder (***496 m***)	n=2	63.84158	20.72413	10/5/16
Anthro #3	Garden (***0 m***)	n=2	63.83894	20.72381	10/4/16
	Grey alder (***224 m***)	n=2	63.83992	20.72634	10/4/16
	Grey alder (***281 m***)	n=2	63.83404	20.72667	10/4/16
	Grey alder (***443 m***)	n=2	63.84116	20.72451	10/5/16
	Grey alder (***496 m***)	n=2	63.84158	20.72413	10/5/16

Padjelanta cultural soils (milking grounds)

Group 5	Milking ground	n=3	67.29961	16.71168	8/6/16
	Control	n=3	67.30055	16.71333	8/6/16
	Birch forest	n=3	67.30122	16.71465	8/6/16
Group 1	Milking ground	n=3	67.30419	16.70508	8/5/16
	Control	n=3	67.30469	16.70355	8/5/16
	Birch forest	n=3	67.30480	16.70244	8/5/16

Group 6	Milking ground	n=3	67.29717	16.71083	8/7/16
	Control	n=3	67.29678	16.71132	8/7/16
	Birch forest	n=3	67.29694	16.71286	8/7/16
Group 12	Milking ground	n=3	67.29378	16.70059	8/7/16
	Control	n=3	67.29438	16.70154	8/7/16
Arctic birch forest invasion gradients					
Staloluokta	Compost (***0 m***)	n=2	67.32459	16.69512	8/8/16
	Lawn (***6 m***)	n=2	67.32461	16.69505	8/8/16
	Birch forest (***88 m***)	n=5	67.32427	16.69696	8/8/16
Kopparåsen	Field (***0 m***)	n=2	68.43115	18.61582	9/14/16
	Field (***32 m***)	n=1	68.43092	18.61557	9/14/16
	Birch forest (***51 m***)	n=1	68.43075	18.61546	9/15/16
	Birch forest (***124 m***)	n=1	68.43017	18.61482	9/15/16
	Birch forest (***171 m***)	n=1	68.42979	18.61510	9/15/16
	Birch forest (***226 m***)	n=2	68.42933	18.61472	9/15/16
	Birch forest (***263 m***)	n=1	68.42905	18.61411	9/14/16
	Birch forest (***301 m***)	n=1	68.42871	18.61384	9/14/16
	Birch forest (***323 m***)	n=1	68.42853	18.61343	9/15/16
Jierpen (2016)	Field (***0 m***)	n=3	68.44772	18.85768	9/13/16
	Field (***20 m***)	n=2	68.44787	18.85788	9/13/16
	Field (***38 m***)	n=2	68.44801	18.85794	9/13/16
	Field (***51 m***)	n=2	68.44806	18.85826	9/17/16
	Field (***94 m***)	n=2	68.44837	18.85885	9/17/16
	Birch forest (***146 m***)	n=1	68.44879	18.85917	9/17/16
	Birch forest (***187 m***)	n=2	68.44908	18.85954	9/17/16
	Birch forest (***263 m***)	n=2	68.44961	18.86023	9/17/16
	Birch forest (***341 m***)	n=1	68.45010	18.86123	9/18/16
	Birch forest (***415 m***)	n=2	68.45025	18.86296	9/18/16
	Birch forest (***595 m***)	n=1	68.45126	18.86497	9/18/16
	Birch forest (***747 m***)	n=2	68.45196	18.86669	9/18/16
	Birch forest (***860 m***)	n=2	68.45232	18.86833	9/19/16
	Birch forest (***926 m***)	n=2	68.45250	18.8692	9/18/16
Jierpen (2017)	Field (***0 m***)	n=3	68.44772	18.85768	8/11/17
	Field (***94 m***)	n=3	68.44837	18.85885	8/11/17
	Birch forest (***187 m***)	n=3	68.44908	18.85954	8/12/17
	Birch forest (***263 m***)	n=3	68.44961	18.86023	8/12/17
	Birch forest (***341 m***)	n=3	68.45010	18.86123	8/12/17
	Birch forest (***415 m***)	n=3	68.45025	18.86296	8/12/17

	Birch forest (***595 m***)	n=3	68.45126	18.86497	8/12/17
	Birch forest (***652 m***)	n=3	68.45138	18.86587	8/13/17
	Birch forest (***747 m***)	n=3	68.45196	18.86669	8/13/17
	Birch forest (***860 m***)	n=3	68.45232	18.86833	8/13/17
	Birch forest (***926 m***)	n=3	68.45250	18.8692	8/13/17
Jierpen control (2017)	Birch forest (***0 m***)	n=3	68.44546	18.86532	8/14/17
	Birch forest (***94 m***)	n=3	68.44652	18.86574	8/16/17
	Birch forest (***187 m***)	n=3	68.44615	18.86767	8/14/17
	Birch forest (***263 m***)	n=3	68.44664	18.86923	8/14/17
	Birch forest (***341 m***)	n=3	68.44701	18.86920	8/14/17
	Birch forest (***415 m***)	n=3	68.44705	18.87162	8/15/17
	Birch forest (***595 m***)	n=3	68.44800	18.87111	8/15/17
	Birch forest (***747 m***)	n=3	68.44841	18.87340	8/15/17
	Birch forest (***860 m***)	n=3	68.44896	18.87464	8/15/17
	Birch forest (***926 m***)	n=3	68.44959	18.87639	8/16/17
Kungsleden (King's trail)	Abiskojaurestugorna	n=4	68°17'17.3"	18°35'26.1	7/19/17
	Alesjaurestugorna	n=2	68° 8'14.50"	18°25'7.02	7/20/17
	Sälkastugorna	n=2	67°56'44.6"	18°17'3.34	7/22/17
	Singistugorna	n=2	67°51'5.98"	18°18'56.0	7/25/17
	Teusajaurestugorna	n=4	67.69468	18.15676	7/27/17
	Vakkotavare	n=3	67°34'54.46	18°6'2.27"	7/28/17
Kiruna-Narvik railway	Kaisepakte ('16)	n=2	68.28593	19.30192	9/16/16
	Kaisepakte ('17)	n=4	68.28659	19.29993	8/17/17
	Stordalen	n=6	68°20'37.6"	19°4'0.01"	8/21/17
	Torneträsk	n=3	68.21792	19.70967	8/18/17
	Stenbacken	n=3	68.24851	19.50687	8/18/17
	Vassijaure	n=6	68.25738	18.25738	8/20/17

Table AA.2. Epigeic earthworm (*Dendrobaena octaedra* and *Dendrodrilus rubidus*) biomass in natural succession gradients of Svensson and Jeglum (2003)

Site name	Latitude	Longitude	Spruce	Alder	Driftwood
			(g m^{-2})	(g m^{-2})	(g m^{-2})
Sladan 3A-1	63.84516N	20.70576E	0.00	0.06	1.06
Sladan 3A-2	63.84527N	20.70559E	0.05	0.14	0.39
Sladan 3A-3	63.84453N	20.70532E	0.00	0.53	0.73
Sladan 3A average			**0.02**	**0.24**	**0.73**
Standard error			0.02	0.14	0.19
Sladan 2A-1	63.84507N	20.70598E	0.02	0.05	0.56
Sladan 2A-2	63.84500N	20.70621E	0.06	0.09	0.22
Sladan 2A-3	63.84506N	20.70616E	0.11	0.63	0.12
Sladan 2A average			**0.07**	**0.26**	**0.30**
Standard error			0.03	0.19	0.13
Sladan 5A-1 island	63.84188N	20.71898E	0.00	0.33	1.09
Sladan 5A-2 island	63.84183N	20.71849E	0.00	0.49	0.81
Sladan 5A-3 island	63.84190N	20.71823E	0.32	0.27	0.19
Sladan 5A average			**0.11**	**0.36**	**0.69**
Standard error			0.11	0.07	0.27
Compiled average			**0.06**	**0.29**	**0.57**
Compiled standard error			**0.03**	**0.07**	**0.12**

Table AA.3. Earthworm (*Dendrobaena octaedra*) biomass in Padjelanta milking grounds

Site	Latitude	Longitude	Biomass
			(g m^{-2})
Milking ground 5-1	67.29956 °N	16.71168 °E	0.68
Milking ground 5-2	67.29970 °N	16.71163 °E	0.75
Milking ground 5-3	67.29961 °N	16.71178 °E	0.13
Milking ground 5 average			**0.52**
Standard error			0.20
Milking ground 1-1	67.30419 °N	16.70508 °E	0.26
Milking ground 1-2	67.30435 °N	16.70483 °E	0.45
Milking ground 1-3	67.30409 °N	16.70493 °E	0.41
Milking ground 1 average			**0.37**
Standard error			0.06
Milking ground 6-1	67.29713 °N	16.71064 °E	0.21
Milking ground 6-2	67.29717 °N	16.71083 °E	0.43
Milking ground 6-3	67.29726 °N	16.71081 °E	0.63
Milking ground 6 average			**0.42**
Standard error			0.12
Milking ground 12-1	67.29400 °N	16.70057 °E	0.00
Milking ground 12-2	67.29381 °N	16.70126 °E	0.50
Milking ground 12-3	67.29378 °N	16.70059 °E	0.36
Milking ground 12 average			**0.29**
Standard error			0.15
Compiled average			**0.40**
Compiled standard error			**0.07**

Table AA.4. Earthworm biomass (*Dendrobaena octaedra*) in Padjelanta control tundra

Site	Latitude	Longitude	Biomass
			(g m^{-2})
Control 5-1	67.30055 °N	16.71333 °E	0.11
Control 5-2	67.30045 °N	16.71332 °E	0
Control 5-3	67.30069 °N	16.71360 °E	0
Control 5 average			**0.04**
Standard error			0.04
Control 1-1	67.30469 °N	16.70355 °E	0
Control 1-2	67.30464 °N	16.70357 °E	0
Control 1-3	67.30469 °N	16.70397 °E	0
Control 1 average			**0**
Standard error			0
Control 6-1	67.29677 °N	16.71150 °E	0
Control 6-2	67.29683 °N	16.71125 °E	0
Control 6-3	67.29678 °N	16.71132 °E	0
Control 6 average			**0**
Standard error			0
Control 12-1	67.29417 °N	16.70146 °E	0
Control 12-2	67.29438 °N	16.70154 °E	0
Control 12-3	67.29420 °N	16.70175 °E	0
Control 12 average			**0**
Standard error			0
Compiled average			**0.01**
Compiled standard error			**0.01**

Table AA.5. Earthworm biomass (*Dendrobaena octaedra*) – Padjelanta birch forest plots

Site	Latitude	Longitude	Biomass
			(g m^{-2})
Birch forest 5-1	67.30110 °N	16.71467 °E	0
Birch forest 5-2	67.30122 °N	16.71465 °E	1.17
Birch forest 5-3	67.30134 °N	16.71524 °E	0
Birch forest 5 average			**0.39**
Standard error			0.39
Birch forest 1-1	67.30490 °N	16.70244 °E	0
Birch forest 1-2	67.30494 °N	16.70233 °E	0
Birch forest 1-3	67.30472 °N	16.70245 °E	0
Birch forest 1 average			**0**
Standard error			0
Birch forest 6-1	67.29694 °N	16.71286 °E	0
Birch forest 6-2	67.29667 °N	16.71272 °E	0
Birch forest 6-3	67.29679 °N	16.71313 °E	0
Birch forest 6 average			**0**
Standard error			0
Compiled average			**0.10**
Compiled standard error			**0.10**

Table AA.6. Earthworm biomass – Staloloukta anthropogenic gradient (Padjelanta, SE)

Distance	**Latitude**	**Longitude**	***Epigeic Biomass***	***Epi-endogeic Biomass****	***Endogeic Biomass***	***Anecic Biomass***
(m)			(g m^{-2})	(g m^{-2})	(g m^{-2})	(g m^{-2})
compost (0)	67.32459 °N	16.69512 °E	0	9.68	0	0
compost (0)	67.32459 °N	16.69512 °E	0	8.72	0	5.97
0 m average			**0**	**9.20**	**0**	**2.98**
Standard error			0	0.48	0	2.98
lawn (4)	67.32461 °N	16.69505 °E	0	6.53	0.27	0
lawn (7)	67.32456 °N	16.69498 °E	0.30	4.84	2.46	5.03
5.5 m average			**0.15**	**5.69**	**1.36**	**2.52**
Standard error			0.15	0.85	1.09	2.52
Birch-1 (90)	67.32422 °N	16.69692 °E	0	0	0	0
Birch-2 (91)	67.32427 °N	16.69696 °E	0.05	0	0	0
Birch-3 (98)	67.32425 °N	16.69711 °E	0.07	0	0	0
Birch-4 (83)	67.32427 °N	16.69680 °E	0.57	0	0	0
Birch-5 (78)	67.32433 °N	16.69668 °E	0.37	0.18	0	0
88 m average			**0.21**	**0.04**	**0**	**0**
Standard error			0.11	0.04	0	0

* All *Lumbricus sp* juveniles were classified as epi-endogeic due to the greater abundance of *Lumbricus rubellus* vs. *Lumbricus terrestris* adults

Table AA.7. Earthworm biomass – Kopparåsen anthropogenic gradient (near Abisko)

Distance	**Latitude**	**Longitude**	***Epigeic Biomass***	***Epi-endogeic Biomass****	***Endogeic Biomass***	***Anecic Biomass***
(m)			(g m^{-2})	(g m^{-2})	(g m^{-2})	(g m^{-2})
barn (0)	68.43115 °N	18.61582 °E	0.22	5.33	0.52	0
barn (0)	68.43115 °N	18.61582 °E	0	1.38	0.38	0
0 m average			**0.11**	**3.36**	**0.45**	**0**
Standard error			0.11	1.97	0.07	0
32 m	68.43092 °N	18.61557 °E	**0**	**3.50**	**4.77**	**0**
51 m	68.43075 °N	18.61546 °E	**0.28**	**3.35**	**1.56**	**0**
124 m	68.43017 °N	18.61482 °E	**0.06**	**1.06**	**0.98**	**0**
171 m	68.42979 °N	18.61510 °E	**0.29**	**0.25**	**0**	**0**
226	68.42933 °N	18.61472 °E	0.03	3.17	0	0
226	68.42933 °N	18.61472 °E	0	5.21	0	0
226 m average			**0.02**	**4.19**	**0**	**0**
Standard error			0.02	1.02	0	0
263 m	68.42905 °N	18.61411 °E	**0.29**	**0**	**0**	**0**
301 m	68.42871 °N	18.61384 °E	**0.06**	**0**	**0**	**0**
323 m	68.42853 °N	18.61343 °E	**0.19**	**0**	**0**	**0**

***** All *Lumbricus sp* juveniles were classified as epi-endogeic due to the absence of *Lumbricus terrestris* adults

Table AA.8. Earthworm biomass – Jierpen anthropogenic gradient (near Abisko, SE)

Distance	**Latitude**	**Longitude**	***Epigeic Biomass***	***Epi-endogeic Biomass***	***Endogeic Biomass***	***Anecic Biomass***
(m)			(g m^{-2})	(g m^{-2})	(g m^{-2})	(g m^{-2})
barn (0)	68.44772 °N	18.85768 °E	0	5.50	3.39	0
barn (0)	68.44772 °N	18.85768 °E	0	1.97	2.49	0
barn (0)	68.44772 °N	18.85768 °E	0	4.73	3.93	0
0 m average			**0**	**4.07**	**3.27**	**0**
Standard error			0	1.07	0.42	0
20	68.44787 °N	18.85788 °E	0	1.90	3.39	0
20	68.44787 °N	18.85788 °E	0	4.55	0.41	0
20 m average			**0**	**3.23**	**1.90**	**0**
Standard error			0	1.33	1.49	0
38	68.44801 °N	18.85794 °E	0	2.90	2.31	0
38	68.44801 °N	18.85794 °E	0	1.93	1.79	0
38 m average			**0**	**2.41**	**2.05**	**0**
Standard error			0	0.49	0.26	0
51	68.44806 °N	18.85826 °E	0	5.58	5.31	0
51	68.44806 °N	18.85826 °E	0	3.64	4.15	0
51 m average			**0**	**4.61**	**4.73**	**0**
Standard error			0	0.97	0.58	0
94	68.44837 °N	18.85885 °E	0	2.44	5.42	0
94	68.44837 °N	18.85885 °E	0	2.67	3.82	0
94 m average			**0**	**2.56**	**4.62**	**0**
Standard error			0	0.11	0.80	0
146 m	68.44879 °N	18.85917 °E	**0**	**0.86**	**2.44**	**0**
187	68.44908 °N	18.85954 °E	0	4.53	4.12	0
187	68.44908 °N	18.85954 °E	0	4.59	2.23	0
187 m average			**0**	**4.56**	**3.17**	**0**
Standard error			0	0.03	0.94	0
263	68.44961 °N	18.86023 °E	0	2.01	4.69	0
263	68.44961 °N	18.86023 °E	0	4.59	6.52	0
263 m average			**0**	**3.30**	**5.61**	**0**

Standard error			0	1.29	0.91	0
S1.7 (cont).						
341 m	68.45010 °N	18.86123 °E	**0**	**2.19**	**0.32**	**0**
415	68.45025 °N	18.86296 °E	0.48	1.03	0	0
415	68.45025 °N	18.86296 °E	0.31	0	0	0
415 m average			**0.40**	**0.52**	**0**	**0**
Standard error			0.09	0.52	0	0
595 m	68.45126 °N	18.86497 °E	**0.03**	**0.23**	**0**	**0**
747	68.45196 °N	18.86669 °E	0.20	0	0	0
747	68.45196 °N	18.86669 °E	0.54	0.98	0	0
747 m average			**0.37**	**0.49**	**0**	**0**
Standard error			0.17	0.49	0	0
860	68.45232 °N	18.86833 °E	0	0	0	0
860	68.45232 °N	18.86833 °E	0.06	0	0	0
860 m average			**0.03**	**0.00**	**0**	**0**
Standard error			0.03	0.00	0	0
926	68.45250 °N	18.86920 °E	0	0.12	0	0
926	68.45250 °N	18.86920 °E	0	0	0	0
926 m average			**0.00**	**0.06**	**0**	**0**
Standard error			0.00	0.06	0	0

Table AA.9. Earthworm biomass in spruce (*Picea abies*) vegetation zone for anthropogenic gradient #1 on the Bay of Ostnas

Distance	**Latitude**	**Longitude**	***Epigeic Biomass***	***Epi-endogeic Biomass***	***Endogeic Biomass***	***Anecic Biomass***
(m)			(g m^{-2})	(g m^{-2})	(g m^{-2})	(g m^{-2})
lawn (0)	63.84427 °N	20.71211 °E	0.22	3.12	1.03	0
lawn (0)	63.84427 °N	20.71211 °E	0.12	6.24	0.72	0
lawn average			**0.17**	**4.68**	**0.88**	**0**
Standard error			0.05	1.56	0.15	0
9	63.84429 °N	20.71195 °E	0.10	0.49	0	0
9	63.84429 °N	20.71195 °E	0	1.13	0	0
9 m average			**0.05**	**0.81**	**0**	**0**
Standard error			0.05	0.32	0	0
32	63.84399 °N	20.71207 °E	0.40	0	0	0
32	63.84399 °N	20.71207 °E	0.14	1.74	0	0
32 m average			**0.27**	**0.87**	**0**	**0**
Standard error			0.13	0.87	0	0
46	63.84386 °N	20.71205 °E	0.05	0	0	0
46	63.84386 °N	20.71205 °E	0	0	0	0
46 m average			**0.03**	**0**	**0**	**0**
Standard error			0.03	0	0	0
75 m	63.84361 °N	20.71193 °E	**0**	**0**	**0**	**0**
111 m	63.84327 °N	20.71202 °E	**0.11**	**0.0**	**0.0**	**0**

Table AA.10. Earthworm biomass in grey alder (*Alnus incana*) zone for anthropogenic gradient #1 on the Bay of Ostnas

Distance	**Latitude**	**Longitude**	***Epigeic Biomass***	***Epi-endogeic Biomass***	***Endogeic Biomass***	***Anecic Biomass***
(m)			(g m^{-2})	(g m^{-2})	(g m^{-2})	(g m^{-2})
lawn (0)	63.84427 °N	20.71211 °E	0.13	1.71	4.25	0
lawn (0)	63.84427 °N	20.71211 °E	0.04	2.70	1.16	3.80
lawn average			**0.08**	**2.21**	**2.70**	**1.90**
Standard error			0.05	0.50	1.55	1.90
9	63.84429 °N	20.71195 °E	0.10	1.69	2.74	0
9	63.84429 °N	20.71195 °E	0.46	0.94	0	0
9 m average			**0.28**	**1.32**	**1.37**	**0**
Standard error			0.18	0.38	1.37	0
32	63.84399 °N	20.71207 °E	0.06	1.11	0	0
32	63.84399 °N	20.71207 °E	0.03	0.28	0	0
32 m average			**0.04**	**0.70**	**0**	**0**
Standard error			0.02	0.42	0	0
46	63.84386 °N	20.71205 °E	0.24	2.59	0	0
46	63.84386 °N	20.71205 °E	0.12	0.39	0	0
46 m average			**0.18**	**1.49**	**0**	**0**
Standard error			0.06	1.10	0	0
75	63.84361 °N	20.71193 °E	0.12	1.20	0	0
75	63.84361 °N	20.71193 °E	0.08	3.14	0	0
75 m average			**0.10**	**2.17**	**0**	**0**
Standard error			0.02	0.97	0	0
111	63.84327 °N	20.71202 °E	0.09	0	0	0
111	63.84327 °N	20.71202 °E	0.27	0	0	0
111 m average			**0.18**	**0**	**0**	**0**
Standard error			0.09	0	0	0

Table AA.11. Earthworm biomass in spruce (*Picea abies*) vegetation zone for anthropogenic gradient #2 on the Bay of Ostnas

Distance	**Latitude**	**Longitude**	***Epigeic Biomass***	***Epi-endogeic Biomass***	***Endogeic Biomass***	***Anecic Biomass***
(m)			(g m^{-2})	(g m^{-2})	(g m^{-2})	(g m^{-2})
lawn (0)	63.83583 °N	20.71586 °E	1.22	5.05	2.34	11.12
lawn (0)	63.83583 °N	20.71586 °E	2.16	3.49	2.58	4.19
lawn average			**1.69**	**4.27**	**2.46**	**7.65**
Standard error			0.47	0.78	0.12	3.47
22	63.83564 °N	20.71584 °E	0.07	1.78	0	0
22	63.83564 °N	20.71584 °E	0.22	0.54	0	0
22 m average			**0.14**	**1.16**	**0**	**0**
Standard error			0.07	0.62	0	0
61	63.83529 °N	20.71576 °E	0.21	0	0	0
61	63.83529 °N	20.71576 °E	0	0	0	0
61 m average			**0.10**	**0**	**0**	**0**
Standard error			0.10	0	0	0
97	63.83497 °N	20.71574 °E	0	0	0	0
97	63.83497 °N	20.71574 °E	0	0	0	0
97 m average			**0.00**	**0**	**0**	**0**
Standard error			0.00	0	0	0
133 m	63.83468 °N	20.71547 °E	**0.58**	**0**	**0**	**0**
181 m	63.83422 °N	20.71551 °E	**0**	**0**	**0**	**0**
298 m	63.83318 °N	20.71529 °E	**0.09**	**0**	**0**	**0**

Table AA.12. Earthworm biomass in grey alder (*Alnus incana*) vegetation zone for anthropogenic gradient #2 on the Bay of Ostnas

Distance	**Latitude**	**Longitude**	***Epigeic Biomass***	***Epi-endogeic Biomass***	***Endogeic Biomass***	***Anecic Biomass***
(m)			(g m^{-2})	(g m^{-2})	(g m^{-2})	(g m^{-2})
lawn (0)	63.83583 °N	20.71586 °E	0.42	3.43	0.54	6.60
lawn (0)	63.83583 °N	20.71586 °E	0.61	2.20	0.32	0.00
lawn average			**0.52**	**2.82**	**0.43**	**3.30**
Standard error			0.10	0.62	0.11	3.30
22	63.83564 °N	20.71584 °E	0.07	1.46	0	0
22	63.83564 °N	20.71584 °E	0.08	3.41	0	0
22 m average			**0.07**	**2.43**	**0**	**0**
Standard error			0.01	0.97	0	0
61	63.83529 °N	20.71576 °E	0.51	3.64	0.44	0
61	63.83529 °N	20.71576 °E	0.22	0.78	0	0
61 m average			**0.36**	**2.21**	**0.22**	**0**
Standard error			0.15	1.43	0.22	0
92	63.83502 °N	20.71562 °E	0.21	3.04	0	0
92	63.83502 °N	20.71562 °E	0.48	3.79	0	0
92 m average			**0.35**	**3.42**	**0**	**0**
Standard error			0.13	0.37	0	0
133 m	63.83468 °N	20.71547 °E	**0.05**	**0**	**0**	**0**
181 m	63.83422 °N	20.71551 °E	**0.27**	**0**	**0**	**0**
298 m	63.83318 °N	20.71529 °E	**0.75**	**0.49**	**0**	**0**

Table AA.13. Earthworm biomass in driftwood zone for anthropogenic gradient #2 on the Bay of Ostnas

Distance	**Latitude**	**Longitude**	***Epigeic Biomass***	***Epi-endogeic Biomass***	***Endogeic Biomass***	***Anecic Biomass***
(m)			(g m^{-2})	(g m^{-2})	(g m^{-2})	(g m^{-2})
92	63.83502 °N	20.71562 °E	0.19	1.64	0	0
92	63.83502 °N	20.71562 °E	0.35	3.82	0	0
92 m average			**0.27**	**2.73**	**0**	**0**
Standard error			0.08	1.09	0	0
133	63.83468 °N	20.71547 °E	0.22	4.37	0	0
133	63.83468 °N	20.71547 °E	0.39	3.02	0	0
133 m average			**0.30**	**3.70**	**0**	**0**
Standard error			0.09	0.67	0	0
181	63.83422 °N	20.71551 °E	0.12	3.80	0	0
181	63.83422 °N	20.71551 °E	0.39	0.25	0	0
181 m average			**0.26**	**2.03**	**0**	**0**
Standard error			0.14	1.77	0	0
298	63.83318 °N	20.71529 °E	0.41	5.32	0	0
298	63.83318 °N	20.71529 °E	0.21	0.00	0	0
298 m average			**0.31**	**2.66**	**0**	**0**
Standard error			0.10	2.66	0	0

Table AA.14. Earthworm biomass in spruce (*Picea abies*) vegetation zone for anthropogenic gradient #3 on the semi-enclosed Bay of Sönnerstgrundsfarden

Distance	**Latitude**	**Longitude**	***Epigeic Biomass***	***Epi-endogeic Biomass***	***Endogeic Biomass***	***Anecic Biomass***
(m)			(g m^{-2})	(g m^{-2})	(g m^{-2})	(g m^{-2})
Garden (0)	63.83894 °N	20.72381 °E	1.31	5.61	0	0
Garden (0)	63.83894 °N	20.72381 °E	0.19	1.96	0	0
0 m average			**0.75**	**3.79**	**0**	**0**
Standard error			0.56	1.82	0	0
97 m	63.83888 °N	20.72573 °E	**0**	**0**	**0**	**0**
224 m	63.83992 °N	20.72634 °E	**0.15**	**0**	**0**	**0**
281 m	63.83404 °N	20.72667 °E	**0.06**	**0**	**0**	**0**
443 m	63.84116 °N	20.72451 °E	**0.11**	**0**	**0**	**0**
496 m	63.84158 °N	20.72413 °E	**0**	**0**	**0**	**0**

Table AA.15. Earthworm biomass in grey alder (*Alnus incana*) vegetation zone for anthropogenic gradient #3 on the semi-enclosed Bay of Sönnerstgrundsfarden

Distance	**Latitude**	**Longitude**	***Epigeic***	***Epi-endogeic***	***Endogeic***	***Anecic***
			Biomass	***Biomass***	***Biomass***	***Biomass***
(m)			(g m^{-2})	(g m^{-2})	(g m^{-2})	(g m^{-2})
Garden (0)	63.83894 °N	20.72381 °E	1.31	5.61	0	0
Garden (0)	63.83894 °N	20.72381 °E	0.19	1.96	0	0
0 m average			**0.75**	**3.79**	**0**	**0**
Standard error			0.56	1.82	0	0
97	63.83888 °N	20.72573 °E	0.48	3.17	0	0
97	63.83888 °N	20.72573 °E	0.03	6.99	0	0
97 m average			**0.25**	**5.08**	**0**	**0**
Standard error			0.22	1.91	0	0
224	63.83992 °N	20.72634 °E	0.17	2.10	0	0
224	63.83992 °N	20.72634 °E	0.11	1.48	0	0
224 m average			**0.14**	**1.79**	**0**	**0**
Standard error			0.03	0.31	0	0
281	63.83404 °N	20.72667 °E	0.06	2.87	0	0
281	63.83404 °N	20.72667 °E	0.55	5.45	0	0
281 m average			**0.31**	**4.16**	**0**	**0**
Standard error			0.24	1.29	0	0
443	63.84116 °N	20.72451 °E	0.10	0.00	0	0
443	63.84116 °N	20.72451 °E	0.12	2.35	0	0
443 m average			**0.11**	**1.18**	**0**	**0**
Standard error			0.01	1.18	0	0
496	63.84116 °N	20.72451 °E	0.44	0.30	0	0
496	63.84116 °N	20.72451 °E	0.09	0.00	0	0
496 m average			**0.26**	**0.15**	**0**	**0**
Standard error			0.17	0.15	0	0

Table AA.16. Earthworm biomass in driftwood zone for anthropogenic gradient #3 on the semi-enclosed Bay of Sönnerstgrundsfarden

Distance	**Latitude**	**Longitude**	***Epigeic***	***Epi-endogeic***	***Endogeic***	***Anecic***
			Biomass	***Biomass***	***Biomass***	***Biomass***
(m)			(g m^{-2})	(g m^{-2})	(g m^{-2})	(g m^{-2})
224	63.83992 °N	20.72634 °E	0.07	2.18	0	0
224	63.83992 °N	20.72634 °E	0.76	4.85	0	0
224 m average			**0.41**	**3.52**	**0**	**0**
Standard error			0.34	1.33	0	0
281	63.83404 °N	20.72667 °E	0.26	2.69	0	0
281	63.83404 °N	20.72667 °E	0.41	6.92	0	0
281 m average			**0.33**	**4.80**	**0**	**0**
Standard error			0.08	2.12	0	0
443	63.84116 °N	20.72451 °E	0.48	4.80	0	0
443	63.84116 °N	20.72451 °E	0.57	0.96	0	0
443 m average			**0.53**	**2.88**	**0**	**0**
Standard error			0.05	1.92	0	0
496	63.84116 °N	20.72451 °E	0.93	0.30	0	0
496	63.84116 °N	20.72451 °E	0.54	0.98	0	0
496 m average			**0.74**	**0.64**	**0**	**0**
Standard error			0.20	0.34	0	0

Appendix B – Soil sampling and morphological descriptions

Methods

We excavated soil pits to variable depths at selected sites within each of the northern forest biome (arctic, boreal, and temperate) types. At the Ottertail (temperate) and the Swedish arctic sites, we placed soil pits at strategic positions behind (invaded) or in front of (pre- or early-invasion) the leading edge of the identified earthworm invasion front to isolate variations in earthworm density and community structure without altering other soil state factors like climate, parent material, or vegetation. Pits at these locations therefore capture the transformation from natural 'pre-invasion' soils to the earthworm-invaded soil regime at a local scale.

Six large (1.5 x 1.5 x 1.5 m) pits were excavated at various positions representing different stages of earthworm invasion along the ~200 m transect through temperate hardwood forest at the Ottertail site in northern Minnesota, USA during Fall 2009. Soil and bulk density samples were collected laterally from the exposed profiles at pre-determined depth intervals. Bulk density samples were collected using a sliding hammer corer and were dried at 105 ºC and weighed in the laboratory. Coarse fragments (>2 mm) were sieved in the laboratory and weighed to determined soil rock contents. See Lyttle *et al.*, (2015) and Resner *et al.*, (2015) for details regarding soil sampling and laboratory methods pertaining to Ottertail.

We opened four 1 x 1 m soil pits at various positions along the Jierpen invasion gradient (Wackett *et al.,* 2018) near Abisko, Sweden during fall of 2016. The pits include an invaded (all geoengineering species present, JW_1) endmember, an intermediate stage (only *Lumbricus rubellus* present, JDI_2), and two geoengineering earthworm-free control pits (only small epigeic species such as *Dendrobaena octaedra* and *Dendrodrilus rubidus* present, JNW_3 and JCNW_4). All pedon descriptions are available in Appendix 2 (Tables AB.1 – AB.4). We collected soils laterally by depth interval and horizon beginning at the base of the pit. Bulk density cores (diameter 3 cm; length 15 cm) were collected by horizon (n = 3), dried, and weighed in the laboratory. For the intermediate and pre-invasion pits, we cut squares (usually 10 x 10 cm) out of the humus with a sharpened blade to determine the bulk density of the O-horizon(s). Surface leaf litter samples were taken from select pits. We collected roughly 200 kg of each O-horizon sample and 1 kg of each mineral horizon soil and sieved to 2 mm in the lab to determine coarse fragment contents in order to account for stoniness in our estimates of organic carbon and nitrogen stocks, since Fennoscandian forest soils are often extremely rocky (Stendahl *et al.,* 2009). In addition to the soil pits, we measured humus thickness (n = 10) with a hand-held soil corer at each earthworm sampling location.

At Kopparåsen we excavated two pits (one invaded, KW_1; one early-invasion, KNW_3) along the ~300 m invasion front during Fall 2016. Because of the rockiness of the Cr horizons, our pits were shallow by necessity (invaded to 30 cm depth, pre-invaded to 25 cm). We again collected soils laterally by depth interval and horizon, and sampled bulk density horizontally by horizon (n = 3) following the same method described previously. Pedon descriptions for the Kopparåsen profiles are available in Appendix 2 (Tables AB.5 – AB.6). We also measured humus thickness (n = 10) with a small soil corer within a 1 m radius of each earthworm sampling subplot along the transect.

We selected sites for additional soil sampling during August 2016 based on the results from our extensive survey (N = 60) of Finnish earthworm communities the previous summer. We chose sites that had earthworm invaded and earthworm-free localities in close proximity to minimize variations in other soil forming factors. We also selected sites to span a range of climates (latitudinal gradient) and soil parent materials (specifically different texture classes). Our identification of sites matching this criteria also tended to select for mixed-wood environments with some deciduous litter (typically birch, aspen, or alder), consistent with previous studies of non-native earthworm distributions in boreal forests reporting an association between earthworm invasions and mixed-wood boreal stands (Tiunov *et al.,* 2006; Cameron *et al.,* 2007; Addison, 2009).

Within this framework, we identified 12 sites (N = 6 invaded; N = 6 pre- or early-invasion) for detailed soil sampling. One pre-invasion site (Tvärminne_627; Table AB.18) was later dropped because the site was situated on a drained peatland and contained a Histosol (O-horizon thickness = 53 cm). At all of the remaining sites (N = 11), 1 x 1 m soil pits were excavated to 20 – 30 cm below the top of the C-horizon (where signs of pedogenesis disappeared). Soils were collected laterally by horizon and depth interval (fining upwards). We also took surface litter samples from select pits. Bulk density cores were collected by horizon (n = 1–3) according to the same procedures outlined above. Coarse fragments were similarly determined by sieving to <2 mm in the laboratory. No additional humus thickness measurements were taken during sampling of Finnish soils; instead, humus thickness is defined by the average O-horizon thickness identified within the exposed soil profiles.

Figure AB.1. a Soil profile photo for the JW_1 (Jierpen heavily invaded) pit with horizons marked and **b** representative vegetation at JW_1.

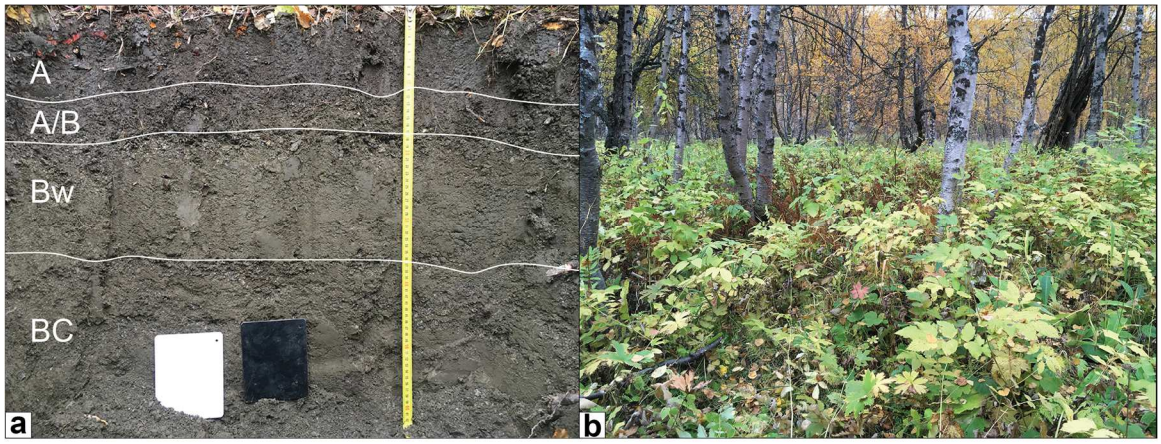

Pit: JW_1 – (Heavily invaded)

Site: Jierpen farm

Earthworm assemblage: Endogeic – *Aporrectodea calignosa*, *Aporrectodea tuberculata*, *Aporrectodea trapezoides*, *Aporrectodea rosea*; Epi-endogeic – *Lumbricus rubellus*; Epigeic – *Dendrobaena octaedra*, *Bimastos rubidus*

Location: 68.44908 °N; 18.85954 °E

Sampling date: 9/18/16

Table AB.1. Pedon description and physiochemical data for the Jierpen invaded (JW_1) soil profile near Abisko, SE (photo above)

Horizon	Depth	Color (field)	Structure	%C	%N	CF (%)	BD (g/cm^3)	$SSA_{occluded}$ (m^2/g)
A	0-10	7.5YR2.5/1	3[a], m to c[b], g[c]	6.2	0.42	3	0.65±0.12	8.7 ± 0.9
AB	10-18	7.5YR 3/1	3, m to c, g	3.9	0.30	6	0.94±0.05	6.0 ± 2.6
Bw	18-35	10YR 4/1	2, f to m, g	0.92	0.06	5	1.1 ± 0.1	3.56
BC	35-63	10YR 4/1	1, sbk	0.79	0.08	15	1.3 ± 0.3	2.74

[a] Structure grade: 0, structureless; 1, weak; 2, moderate; 3, strong
[b] Structure size: f, fine; m, medium; c, coarse
[c] Structure type: g, granular; sgl, single grain; sbk, subangular blocky; pl, platy; m, massive

Figure AB.2. a Soil profile photo for the JDI_2 (Jierpen intermediate invaded) pit with horizons marked and **b** representative vegetation at the JDI_2 site

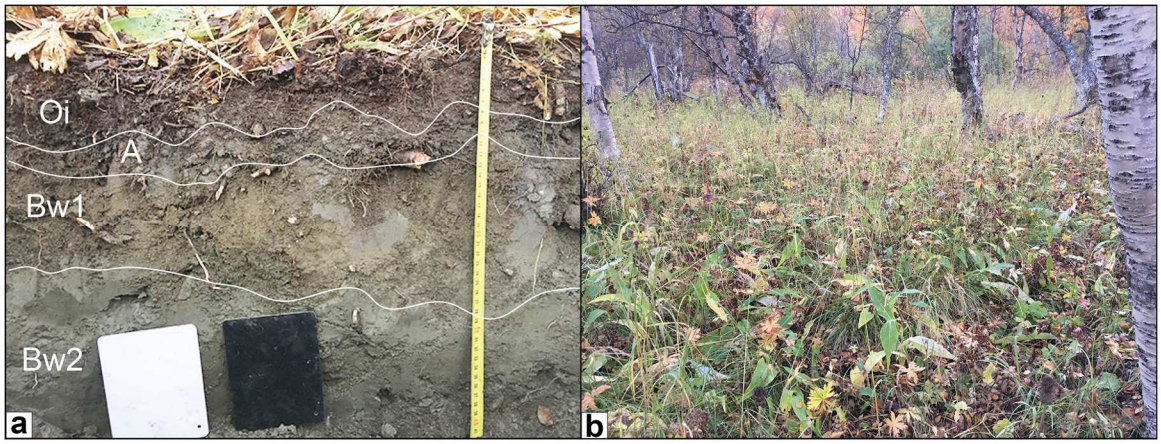

Pit: JDI_2 – (Intermediate invasion, *Lumbricus rubellus* only)

Site: Jierpen farm

Earthworm assemblage: Epi-endogeic – *Lumbricus rubellus*; Epigeic – *Dendrobaena octaedra*, *Bimastos rubidus*

Location: 68.44819 °N; 18.85611 °E

Sampling date: 9/19/16

Table AB.2. Pedon description and physiochemical data for the Jierpen intermediate invasion (JDI_2) soil profile near Abisko, SE

Horizon	Depth	Color (field)	Structure	%C	%N	CF (%)	BD (g/cm^3)	$SSA_{occluded}$ (m^2/g)
Oi/Oe	0-5	5YR2.5/1	fibric/hemic[a]	18.0	1.00	5	0.11±0.02	–[e]
A	5-10	7.5YR 3/1	2[b], m[c], gr[d]	3.8	0.27	10	0.87±0.12	6.5 ± 2.6
Bw1	10-21	7.5YR 4/1	1, f to m, sbk	0.79	0.07	19	1.42±0.08	1.4 ± 0.3
Bw2	21-42	7.5YR 4/1	2, m to c, sbk	0.46	0.01	11	1.6 ± 0.1	0.41

[a] Fibric (Oi), hemic (Oe), and sapric (Oa) designations used for organic horizons/soils
[b] Structure grade: 0, structureless; 1, weak; 2, moderate; 3, strong
[c] Structure size: f, fine; m, medium; c, coarse
[d] Structure type: gr, granular; sgl, single grain; sbk, subangular blocky; pl, platy; m, massive
[e] Mineral SSA values ($SSA_{occluded}$) were not determined for organic horizons

Figure AB.3. a Soil profile photo for the JNW_3 (Jierpen Pre-invasion) pit with horizons marked and **b** representative vegetation at JNW_3

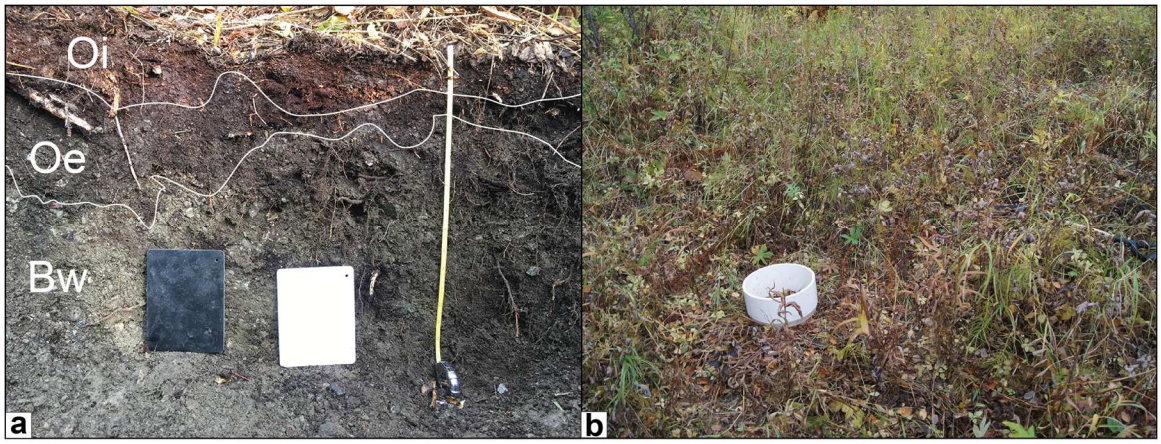

Pit: JNW_3 – (Pre-invasion, *Dendrobaena octaedra* only)

Site: Jierpen farm

Earthworm assemblage: Epigeic – *Dendrobaena octaedra*

Location: 68.45232 °N; 18.86833 °E

Sampling date: 9/17/16

Table AB.3. Pedon description and physiochemical data for the Jierpen Pre-invasion (JNW_3) soil profile near Abisko, SE

Horizon	Depth	Color (field)	Structure	%C	%N	CF (%)	BD (g/cm^3)	$SSA_{occluded}$ (m^2/g)
Oi	0-6	5YR 2.5/2	fibric/hemic[a]	43.0	3.09	6	0.10±0.02	–[d]
Oe/Oa	6-13	5YR 2.5/1	hemic/sapric	33.7	2.37	10	0.22±0.12	–
Bw	13-51	10YR 4/1	0 to 1[b], sgl[c]	1.7	0.13	43	1.2±0.1	3.7 ± 1.8

[a] Fibric (Oi), hemic (Oe), and sapric (Oa) designations used for organic horizons/soils
[b] Structure grade: 0, structureless; 1, weak; 2, moderate; 3, strong
[c] Structure type: sgl, single grain
[d] Mineral SSA values ($SSA_{occluded}$) were not determined for organic horizons

Figure AB.4. a Soil upper profile (to ~40 cm) photo for the JCNW_4 (Jierpen Shoreline Pre-invasion) pit with horizons marked and **b** representative vegetation at JCNW_4

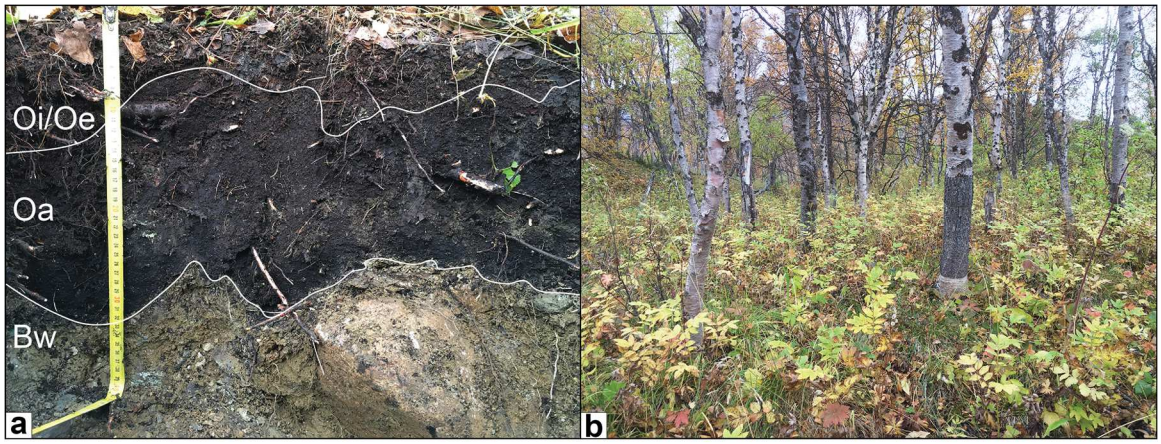

Pit: JCNW_4 – (Shoreline Pre-invasion, *Dendrobaena octaedra* only)

Site: Jierpen farm

Earthworm assemblage: Epigeic – *Dendrobaena octaedra*

Location: 68.44706 °N; 18.86072 °E

Sampling date: 9/19/16

Table AB.4. Pedon description and physiochemical data for the Jierpen Shoreline Pre-invasion (JCNW_4) soil profile near Abisko, SE

Horizon	Depth	Color (field)	Structure	%C	%N	CF (%)	BD (g/cm^3)	$SSA_{occluded}$ (m^2/g)
Oi/Oe	0-7	5YR 2.5/1	fibric/hemic[a]	40.4	2.16	4	0.12±0.03	–[d]
Oa	7-27	2.5YR2.5/0	sapric	30.6	2.14	9	0.26±0.05	–
Bw	27-41	10YR 4/3	0 to 1[b], sgl[c]	0.91	0.07	54	1.6 ± 0.2	1.35

[a] Fibric (Oi), hemic (Oe), and sapric (Oa) designations used for organic horizons/soils
[b] Structure grade: 0, structureless; 1, weak; 2, moderate; 3, strong
[c] Structure type: sgl, single grain
[d] Mineral SSA values ($SSA_{occluded}$) were not determined for organic horizons

Figure AB.5. a Soil upper profile (to ~25 cm) photo for the KW_1 (Kopparåsen heavily invaded) pit with horizons marked and **b** representative vegetation at KW_1

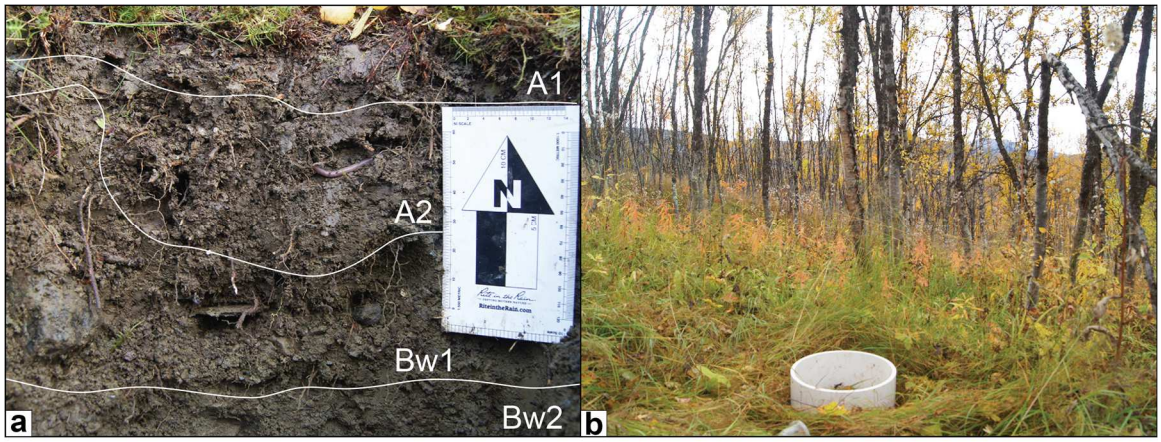

Pit: KW_1 – (Heavily invaded)

Site: Kopparåsen farm

Earthworm assemblage: Endogeic – *Aporrectodea caliginosa*, *Aporrectodea tuberculata*, *Aporrectodea rosea*; Epi-endogeic – *Lumbricus rubellus*; Epigeic – *Dendrobaena octaedra*, *Bimastos rubidus*

Location: 68.43075 °N; 18.61546 °E

Sampling date: 9/14/16

Table AB.5. Pedon description and physiochemical data for the Kopparåsen heavily invaded (KW_1) soil profile near Riksgränsen, SE

Horizon	Depth	Color (field)	Structure	%C	%N	CF (%)	BD (g/cm^3)	$SSA_{occluded}$ (m^2/g)
A1	0-4	10YR 3/2	3[a], f to c[b], gr[c]	5.3	0.25	21	0.59±0.13	6.3 ± 0.6
A2	4-11	10YR 4/2	2, f to m, gr	4.5	0.21	38	0.88±0.13	6.5 ± 1.1
Bw1	11-21	10YR 4/3	1, f to m, gr	1.1	0.09	29	1.07±0.09	1.9 ± 0.9
Bw2	21-30	2.5Y 4/4	2, m to c, sbk	0.88	0.07	39	1.2 ± 0.1	1.65

[a] Structure grade: 0, structureless; 1, weak; 2, moderate; 3, strong
[b] Structure size: f, fine; m, medium; c, coarse
[c] Structure type: gr, granular; sgl, single grain; sbk, subangular blocky; pl, platy; m, massive

Figure AB.6. a Soil upper profile (to ~25 cm) photo for the KW_3 (Kopparåsen Pre-Invasion, KW_3) pit with horizons marked and **b** representative vegetation at KW_3

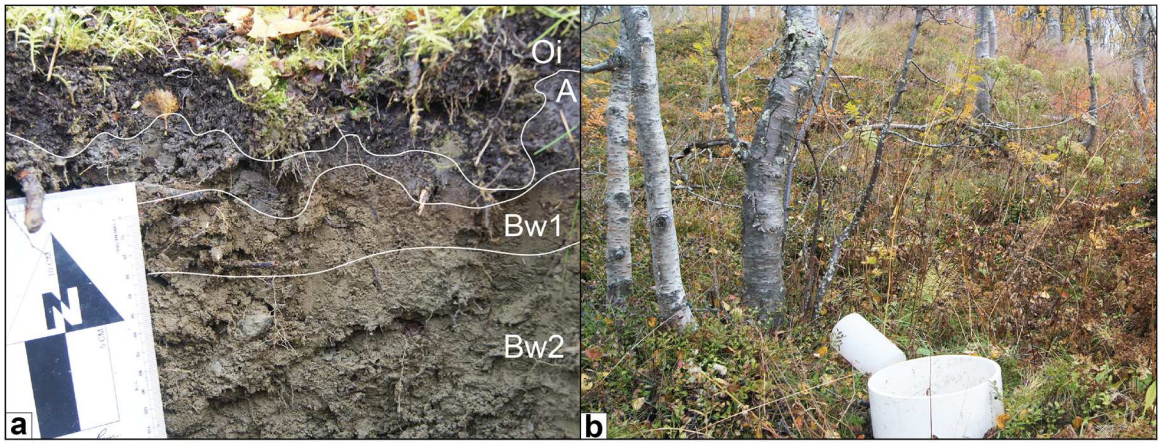

Pit: KW_3 – (Pre-invasion)

Site: Kopparåsen farm

Earthworm assemblage: Epigeic – *Dendrobaena octaedra*, *Bimastos rubidus*

Location: 68.42853 °N; 18.61343 °E

Sampling date: 9/15/16

Table AB.6. Pedon description and physiochemical data for the Kopparåsen Pre-invasion (KW_3) soil profile near Riksgränsen, SE

Horizon	Depth	Color (field)	Structure	%C	%N	CF (%)	BD (g/cm^3)	$SSA_{occluded}$ (m^2/g)
Oi	0-7	5YR 2.5/1	fibric [a]	13.1	0.66	18	0.10±0.04	– [e]
A	7-9	2.5Y 5/0	0 to 1[b], sgl [c]	4.3	0.23	16	0.7 ± 0.1	5.1 ± 2.2
Bw1	9-14	5YR 4/3	1, f to m[d], sbk	2.5	0.11	27	0.99±0.08	1.4 ± 0.8
Bw2	14-25	2.5Y 4/4	2, f to c, sbk	0.89	0.07	15	1.3 ± 0.1	0.30 ± 0.26

[a] Fibric (Oi), hemic (Oe), and sapric (Oa) designations used for organic horizons/soils
[b] Structure grade: 0, structureless; 1, weak; 2, moderate; 3, strong
[c] Structure type: gr, granular; sgl, single grain; sbk, subangular blocky; pl, platy; m, massive
[d] Structure size: f, fine; m, medium; c, coarse
[e] Mineral SSA values ($SSA_{occluded}$) were not determined for organic horizons

Figure AB.7. a Soil profile photo for Kuhmo heavily invaded (Kuhmo_176, KW_176) pit with horizons marked **b** representative vegetation w/ adjacent human-made stone pile

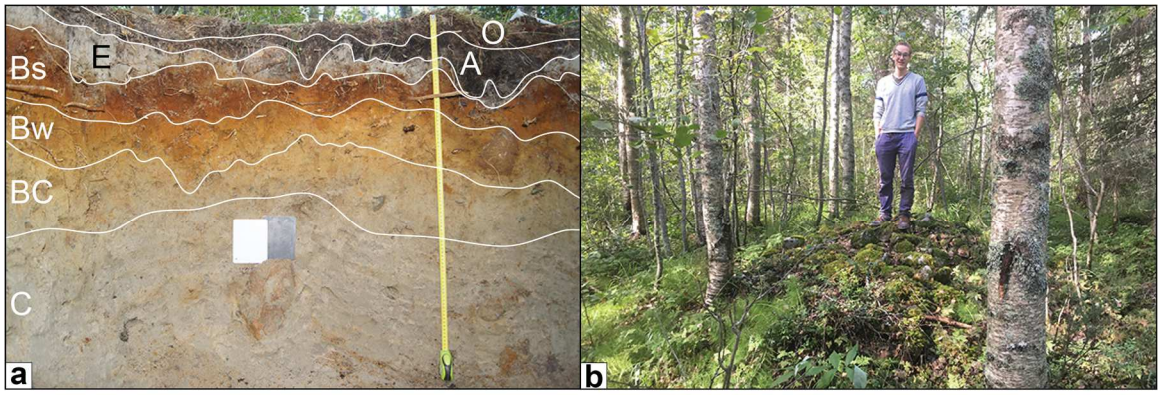

Pit: Kuhmo_176 – (Heavily Invaded)

Site: Kuhmo, Finland (Northern/Middle boreal transition zone)

Earthworm assemblage: Anecic – *Lumbricus terrestris*; Endogeic – *Aporrectodea tuberculata*, *Aporrectodea sp.*; Epi-endogeic – *Lumbricus rubellus*, *Lumbricus sp.* (juveniles)

Location: 63.84763°N; 30.15834°E

Sampling date: 8/17/16

Table AB.7. Pedon description and physiochemical data for the Kuhmo heavily invaded (Kuhmo_176, KW_176) soil profile near Kuhmo, Finland

Horizon	Depth	Color (field)	Structure	%C	%N	CF (%)	BD (g/cm^3)	$SSA_{occluded}$ (m^2/g)
Oi	0-5	2.5YR2.5/3	fibric [a]	27.9	1.60	6	0.13	– [d]
A	5-12	7.5YR 3/1	1[b], gr [c]	11.4	0.76	11	0.25	3.6 ± 0.6
E	12-21	10YR 6/1	1, sgl	0.43	0.05	30	1.22	0.9 ± 0.4
Bs	21-32	2.5YR 3/4	1, sgl	2.8	0.13	23	1.28	5.9 ± 2.2
Bw	32-45	10YR 5/6	1, sgl	0.76	0.04	26	1.2	1.21
BC	45-78	2.5Y 5/3	1, sgl	0.16	0.02	49	1.47	0.35
C	78-102	2.5Y 5/2	1, sgl	0.12	0.01	43	1.41	0.23

[a] Fibric (Oi), hemic (Oe), and sapric (Oa) designations used for organic horizons/soils
[b] Structure grade: 0, structureless; 1, weak; 2, moderate; 3, strong
[c] Structure type: gr, granular; sgl, single grain
[d] Mineral SSA values ($SSA_{occluded}$) were not determined for organic horizons

Vegetation Survey
Site: Kuhmo_176 (KW_176, Invaded)
Location: 63.84763°N; 30.15834°E
Survey date: 08/17/2016

(Pit) Vegetation – Survey taken 0.5 m away, due 100° from soil pit: canopy of *Alnus incana*, *Sorbus aucuparia*, and *Betula* (both species)

% cover – *Vaccinium myrtillus* (**35%**); *Melica nutans* (**3%**); *Solidago virgaurea* (**1%**); *Trientalis europaea* (**0.5%**); *Maianthemum bifolium* (**0.5%**); *Luzula pilosa* (**0.5%**); *Melampyrum sylvaticum* (**0.5%**);
Moss cover on forest floor (**7%**) – *Hylocomium splendens* (**5%**); *Rhytidiadelphus triquetrus* (**2%**)

(Clearing) Vegetation – Survey taken 10 m away from pit, due 100° in adjacent forest clearing with *Betula*, *Alnus incana*, *Sorbus aucuparia*, *Salix caprea* and *Juniperus communis* in canopy at edges of the opening

% cover – *Calamagrostis arundinacea* (**55%**); *Viola palustris* (**7%**); *Geranium sylvaticum* (**5%**); *Maianthemum bifolium* (**5%**); *Equisetum sylvaticum* (**3%**); *Solidago virgaurea* (**1%**); *Trientalis europaea* (**0.5%**); *Prunella vulgaris* (**0.5%**);
Moss cover (**45%**) – *Rhytidiadelphus squarrosus* (**35%**); *Hylocomium splendens* (**5%**); *Plagiomnium cuspidatum* (**3%**)

Figure AB.8. a Soil profile photo for the Kuhmo Pre-invasion (Kuhmo_k02, KNW_02) pit with horizons marked and **b** representative vegetation at KNW_02

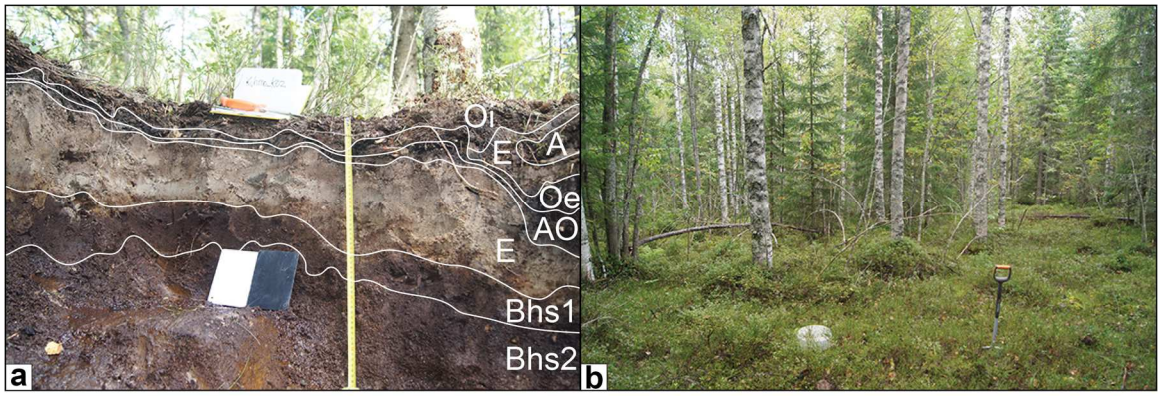

Pit: Kuhmo_k02 – (Pre-Invasion)
Site: Kuhmo, Finland (Northern/Middle boreal transition zone)
Earthworm assemblage: Epigeic – *Dendrobaena octaedra*
Location: 63.83765°N; 29.45825°E
Sampling date: 8/18/16

Table AB.8. Pedon description and physiochemical data for the Kuhmo Pre-Invasion (Kuhmo_k02, KNW_02) soil profile near Kuhmo, Finland

Horizon	Depth	Color (field)	Structure	%C	%N	CF (%)	BD (g/cm^3)	$SSA_{occluded}$ (m^2/g)
Oi	0-6	5YR2.5/2	fibric [a]	46.1	1.93	4	0.09±0.03	– [d]
Oe	6-8	7.5YR2.5/1	hemic	33.7	1.42	3	0.22±0.07	–
AO	8-10	10YR 2/1	1[b], gr [c]	19.1	0.88	19	0.38±0.08	1.51 ± 0.09
E	10-25	2.5Y 5/2	1, sgl	0.61	0.05	34	1.4 ± 0.2	1.2 ± 0.5
Bhs1	25-32	2.5YR2.5/1	cemented, sgl	5.8	0.20	59	1.5 ± 0.4	5.64 ± 0.06
Bhs2	32-60	2.5YR2.5/2	cemented, m	3.4	0.10	71	1.7 ± 0.5	4.3 ± 0.7

[a] Fibric (Oi), hemic (Oe), and sapric (Oa) designations used for organic horizons/soils
[b] Structure grade: 0, structureless; 1, weak; 2, moderate; 3, strong
[c] Structure type: gr, granular; sgl, single grain; m, massive
[d] Mineral SSA values ($SSA_{occluded}$) were not determined for organic horizons

Vegetation – Survey taken 2 m away from pit, due NW: canopy of *Betula pendula* and *Picea abies*

% cover – *Vaccinium myrtillus* (**65%**); *Vaccinium vitis-idaea* (**7%**); *Solidago virgaurea* (**1%**); *Trientalis europaea* (**0.5%**); *Maianthemum bifolium* (**0.5%**); *Deschampsia flexuosa* (**0.5%**); Moss cover on forest floor (**85%**) – *Pleurozium schreberi* (**55%**); *Hylocomium splendens* (**25%**); *Dicronum polysetum* (**3%**); *Polytrichum commune* (**2%**)

Figure AB.9. a Soil profile photo for the Hyytiälä_1A Invaded (Hyytiälä_1A, HW_1A) pit with horizons marked and **b** representative vegetation at HW_1A

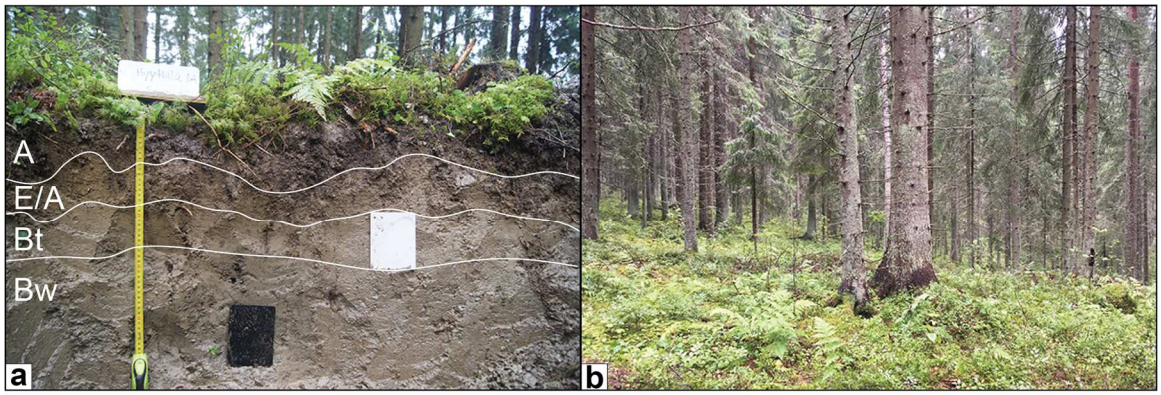

Pit: Hyytiälä _1A – (Heavily Invaded)

Site: Hyytiälä, Finland (Middle/Southern boreal transition zone)

Earthworm assemblage: Anecic – *Lumbricus terrestris*; Endogeic – *Aporrectodea sp.*; Epi-anecic – *Lumbricus* (juveniles); Epigeic – *Dendrobaena octaedra*, *Bimastos rubidus*

Location: 61.62291°N; 24.29813°E

Sampling date: 8/20/16

Table AB.9. Pedon description and physiochemical data for the Hyytiälä Invaded (Hyytiälä_1A, HW_1A) soil profile near Hyytiälä, Finland

Horizon	Depth	Color (field)	Structure	%C	%N	CF (%)	BD (g/cm^3)	$SSA_{occluded}$ (m^2/g)
A	0-9	10YR 3/2	2 [a], m [b], gr [c]	10.0	0.64	5	0.53	11.0 ± 2.2
E/A	9-17	2.5Y 4/3	1, f, sbk	1.32	0.10	3	0.84	3.5 ± 2.2
Bt	17-27	2.5Y 5/3	2, f to m, sbk	0.42	0.00	11	1.1	0.9 ± 0.4
Bw	27-60	2.5Y 5/1	1, f to m, sbk	0.37	0.00	27	1.24	0.80

[a] Structure grade: 0, structureless; 1, weak; 2, moderate; 3, strong
[b] Structure size: f, fine; m, medium; c, coarse
[c] Structure type: gr, granular; sgl, single grain; sbk, subangular blocky; pl, platy; m, massive

Vegetation – Myrtillus-type *Picea* stand survey taken 3 m away from pit, 300°

% cover (non-additive) – *Vaccinium myrtillus* (**45%**); *Oxalis acetosella* (**7%**); *Rubus saxatilis* (**2%**); *Maianthemum bifolium* (**1%**); *Vaccinium vitis-idaea* (**0.5%**)
Moss cover on forest floor (**100%**) – *Hylocomium splendens* (**100%**)

Figure AB.10. a Soil profile photo for the Hyytiälä_H4 Invaded (Hyytiälä_H4, HW_H4) pit with horizons marked and **b** representative vegetation at HW_H4

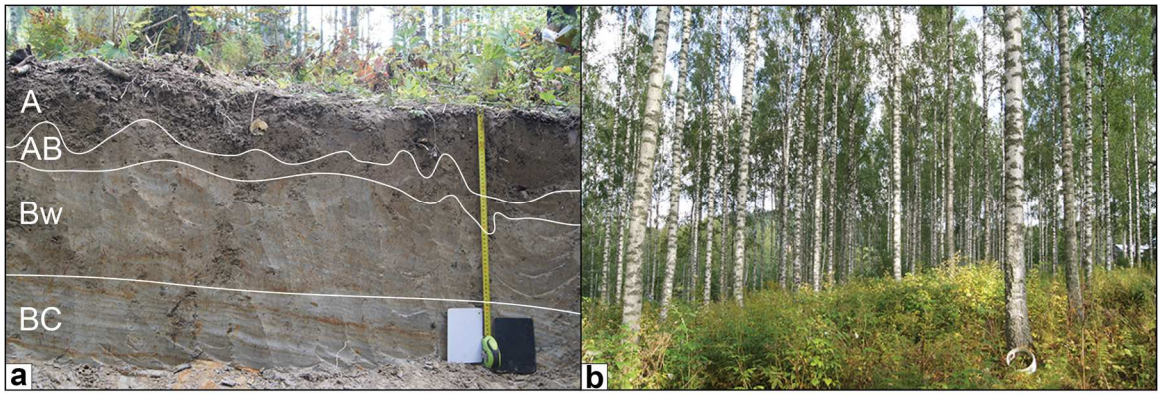

Pit: Hyytiälä _H4 – (Heavily Invaded)
Site: Hyytiälä, Finland (Middle/Southern boreal transition zone)
Earthworm assemblage: Anecic – *Lumbricus terrestris*; Endogeic – *Aporrectodea tuberculata*, *Aporrectodea rosea*; Epi-endogeic – *Lumbricus rubellus*, *Lumbricus* (juv.)
Location: 61.87703°N; 24.10126°E
Sampling date: 8/19/16

Table A2.10. Pedon description and physiochemical data for the Hyytiälä Invaded (Hyytiälä_H4, HW_H4) soil profile near Hyytiälä, Finland

Horizon	Depth	Color (field)	Structure	%C	%N	CF (%)	BD (g/cm^3)	SSA$_{occluded}$ (m^2/g)
A	0-17	10YR 4/3	1[a], m[b], gr[c]	2.62	0.20			
AB	17-24	2.5Y 5/3	1, f to m, sbk	0.50	0.01			
Bw	24-45	2.5Y 5/3	1, f, sbk	0.16	0.00			
BC	45-65	2.5Y 5/2	2, pl	0.16	0.00			

[a] Structure grade: 0, structureless; 1, weak; 2, moderate; 3, strong
[b] Structure size: f, fine; m, medium; c, coarse
[c] Structure type: gr, granular; sgl, single grain; sbk, subangular blocky; pl, platy; m, massive

Vegetation – Survey taken 1 m away from pit, due 180°: canopy of *Betula pendula*

% cover – *Geum rivale* (**35%**); *Rubus idaeus* (**15%**); *Filipendula ulmaria* (**10%**); *Veronica chamaedrys* (**7%**); *Oxalis acetosella* (**5%**); *Geranium sylvaticum* (**2%**); *Equisetum sylvaticum* (**1%**); *Anthriscus sylvestris* (**1%**); *Urtica dioica* (**0.5%**); *Ranunculus repens* (**0.5%**); *Lathyrus pratensis* (**0.5%**); *Vicia sepium* (**0.5%**);

Moss cover on forest floor (**~1%**) – some *Brachytheciaceae sp.*

Figure AB.11. a Soil profile photo for the Hyytiälä_4C Pre-Invasion (Hyytiälä_4C, HNW_4C) pit with horizons marked and **b** representative vegetation at HNW_4C

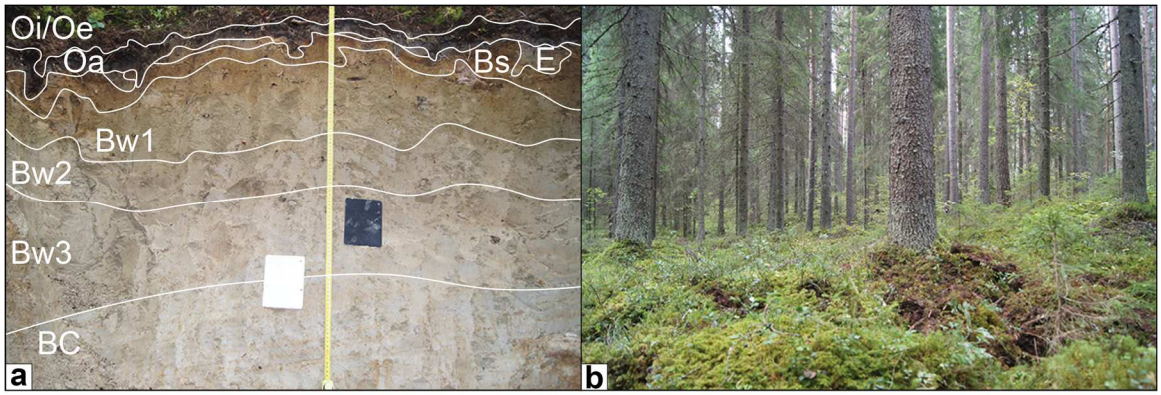

Pit: Hyytiälä _4C – (Pre-Invasion)
Site: Hyytiälä, Finland (Middle/Southern boreal transition zone)
Earthworm assemblage: Epigeic – *Dendrobaena octaedra*
Location: 61.92270°N; 24.35137°E
Sampling date: 8/21/16

Table AB.11. Pedon description and physiochemical data for the Hyytiälä Pre-Invasion (Hyytiälä_4C, HNW_4C) soil profile near Hyytiälä, Finland

Horizon	Depth	Color (field)	Structure	%C	%N	CF (%)	BD (g/cm^3)	$SSA_{occluded}$ (m^2/g)
Oi/Oe	0-9	2.5YR2.5/2	fibric/hemic [a]	46.8	1.38	12	0.07	– [e]
Oa	9-14	2.5YR2.5/1	sapric	23.2	0.67	6	0.16	–
E	14-16	10YR 5/2	1[b], sgl [c]	3.9	0.18	13	0.85	6.2 ± 0.7
Bs	16-25	7.5YR 4/4	1, f to m[d], sbk	2.1	0.10	41	1.09	4.0 ± 2.9
Bw1	25-44	2.5YR 5/4	1, m, sbk	0.59	0.00	26	1.11	1.1 ± 0.9
Bw2	44-54	2.5Y 5/2	1, f to m, sbk	0.27	0.01	22	1.31	2.14
Bw3	54-79	2.5Y 5/2	1, f, sbk	0.21	0.01	19	1.46	0.93
BC	79-115	2.5Y 5/3	2, pl	0.13	0.01	11	1.64	–1.07

[a] Fibric (Oi), hemic (Oe), and sapric (Oa) designations used for organic horizons/soils
[b] Structure grade: 0, structureless; 1, weak; 2, moderate; 3, strong
[c] Structure type: gr, granular; sgl, single grain; sbk, subangular blocky; pl, platy; m, massive
[d] Structure size: f, fine; m, medium; c, coarse
[e] Mineral SSA values ($SSA_{occluded}$) were not determined for organic horizons

Vegetation – Survey taken 2 m away, due 140° from soil pit HNW_4C: canopy of *Picea abies*

% cover – *Vaccinium vitis-idaea* (**10%**); *Vaccinium myrtillus* (**7%**); *Deschampsia flexuosa* (**0.5%**); *Luzula pilosa* (**0.5%**); *Linnaea borealis* (**0.5%**); *Maianthemum bifolium* (**0.5%**)

Moss cover on forest floor (**100%**) – *Hylocomium splendens* (**99%**); *Polytrichum commune* (**0.5%**); *Pleurozium schreberi* (**0.5%**)

Adjacent Vegetation – *Diphasiastrum complanatum* (NT) and *Goodyera repens* (LC) occur in close proximity to the soil pit but not within the vegetation survey area.

Figure AB.12. a Soil profile photo for the Hyytiälä_5C Early Invasion (Hyytiälä_5C, HNW_5C) pit with horizons marked and **b** representative vegetation at HNW_5C

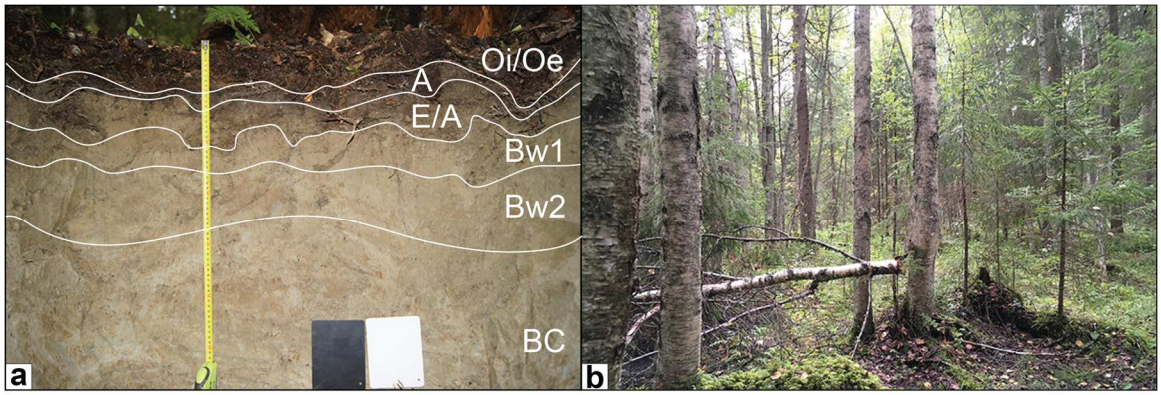

Pit: Hyytiälä_5C – (Early Invasion)
Site: Hyytiälä, Finland (Middle/Southern boreal transition zone)
Earthworm assemblage: Epi-endogeic – *Lumbricus sp.*; Epigeic – *Dendrobaena octaedra*
Location: 61.72920°N; 24.56165°E
Sampling date: 8/21/16

Table AB.12. Pedon description and physiochemical data for the Hyytiälä Early Invasion (Hyytiälä_5C, HNW_5C) soil profile near Hyytiälä, Finland

Horizon	Depth	Color (field)	Structure	%C	%N	CF (%)	BD (g/cm^3)	$SSA_{occluded}$ (m^2/g)
Oi/Oe	0-9	5YR3/3	fibric [a]	39.9	1.92			
A	9-11	10YR 3/2	1[b], gr[c]	7.0	0.35			
E/A	11-19	2.5Y 4/3	1, f[d], sbk	1.18	0.09			
Bw1	19-26	2.5Y 5/3	1, f to m, sbk	0.32	0.00			
Bw2	26-35	2.5YR 5/2	2, m, sbk	0.24	0.01			
BC	35-62	2.5Y 5/2	pl, sbk	0.18	0.01			

[a] Fibric (Oi), hemic (Oe), and sapric (Oa) designations used for organic horizons/soils
[b] Structure grade: 0, structureless; 1, weak; 2, moderate; 3, strong
[c] Structure type: gr, granular; sgl, single grain; sbk, subangular blocky; pl, platy; m, massive
[d] Structure size: f, fine; m, medium; c, coarse

Vegetation – Survey taken 3 m away, due 300° from soil pit: canopy of *Betula pendula* % cover – *Maianthemum bifolium* (**10%**); *Fragaria vesca* (**7%**); *Oxalis acetosella* (**5%**); *Dryopteris carthusiana* (**5%**); *Salidago virgaurea* (**1%**); *Deschampsia cespitosa* (**1%**); *Melica nutans* (**1%**); *Trientalis europaea* (**1%**); *Melampyrum sylvaticum* (**0.5%**); *Luzula pilosa* (**0.5%**); *Equisetum sylvaticum* (**0.5%**); *Vaccinium vitis-idaea* (**0.5%**); *Deschampsia flexuosa* (**0.5%**); *Rubus saxatilis* (**0.5%**); *Viola riviniana* (**0.5%**)
Moss cover on forest floor (**15%**) – some *Brachytheciaceae sp.*

Figure AB.13. a Soil profile photo for the Lammi Invaded (Lammi_12, LW_12) pit with horizons marked and **b** representative vegetation at Lammi_12

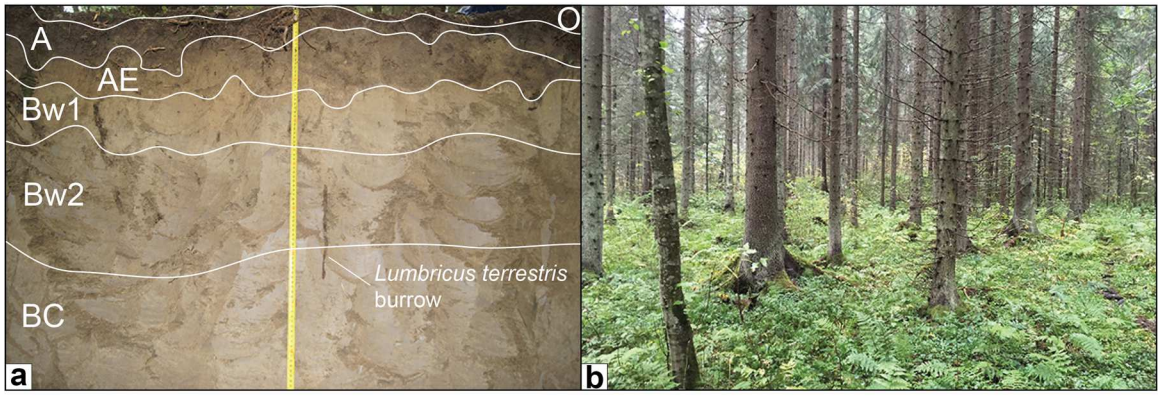

Pit: Lammi_12 – (Heavily Invaded)
Site: Lammi, Finland (Southern boreal zone)
Earthworm assemblage: Anecic – *Lumbricus terrestris*; Endogeic – *Aporrectodea calignosa*, *Aporrectodea rosea*, *Aporrectodea sp.* (juveniles); Epi-endogeic – *Lumbricus rubellus*; Epi-anecic – *Lumbricus sp.* (juveniles); Epigeic – *Dendrobaena octaedra*
Location: 61.03999°N; 25.08480°E
Sampling date: 8/22/16

Table AB.13. Pedon description and physiochemical data for the Lammi Heavily Invaded (Lammi_12, LW_12) soil profile near Lammi, Finland

Horizon	Depth	Color (field)	Structure	%C	%N	CF (%)	BD (g/cm^3)	$SSA_{occluded}$ (m^2/g)
Oi	0-2	5YR 2.5/1	fibric [a]	13.3	0.61			
A	2-14	7.5YR 3/2	2[b], m[c], gr[d]	5.3	0.34			
AE	14-24	2.5Y 4/4	1, f to m, gr	3.2	0.15			
Bw1	24-42	2.5Y 5/3	1, sgl	0.46	0.00			
Bw2	42-58	2.5Y 4/2	1, m to c, sbk	0.34	0.01			
BC	58-110	2.5Y 5/2	pl, sbk	0.33	0.00			

[a] Fibric (Oi), hemic (Oe), and sapric (Oa) designations used for organic horizons/soils
[b] Structure grade: 0, structureless; 1, weak; 2, moderate; 3, strong
[c] Structure size: f, fine; m, medium; c, coarse
[d] Structure type: gr, granular; sgl, single grain; sbk, subangular blocky; pl, platy; m, massive

Vegetation – Survey taken 3 m away, due 60° from soil pit

Herb-rich *Picea* stand with some *Alnus incana* (alder) in the canopy and sparse *Sorbus aucuparia* and small *Acer platanoides*, *Ribes alpinum*, and *Lonicera xylosteum* in the understory/shrub layer

% cover – *Oxalis acetosella* (**65%**); *Phegopteris connectilis* (**10%**); *Dryopteris carthusiana* (**7%**); *Viola riviniana* (**3%**); *Dryopteris filix-mas* (**3%**); *Maianthemum bifolium* (**2%**); *Anemone hepatica* (**2%**); *Vaccinium myrtillus* (**0.5%**); *Gymnocarpium dryopteris* (**2%**); *Fragaria vesca* (**1%**); *Lonicera xylosteum* (**1%**); *Veronica officinalis* (**0.5%**); *Carex digitata* (**0.5%**); *Paris quadrifolia* (**0.5%**); *Luzula pilosa* (**0.5%**)

Moss cover on forest floor (**70%**) – *Hylocomium splendens* (**60%**); *Pleurozium schreberi* (**7%**); *Plagiochila asplenioides* (**3%**)

NOTE – Some rare and endangered species including *Ranunculus cassubicus*, **(abundant) *Circaea alpina***, and *Stellaria nemorum* were observed in close proximity to the soil pit.

Figure AB.14. a Soil profile photo for Lammi Early Invasion (Lammi_S02, LNW_S02) pit with horizons marked and **b** representative vegetation at Lammi_S02

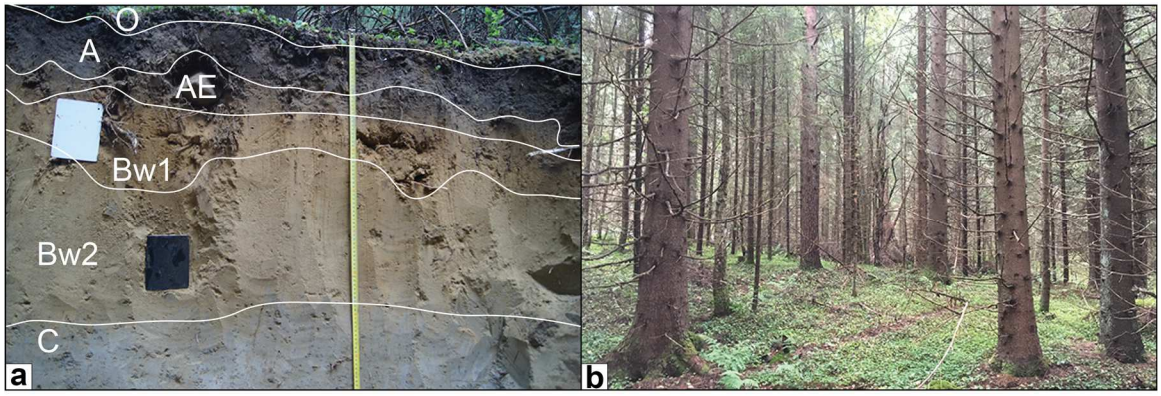

Pit: Lammi_S02 – (Early Invasion)
Site: Lammi, Finland (Southern boreal zone)
Earthworm assemblage: Epi-endogeic – *Lumbricus sp.*; Epigeic – *Dendrobaena octaedra*
Location: 61.05502°N; 25.05164°E
Sampling date: 8/23/16

Table AB.14. Pedon description and physiochemical data for the Lammi Early Invasion (Lammi_S02, LNW_S02) soil profile near Lammi, Finland

Horizon	Depth	Color (field)	Structure	%C	%N	CF (%)	BD (g/cm^3)	$SSA_{occluded}$ (m^2/g)
Oi	0-3	5YR 2.5/1	fibric [a]	41.5	2.06			
A	3-15	10YR 3/2	1[b], f[c], gr[d]	5.2	0.36			
AE	15-22	10YR 4/3	1, sgl	2.4	0.18			
Bw1	22-32	10YR 4/6	1, sgl	1.2	0.09			
Bw2	32-67	2.5Y 5/6	1, sgl	0.57	0.05			
C	67-95	2.5Y 5/3	m	0.44	0.02			

[a] Fibric (Oi), hemic (Oe), and sapric (Oa) designations used for organic horizons/soils
[b] Structure grade: 0, structureless; 1, weak; 2, moderate; 3, strong
[c] Structure size: f, fine; m, medium; c, coarse
[d] Structure type: gr, granular; sgl, single grain; m, massive

Vegetation – Survey taken 3 m away, due 280° from soil pit
% cover – *Oxalis acetosella* (**80%**); *Maianthemum bifolium* (**7%**); *Anemone hepatica* (**5%**); *Dryopteris carthusiana* (**5%**); *Rubus saxatilis* (**3%**); *Convallaria majalis* (**1%**); *Fragaria vesca* (**1%**); *Trientalis europaea* (**0.5%**); *Carex digitata* (**0.5%**); *Viola riviniana* (**0.5%**); *Vaccinium myrtillus* (**0.5%**); Moss cover on forest floor (**15%**) – *Rhodobryum roseum* (**10%**); *Hylocomium splendens* (**3%**); *Climacium dendroides* (**2%**)

Figure AB.15. a Soil profile photo for Tvärminne_61 heavily invaded (Tvärminne_61, TW_61) pit with horizons marked and **b** representative vegetation at Tvärminne_61

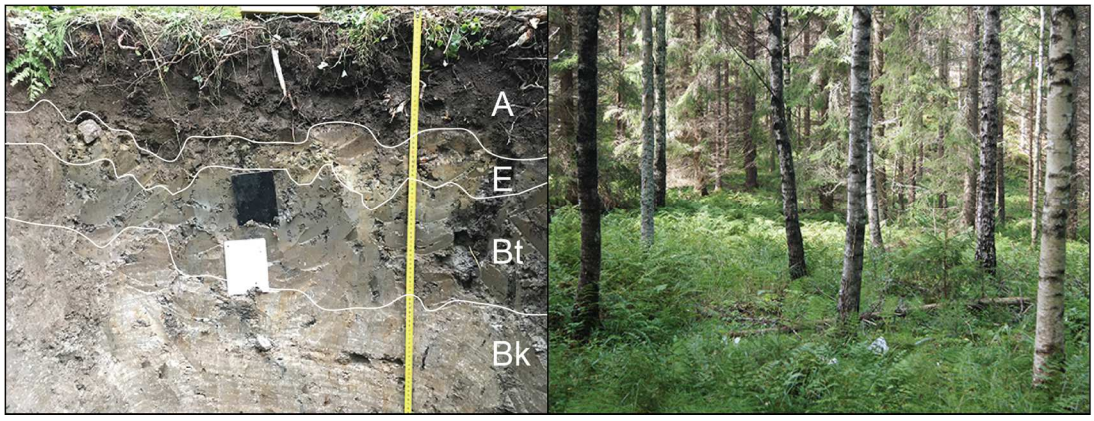

Pit: Tvärminne_61 – (Heavily Invaded)

Site: Tvärminne, Finland (Boreo-nemoral zone)

Earthworm assemblage: Anecic – *Lumbricus terrestris*; Endogeic – *Aporrectodea tuberculata*, *Aporrectodea sp.*, *Octolasion tyrtaeum*; Epi-anecic – *Lumbricus sp.* (juv.); Epigeic – *Dendrobaena octaedra*, *Bimastos rubidus*

Location: 60.00135°N; 23.17143°E

Sampling date: 8/14/16

Table AB.15. Pedon description and physiochemical data for the Tvärminne_61 heavily invaded (Tvärminne_61, TW_61) soil profile near Tvärminne, Finland

Horizon	Depth	Color (field)	Structure	%C	%N	CF (%)	BD (g/cm^3)	$SSA_{occluded}$ (m^2/g)
A1	0-16	7.5YR2.5/1	3[a], m[b], gr[c]	8.0	0.59			
A2	16-28	10YR 3/1	2, f to c, gr					
E	28-38	2.5Y 4/2	2, f to m, sbk	0.50	0.00			
Bt	38-57	2.5Y 4/1	3, f to c, sbk	0.37	0.00			
Bk1	57-73	2.5Y 5/2	2, m to c, sbk					
Bk2	73-96	2.5Y 4/2	2, sbk, pl					
Bk3	96-103	2.5Y 5/2	2, pl	0.14	0.00			

[a] Structure grade: 0, structureless; 1, weak; 2, moderate; 3, strong
[b] Structure size: f, fine; m, medium; c, coarse
[c] Structure type: gr, granular; sgl, single grain; sbk, subangular blocky; pl, platy; m, massive

Vegetation – Survey taken 2 m away 18° from soil pit

Betula pendula stand in a *Picea*-dominated moist, calcareous, herb-rich forest

% cover – *Oxalis acetosella* (**30%**); *Gymnocarpium dryopteris* (**30%**); *Dryopteris carthusiana* (**15%**); *Pteridium aquilinum* (**7%**); *Calamagrostis arundinacea* (**3%**); *Athyrium filix-femina* (**3%**); *Deschampsia cespitosa* (**1%**); *Poa nemoralis* (**1%**); *Veronica chamaedrys* (**0.5%**); *Equisetum sylvaticum* (**0.5%**); *Viola riviniana* (**0.5%**); *Lactuca muralis* (**0.5%**); *Trientalis europaea* (**0.5%**); *Paris quadrifolia* (**1%**); Moss cover on forest floor (**95%**) – *Plagiomnium cuspidatum* (**80%**); *Rhytidiadelphus triquetrus* (**15%**); *Pleurozium schreberi* (**2%**)

NOTE – *Circaea alpina* (protected plant species in Finland) was observed close to the pit in a localized moist depression.

Figure AB.16. a Soil profile photo for Tvärminne_34 heavily invaded (Tvärminne_34, TW_34) pit with horizons marked and **b** representative vegetation at Tvärminne_34

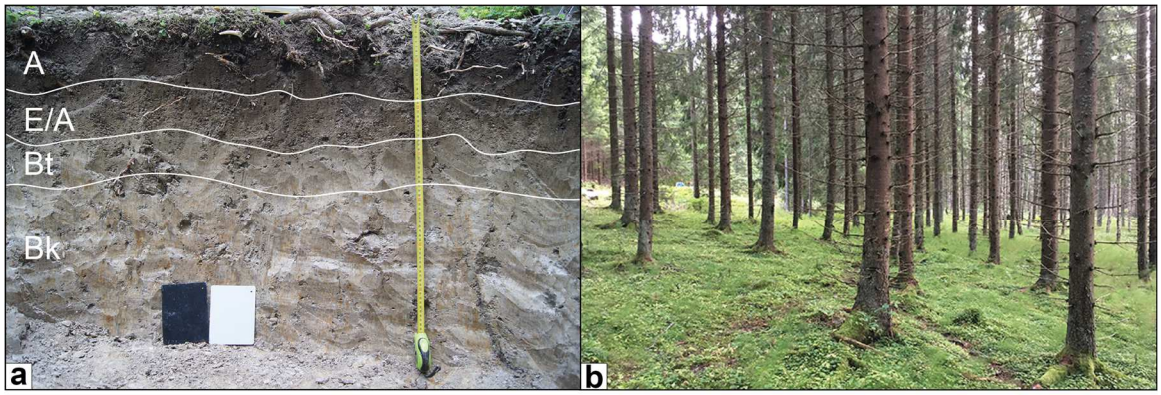

Pit: Tvärminne_34 – (Heavily Invaded)

Site: Tvärminne, Finland (Boreo-nemoral zone)

Earthworm assemblage: Anecic – *Lumbricus terrestris*; Endogeic – *Aporrectodea tuberculata*, *Aporrectodea rosea*, *and Aporrectodea sp.*; Epi-anecic – *Lumbricus sp.* (juv.); Epigeic – *Dendrobaena octaedra*

Location: 60.00246°N; 23.17609°E

Sampling date: 8/15/16

Table AB.16. Pedon description and physiochemical data for the Tvärminne_34 heavily invaded (Tvärminne_34, TW_34) soil profile near Tvärminne, Finland

Horizon	Depth	Color (field)	Structure	%C	%N	CF (%)	BD (g/cm^3)	$SSA_{occluded}$ (m^2/g)
A1	0-6	7.5YR 3/1	2[a], m[b], gr[c]	4.5	0.32			
A2	6-13	10YR 3/1	2, f to m, gr	2.9	0.22			
AE	13-25	10YR 4/2	1, f to m, gr					
E/A	25-31	10YR 5/2	1, f, sbk	0.50	0.01			
Bt	31-44	2.5Y 5/2	2, f to c, sbk	0.32	0.01			
Bk1	44-51	2.5Y 5/2	2, m to c, sbk	0.21	0.00			
Bk2	51-73	2.5Y 5/3	2, sbk, pl	0.14	0.00			

[a] Structure grade: 0, structureless; 1, weak; 2, moderate; 3, strong
[b] Structure size: f, fine; m, medium; c, coarse
[c] Structure type: gr, granular; sgl, single grain; sbk, subangular blocky; pl, platy; m, massive

Vegetation – Survey taken 2 m away 10° from soil pit

60-year-old *Picea abies* stand in productive, calcareous herb-rich forest

% cover – *Oxalis acetosella* (**65%**); *Maianthemum bifolium* (**10%**); *Equisetum sylvaticum* (**5%**); *Viola riviniana* (**3%**); *Veronica chamaedrys* (**0.5%**); *Luzula pilosa* (**0.5%**); *Carex digitata* (**0.5%**); *Melica nutans* (**0.5%**); *Anemone nemorosa* (**0.5%**); *Trientalis europaea* (**0.5%**); *Paris quadrifolia* (**0.5%**);

Moss cover on forest floor (**95%**) – *Plagiomnium cuspidatum* (**40%**); *Pleurozium schreberi* (**30%**); *Plagiochila asplenioides* (**15%**); *Rhytidiadelphus triquetrus* (**5%**); *Hylocomium splendens* (**5%**)

Figure AB.17. a Soil profile photo for the Tvärminne_8 Pre-invasion (Tvärminne_8, TNW_8) pit with horizons marked and **b** representative vegetation at Tvärminne_8

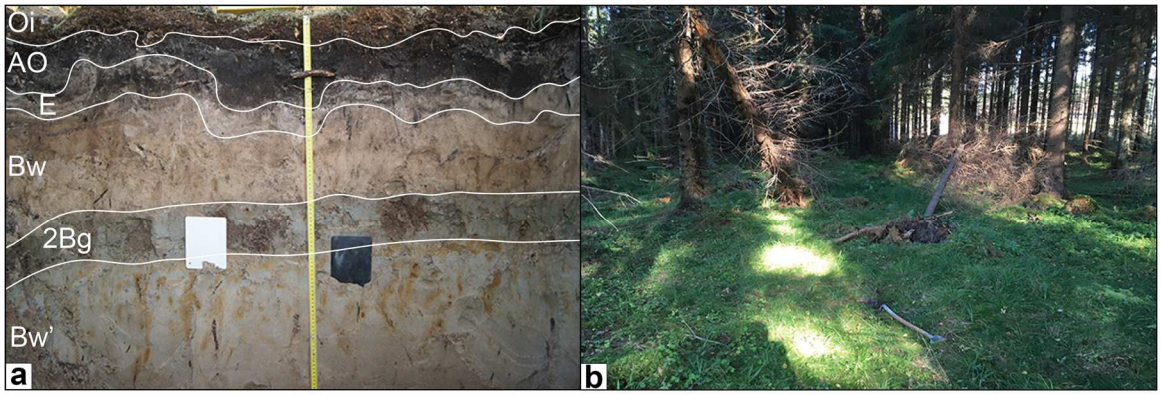

Pit: Tvärminne_8 – (Pre-Invasion)
Site: Tvärminne, Finland (Boreo-nemoral zone)
Earthworm assemblage: Epigeic – *Dendrobaena octaedra*
Location: 59.98125°N; 23.36439°E
Sampling date: 8/15/16

Table AB.17. Pedon description and physiochemical data for the Tvärminne_8 Pre-invasion (Tvärminne_8, TNW_8) soil profile near Tvärminne, Finland

Horizon	Depth	Color (field)	Structure	%C	%N	CF (%)	BD (g/cm^3)	$SSA_{occluded}$ (m^2/g)
Oi	0-8	2.5YR2.5/3	fibric	47.5	2.27	0	0.15±0.04	–
AO	8-15	7.5YR2.5/1	1[a], f [b], gr [c]	19.7	0.89	1	0.28±0.09	12.4 ± 7.8
E	15-21	2.5Y 3/2	1, sgl	0.28	0.01	0	1.1 ± 0.1	0.7 ± 0.2
Bw	21-44	10YR 5/3	1, sgl	0.30	0.01	3	1.2 ± 0.2	0.45±0.07
2Bg	44-53	10YR 5/1 (2.5YR3/3)	2, m to c, sbk	1.6	0.15	4	1.08±0.07	7.89
Bw'	53-75	10YR 6/2 (10YR 4/6)	1, sgl	0.13	0.00	0	1.4 ± 0.2	0.14
BC	75-100	10YR 5/2	1, sgl	0.09	0.01	2	1.3 ± 0.3	0.45

[a] Structure grade: 0, structureless; 1, weak; 2, moderate; 3, strong
[b] Structure size: f, fine; m, medium; c, coarse
[c] Structure type: gr, granular; sgl, single grain; sbk, subangular blocky; pl, platy; m, massive

Vegetation – Survey taken 0.5 m away, 5° from soil pit
% cover – *Oxalis acetosella* (**15%**); *Deschampsia flexuosa* (**15%**); *Luzula pilosa* (**10%**); *Dryopteris carthusiana* (**2%**); *Maianthemum bifolium* (**1%**); *Solidago virgaurea* (**0.5%**); *Carex canescens* (**0.5%**); *Melampyrum sylvaticum* (**0.5%**)
Moss cover on forest floor (**100%**) –*Pleurozium schreberi* (**70%**); *Dicranum sp.* (**30%**)

Figure AB.18. a Soil profile photo for Tvärminne_627 Pre-invasion (Tvärminne_627, TNW_627) pit with horizons marked and **b** representative vegetation at Tvärminne_627

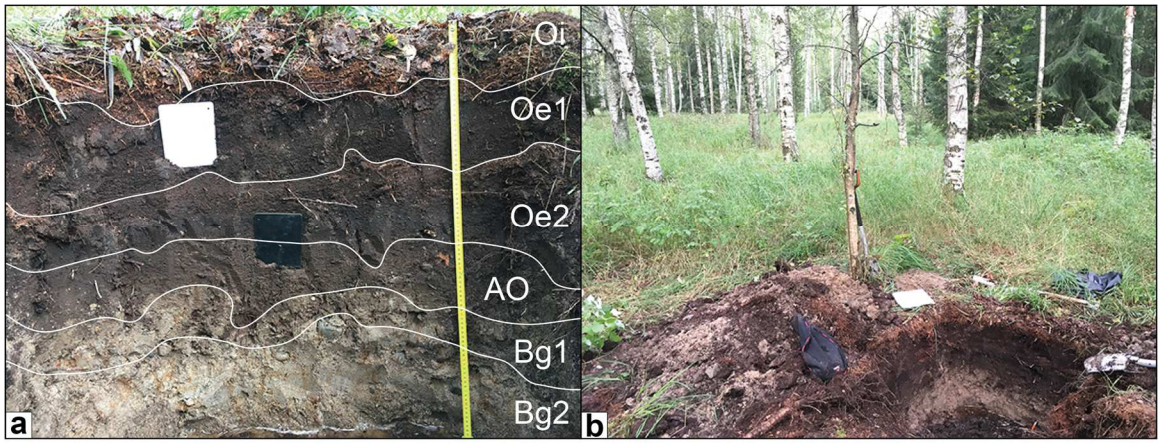

Pit: Tvärminne_627 – (Pre-Invasion)
Site: Tvärminne, Finland (Boreo-nemoral zone)
Earthworm assemblage: Epigeic – *Dendrobaena octaedra*
Location: 59.85241°N; 23.06847°E
Sampling date: 8/13/16

Table AB.18. Pedon description and physiochemical data for the Tvärminne_627 Pre-invasion (Tvärminne_627, TNW_627) organic soil profile near Tvärminne, Finland

Horizon	Depth	Color (field)	Structure	%C	%N	CF (%)	BD (g/cm^3)	$SSA_{occluded}$ (m^2/g)
Oi	0-13	2.5YR2.5/4	fibric [a]	49.3	2.60			
Oe1	13-33	2.5YR2.5/1	hemic	45.6	2.58			
Oe2	33-43	7.5YR2.5/1	hemic	41.4	3.07			
AO	43-53	7.5YR2.5/1	hemic	8.8	0.81			
Bg1	53-65	10YR 3/2	1[b], c [c], sgl [d]	1.13	0.10			
Bg2	65-76	10YR 4/2	1, c, sgl	0.13	0.01			
BC	76-85	10YR 4/2	1, vc, sgl	0.10	0.02			

[a] Fibric (Oi), hemic (Oe), and sapric (Oa) designations used for organic horizons/soils
[b] Structure grade: 0, structureless; 1, weak; 2, moderate; 3, strong
[c] Structure size: f, fine; m, medium; c, coarse; vc, very coarse
[d] Structure type: sgl, single grain

Vegetation –
% cover – *Calamagrostis canescens* (**25%**); *Rubus idaeus* (**15%**); *Salix starkeana* (**10%**); *Luzula pilosa* (**7%**); *Lysimachia thyrsiflor* (**1%**); *Moehringia trinervia* (**0.5%**); *Trientalis europaeus* (**0.5%**); *Molinia coerulea* (**0.5%**); Moss cover (**5%**) non-sphagnum *Brachytheciaceae sp.*

Appendix C – Constraining the timing of earthworm arrival to study areas

Methods

We identified earthworm invasion sites where the timing of earthworm introduction could be more-or-less constrained (Table 2, main text), allowing us the opportunity to assess how upper profile SOC dynamics in northern forests are influenced by earthworm invasion through time. We placed the timing of earthworm introduction at Otter Tail in northern Minnesota in the late 1970s, when tree rings first detect the effects of earthworm invasion (Larson *et al.,* 2010). Our six soil pits were arranged along this gradient to capture differences in the forest soils as a function of different stages and timing of earthworm invasion (see Lyttle *et al.,* 2015 or Resner *et al.,* 2015 for details on sampling design). On this basis, we place the age of earthworm invasion at 40 years for the most heavily invaded soil profile (OT_8) and make the simple assumption that the age decreases linearly along the gradient, with the geoengineering earthworm-free pit at ~190 m (OT_3) representing 0 years (Table 2.2 main text).

The sampling approach at the two arctic invasion gradients (Jierpen and Kopparåsen) was designed to mimic the Otter Tail site, where earthworm and soil sampling locations are placed at increasing distances from the presumed earthworm source (see Wackett *et al.,* 2018 for details). At Jierpen, we estimate the timing of earthworm introduction to be ca. mid-1860s, when homesteading farmers from southern Sweden were first sent to the Abisko area (Andersson *et al.,* 2005). The length of the earthworm invasion 'front' further supports this determination: our earthworm surveys indicated that geoengineering earthworms have moved ~750 m away from the farm into the adjacent birch forest, corresponding to a dispersal rate of 5 m yr^{-1} that directly matches N. American analogues (Wackett *et al.,* 2018). We assign a median age to the 'intermediate' soil pit invaded by *Lumbricus rubellus* only (Figure S2.3) and ages of 0 years to the two soil profiles free of geoengineering earthworms (Table 2.2). At Kopparåsen, we estimate the timing of earthworm arrival to be ca. early 1900s, the time at which the Kiruna-Narvik railway line was completed and railway operator cabins were constructed (Wackett *et al.,* 2018). On this basis, we place the age of invasion at ~100 years for the earthworm-invaded profile (Table 2.2).

Appendix D – Correcting erroneous mineral SSA data from Otter Tail

Methods

It is important to highlight and address two methodological errors in a previous study of earthworm effects on organo-mineral associations (Lyttle *et al.,* 2013, 2015) that has bearing on this study: we have corrected and re-presented much of this data here. The first error is the incorrect assignment of topsoil in earthworm-free forest plots as mineral topsoil (A-horizon) rather than organic horizons, despite these layers having SOC weight percent's as high as ~27%. This violates the classification guidelines of USDA Soil Taxonomy, which sets 12 wt % as the cut-off between organic and mineral soil horizons with a 1% increase in the threshold with every 10% increase in soil clay content (Soil Survey Staff, 2014).

The most important of these methodological issues is that muffling of organic horizons – as Lyttle *et al.* (2013, 2015) did to remove organic matter – leads to the production of significant quantities of black carbon (e.g. Accardi-Dey and Gschwend, 2002) during the muffling process. This combustion product has large BET surface areas often exceeding 100 m^2/g (Atkins, 1964). By considering organic layers to be part of the mineral soil and muffling their soil samples to determine $SSA_{occluded}$ values according to Eq. 1 (main text), Lyttle *et al.* (2015) came to the surprising conclusion that earthworm invasion decreases the total amount of mineral surfaces occluded by soil organic matter (SOM). However, the large apparent $SSA_{occluded}$ values determined for earthworm-free topsoils can be explained almost entirely by black carbon production during heat treatment, rather than true occlusion of mineral surfaces via organo-mineral associations.

To avoid this issue, we elected not to analyze organic topsoil layers (where present) and constrained our measurements of $SSA_{occluded}$ to mineral soils only. Thus, for forest sites with organic horizons at the surface (most sites lacking geoengineering earthworms), we measured $SSA_{occluded}$ inventories (see Eq. 4, main text) for the upper 25 cm of the soil column beginning directly below the organic-mineral soil interface. We also correct the $SSA_{occluded}$ inventory values reported by Lyttle *et al.* (2015) and present them here (without the O-horizon inventories) to facilitate direct comparison between organo-mineral interactions in soils at the well-studied Otter Tail site in northern MN (Hale et al., 2005a, 2005b, 2006; Resner et al., 2015) and our newly identified high-latitude earthworm invasion sites in Finland and Sweden (this study).

Appendix E – Geospatial mapping

Methods

We compiled global datasets for land cover (ESA GlobCover 2009), croplands (Ramankutty *et al.,* 2008), topographic roughness index (TRI; Gruber, 2012) and permafrost zonation index (PZI; Gruber, 2012). All datasets were re-projected to the WGS84 Geodetic model and interpolated to match the resolution of the coarsest dataset (Latitudinal/longitudinal resolution of 0.008333 degrees, or ~10 km; Ramankutty *et al.,* 2008). Following unification of grid resolution, rasters were clipped to 40°N latitude and re-projected to the North Pole Azimuthal Equidistant projection. Following re-projection, the croplands (scale 0 – 1; representing 0 – 100% cropland cover per unit cell), TRI (artificial scaling 0 – 5.56; see Gruber, 2012 for details), and PZI (scale 0.01 – 1; representing 1 – 100% permafrost probability) were scaled by 100 before conversion from float to integer values to allow for subsequent construction of raster attribute tables. All rasters were then multiplied (or divided) by a 'dummy value' to scale the factors on multiple orders of magnitude before using raster algebra to sum the pre-scaled datasets, creating a master raster with sums that correspond to known values encoding the land cover type, topographic roughness, and the likelihood of permafrost incidence for each 10 x 10 km cell.

The generated map (Figure S2.1) was then used to identify dominant soil mixing modes according to criteria outlined in Table S2.1. Mixing regimes following tree throw in boreal and arctic forests are slower and act over centennial to millennial time-scales (Bormann et al., 1995; Ulanova, 2000). We focused our analysis on areas where cryoturbation and tree throw are dominant (Figure 2.8, main text), which covers most of the world's northern boreal and arctic landscapes.

Appendix F – Soil organic carbon and nitrogen contents

Methods

Splits of the fine earth (<2 mm) fraction from all soil samples were hand-homogenized and dried at 60 ºC for 48 hours. Carbon and nitrogen contents were determined on an elemental analyzer in the department of Forest Resources at the University of Helsinki.

Table AF.1. Elemental chemistry (C and N) for the Jierpen Invaded (JW_1) soil profile

Sample	**Initial** (cm)	**Final** (cm)	**Weight** (mg)	**Org. N** (%)	**Org. C** (%)	**C:N**
			Horizons			
A horizon	0	10	869	0.42	6.19	14.6
AB horizon	10	18	719	0.30	3.92	13.1
Bw1 horizon	18	35	887	0.06	0.92	15.2
Bw2 horizon	35	62	945	0.08	0.79	9.9
			Depth Intervals			
DI 0-3 cm	0	3	866	0.48	7.81	16.3
DI 3-6 cm	3	6	661	0.41	6.27	15.4
DI 6-9 cm	6	9	694	0.35	5.08	14.4
DI 9-12 cm	9	12	706	0.33	4.97	15.1
DI 12-16 cm	12	16	865	0.29	4.15	14.1
DI 16-20 cm	16	20	845	0.11	1.42	13.0
DI 20-30 cm	20	30	735	0.08	1.24	14.9

Table AF.2. Elemental chemistry for the JDI_2 (Jierpen Intermediate Invasion) pit

Sample	Initial (cm)	Final (cm)	Weight (mg)	Org. N (%)	Org. C (%)	C:N
			Horizons			
Surface litter	0	0	115	1.63	40.90	25.1
Oi horizon	0	5	602	1.01	18.00	17.9
A horizon	5	10	700	0.27	3.75	14.1
Bw1 horizon	10	21	640	0.07	0.79	11.0
Bw2 horizon	21	42	863	0.01	0.46	35.5
			Depth Intervals			
DI 0-3 cm	0	3	285	1.94	40.21	20.7
DI 3-6 cm	3	6	489	0.86	15.07	17.6
DI 6-9 cm	6	9	418	0.30	4.79	16.0
DI 9-12 cm	9	12	809	0.10	1.15	11.0
DI 12-16 cm	12	16	693	0.08	0.87	10.9
DI 16-20 cm	16	20	840	0.05	0.64	13.0
DI 20-30 cm	20	30	850	0.05	0.58	11.1

Table AF.3. Elemental chemistry (C and N) for the JNW_3 (Jierpen Pre-Invasion) pit

Sample	Initial (cm)	Final (cm)	Weight (mg)	Org. N (%)	Org. C (%)	C:N
			Horizons			
Oi horizon	0	6	393	3.09	43.11	13.9
Oe/Oa horizon	6	13	397	2.37	33.72	14.2
Bw horizon	13	51	643	0.13	1.66	12.4
			Depth Intervals			
DI 0-3 cm	0	3	292	2.83	43.39	15.3
DI 3-6 cm	3	6	299	2.79	40.32	14.5
DI 6-9 cm	6	9	331	2.86	41.42	14.5
DI 9-12 cm	9	12	564	1.24	13.25	10.7
DI 12-16 cm	12	16	496	0.76	9.32	12.2
DI 16-20 cm	16	20	859	0.09	1.14	12.2
DI 20-30 cm	20	30	912	0.12	1.21	9.8

Table AF.4. Elemental chemistry for the JCNW_4 (Jierpen Shoreline Pre-Invasion) pit

Sample	Initial (cm)	Final (cm)	Weight (mg)	Org. N (%)	Org. C (%)	C:N
			Horizons			
Surface litter	0	0	262	1.54	43.26	28.0
Oe horizon	0	7	332	2.16	40.37	18.7
Oa horizon	7	27	681	2.14	30.62	14.3
Bw horizon	27	41	743	0.07	0.91	12.8
			Depth Intervals			
DI 0-3 cm	0	3	357	2.00	38.04	19.0
DI 3-6 cm	3	6	357	2.16	32.27	14.9
DI 6-9 cm	6	9	506	2.20	34.39	15.6
DI 9-12 cm	9	12	582	2.28	32.45	14.2
DI 12-16 cm	12	16	449	2.43	35.88	14.7
DI 16-20 cm	16	20	700	2.04	28.63	14.0
DI 20-27 cm	20	27	693	1.59	20.58	13.0

Table AF.5. Elemental chemistry for the KW_1 (Kopparåsen Invaded) soil profile

Sample	Initial (cm)	Final (cm)	Weight (mg)	Org. N (%)	Org. C (%)	C:N
			Horizons			
A1 horizon	0	4	807	0.25	5.26	21.1
A2 horizon	4	11	723	0.21	4.49	21.5
Bw1 horizon	11	21	743	0.09	1.07	12.1
Bw2 horizon	21	30	766	0.07	0.88	11.9
			Depth Intervals			
DI 0-3 cm	0	3	691	0.28	5.70	20.4
DI 3-6 cm	3	6	704	0.20	4.82	23.9
DI 6-9 cm	6	9	690	0.20	3.82	18.7
DI 9-12 cm	9	12	626	0.18	3.27	18.3
DI 12-16 cm	12	16	877	0.13	2.19	16.3
DI 16-20 cm	16	20	679	0.07	1.24	17.0

Table AF.6. Elemental chemistry for the KW_3 (Kopparåsen Pre-Invasion) soil pit

Sample	**Initial** (cm)	**Final** (cm)	**Weight** (mg)	**Org. N** (%)	**Org. C** (%)	**C:N**
			Horizons			
Oi horizon	0	7	391	0.66	13.13	19.8
A horizon	7	9	714	0.23	4.27	18.6
Bw1 horizon	9	14	832	0.11	2.49	22.9
Bw2 horizon	14	25	811	0.07	0.89	13.1
			Depth Intervals			
DI 0-3 cm	0	3	242	0.88	19.91	22.5
DI 3-6 cm	3	6	715	0.40	7.41	18.3
DI 6-9 cm	6	9	927	0.13	2.24	16.7
DI 9-12 cm	9	12	746	0.10	1.31	12.8
DI 12-16 cm	12	16	976	0.07	0.99	14.9
DI 16-20 cm	16	20	957	0.07	0.80	11.0

Table AF.7. Elemental chemistry – Kuhmo Heavily Invaded (Kuhmo_176, KW_176) pit

Sample	Initial (cm)	Final (cm)	Weight (mg)	Org. N (%)	Org. C (%)	C:N
			Horizons			
Oi horizon	0	5	647	1.60	27.93	17.5
AO horizon	5	12	402	0.76	11.42	15.0
E horizon	12	21	697	0.05	0.43	8.6
Bs horizon	21	32	762	0.13	2.83	22.5
Bw horizon	32	45	865	0.04	0.76	17.9
BC horizon	45	78	878	0.02	0.16	6.8
C horizon	78	102	1045	0.01	0.13	9.5
			Depth Intervals			
DI 0-3 cm	0	3	336	1.29	22.76	17.7
DI 3-5 cm	3	5	365	1.17	17.23	14.7
DI 5-8 cm	5	8	481	0.96	12.55	13.1
DI 8-11 cm	8	11	553	0.73	9.98	13.7
DI 11-13 cm	11	13	937	0.19	2.96	15.6
DI 13-17 cm	13	17	938	0.04	0.56	14.5
DI 17-20 cm	17	20	694	0.05	0.61	12.4
DI 20-23 cm	20	23	702	0.07	1.23	17.9
DI 23-25 cm	23	25	964	0.18	3.60	20.0
DI 25-29 cm	25	29	953	0.14	2.48	17.8
DI 29-34 cm	29	34	624	0.13	1.97	15.1

Table AF.8. Elemental chemistry – Kuhmo Pre-Invasion (Kuhmo_k02, KNW_02) pit

Sample	Initial (cm)	Final (cm)	Weight (mg)	Org. N (%)	Org. C (%)	C:N
			Horizons			
Oi horizon	0	6	282	1.93	46.10	23.9
Oe horizon	6	8	436	1.42	33.72	23.7
A horizon	8	10	386	0.88	19.06	21.7
E horizon	10	25	997	0.05	0.61	12.4
Bhs1 horizon	25	32	753	0.20	5.77	28.5
Bhs2 horizon	32	60	916	0.10	3.39	34.4
			Depth Intervals			
DI 0-2 cm	0	2	248	1.93	43.13	22.3
DI 2-5 cm	2	5	199	1.95	44.17	22.7
DI 5-8 cm	5	8	251	1.79	45.50	25.5
DI 8-11 cm	8	11	397	0.48	13.10	27.5
DI 11-14 cm	11	14	767	0.08	1.39	16.4
DI 14-16 cm	14	16	782	0.04	0.72	19.3
DI 16-19 cm	16	19	748	0.02	0.42	27.3
DI 19-23 cm	19	23	760	0.06	0.49	8.4
DI 23-26 cm	23	26	631	0.06	1.54	26.7
DI 26-30 cm	26	30	714	0.19	5.52	29.4
DI 30-37 cm	30	37	666	0.16	5.14	31.2
DI 37-43 cm	37	43	805	0.17	4.85	28.7
DI 43-60 cm	43	60	963	0.15	4.11	27.2

Table AF.9. Elemental chemistry – Hyytiälä_1A Invaded (Hyytiälä_1A, HW_1A) pit

Sample	**Initial** (cm)	**Final** (cm)	**Weight** (mg)	**Org. N** (%)	**Org. C** (%)	**C:N**
			Horizons			
A horizon	0	9	793	0.64	10.04	15.7
E/A horizon	9	17	974	0.10	1.32	13.0
Bt horizon	17	27	836	0.00	0.42	0.0
Bw horizon	27	60	962	0.00	0.37	0.0
			Depth Intervals			
Surface litter	0	0	305	1.25	40.13	32.2
Surface litter	0	0	329	1.18	40.49	34.3
Surface litter	0	0	411	1.21	34.43	28.4
Di 0-3 cm	0	3	761	0.82	13.56	16.5
DI 3-5 cm	3	5	856	0.44	7.20	16.3
DI 5-7 cm	5	7	779	0.37	5.75	15.6
DI 7-10 cm	7	10	929	0.26	4.36	16.8
DI 10-12 cm	10	12	745	0.24	4.08	16.7
DI 12-14 cm	12	14	821	0.18	3.04	16.9
DI 14-16 cm	14	16	997	0.15	2.29	15.3
DI 16-19 cm	16	19	841	0.12	1.69	14.4
DI 19-21 cm	19	21	791	0.11	1.49	13.9
DI 21-24 cm	21	24	942	0.00	0.61	0.0
DI 24-27 cm	24	27	802	0.01	0.77	105.0
DI 27-29 cm	27	29	928	0.00	0.59	0.0
DI 29-33 cm	29	33	961	0.00	0.33	69.1

Table AF.10. Elemental chemistry – Hyytiälä_H4 Invaded (Hyytiälä_H4, HW_H4) pit

Sample	**Initial** (cm)	**Final** (cm)	**Weight** (mg)	**Org. N** (%)	**Org. C** (%)	**C:N**
			Horizons			
A horizon	0	17	958	0.20	2.62	12.9
AB horizon	17	24	886	0.01	0.50	95.6
Bw horizon	24	45	938	0.00	0.16	72.7
BC horizon	45	65	1008	0.00	0.16	0.0
			Depth Intervals			
Surface litter	0	0	312	1.71	48.89	28.6
Surface litter	0	0	302	1.62	48.60	30.1
DI 0-2 cm	0	2	735	0.28	4.07	14.6
DI 2-4 cm	2	4	765	0.24	3.25	13.5
DI 4-7 cm	4	7	767	0.23	2.97	12.9
DI 7-10 cm	7	10	796	0.21	2.59	12.6
DI 7-10 cm	7	10	885	0.21	2.64	12.6
DI 10-13 cm	10	13	632	0.19	2.46	12.7
DI 13-15 cm	13	15	753	0.16	1.97	12.4
DI 15-18 cm	15	18	769	0.13	1.51	11.8
DI 18-21 cm	18	21	906	0.09	1.33	14.8
DI 21-24 cm	21	24	758	0.08	0.89	11.0
DI 24-27 cm	24	27	835	0.00	0.44	102.1
DI 27-31 cm	27	31	858	0.00	0.25	0.0

Table AF.11. Elemental chemistry – Hyytiälä Pre-Invasion (Hyytiälä_4C, HNW_4C) pit

Sample	**Initial** (cm)	**Final** c(cm)	**Weight** (mg)	**Org. N** (%)	**Org. C** (%)	**C:N**
			Horizons			
Oi/Oe horizon	0	9	310	1.38	46.79	33.9
Oa horizon	9	14	686	0.67	23.22	34.4
E horizon	14	16	731	0.18	3.90	22.0
Bs horizon	16	25	979	0.10	2.05	20.0
Bw1 horizon	25	44	765	0.00	0.59	136.0
Bw2 horizon	44	54	925	0.01	0.27	23.7
Bw3 horizon	54	79	1011	0.01	0.21	18.7
BC horizon	79	115	1132	0.01	0.13	16.7
			Depth Intervals			
Surface litter	0	0	311	1.51	47.44	31.3
DI 0-3 cm	0	3	282	1.21	48.14	39.7
DI 3-6 cm	3	6	352	1.34	46.36	34.6
DI 6-10 cm	6	10	459	0.97	26.93	27.8
DI 10-14 cm	10	14	663	0.56	14.57	26.0
DI 14-17 cm	14	17	790	0.17	3.84	23.2
DI 17-20 cm	17	20	649	0.15	2.72	17.7
DI 20-23 cm	20	23	992	0.14	2.87	20.7
DI 23-25 cm	23	25	713	0.09	1.44	15.6
DI 25-28 cm	25	28	931	0.06	1.17	17.9
DI 28-32 cm	28	32	989	0.07	1.04	14.4

Table AF.12. Elemental chemistry – Hyytiälä Early Invasion (Hyytiälä5C, HNW_5C) pit

Sample	Initial (cm)	Final (cm)	Weight (mg)	Org. N (%)	Org. C (%)	C:N
			Horizons			
Oi/Oe horizon	0	9	469	1.92	39.85	20.8
A horizon	9	11	683	0.35	6.97	19.9
E/A horizon	11	19	868	0.09	1.18	13.1
Bw1 horizon	19	26	973	0.00	0.32	0.0
Bw2 horizon	26	35	991	0.01	0.24	23.4
BC horizon	35	62	736	0.01	0.18	35.3
			Depth Intervals			
surface litter	0	0	376	2.13	50.24	23.6
DI 0-3 cm	0	3	337	2.16	40.55	18.8
DI 3-6 cm	3	6	491	1.61	28.66	17.8
DI 6-10 cm	6	10	469	1.66	29.51	17.8
DI 10-13 cm	10	13	894	0.38	6.10	16.1
DI 13-15 cm	13	15	828	0.24	4.29	17.5
DI 15-18 cm	15	18	782	0.20	2.81	14.4
DI 18-20 cm	18	20	772	0.17	2.41	14.1
DI 20-23 cm	20	23	957	0.08	1.37	16.6
DI 23-26 cm	23	26	939	0.01	0.99	158.8
DI 26-28 cm	26	28	888	0.00	0.90	1339.3
DI 28-31 cm	28	31	972	0.00	0.27	0.0

Table AF.13. Elemental chemistry for the Lammi Invaded (Lammi_12, LW_12) soil pit

Sample	Initial (cm)	Final (cm)	Weight (mg)	Org. N (%)	Org. C (%)	C:N
			Horizons			
Oi horizon	0	2	496	0.61	13.25	21.8
A horizon	2	14	857	0.34	5.34	15.8
AE horizon	14	24	663	0.15	3.23	21.1
Bw1 horizon	24	42	644	0.00	0.46	0.0
Bw2 horizon	42	58	816	0.01	0.34	47.1
BC horizon	58	110	819	0.00	0.33	0.0
			Depth Intervals			
Surface litter	0	0	366	1.39	41.01	29.4
Surface litter	0	0	305	1.26	40.92	32.6
DI 0-2 cm	0	2	545	0.77	13.71	17.8
DI 2-5 cm	2	5	777	0.80	13.18	16.5
DI 5-8 cm	5	8	775	0.56	7.81	13.9
DI 8-10 cm	8	10	723	0.45	7.25	16.1
DI 10-13 cm	10	13	745	0.31	5.01	16.1
DI 13-16 cm	13	16	940	0.21	3.54	16.8
DI 16-18 cm	16	18	925	0.16	2.95	18.6
DI 18-21 cm	18	21	671	0.13	2.39	18.6
DI 21-24 cm	21	24	925	0.00	1.66	757.1
DI 24-29 cm	24	29	971	0.00	1.19	358.4
DI 29-35 cm	29	35	687	0.00	0.76	0.0

Table AF.14. Elemental chemistry – Lammi Early Invasion (Lammi_S02, LNW_S02)

Sample	**Initial** (cm)	**Final** (cm)	**Weight** (mg)	**Org. N** (%)	**Org. C** (%)	**C:N**
			Horizons			
Oi horizon	0	3	234	2.06	41.51	20.2
A horizon	6	15	627	0.36	5.18	14.2
AE horizon	15	22	534	0.18	2.37	13.5
Bw1 horizon	22	32	750	0.09	1.23	13.0
Bw2 horizon	32	67	721	0.05	0.57	12.5
C horizon	67	95	665	0.02	0.44	19.6
			Depth Intervals			
Surface litter	0	0	176	1.77	49.15	27.8
DI 0-3 cm	0	3	247	1.70	30.28	17.9
DI 3-7 cm	3	7	325	0.69	9.59	14.0
DI 7-10 cm	7	10	462	0.44	6.46	14.5
DI 10-15 cm	10	15	614	0.28	4.37	15.4
DI 15-19 cm	15	19	776	0.21	3.25	15.7
DI 19-23 cm	19	23	702	0.14	2.27	15.8
DI 23-28 cm	23	28	758	0.10	1.43	14.7
DI 28-33 cm	28	33	747	0.09	1.03	11.5

Table AF.15. Elemental chemistry – Tvärminne_61 Invaded (Tvärminne_61, TW_61)

Sample	Initial (cm)	Final (cm)	Weight (mg)	Org. N (%)	Org. C (%)	C:N
			Horizons			
A1 horizon	0	16	762	0.59	7.98	13.5
A2 horizon	16	28				
E horizon	28	38	862	0.00	0.50	513.3
Bt horizon	38	57	898	0.00	0.37	132.8
Bk1 horizon	57	73				
Bk2 horizon	73	96				
Bk3 horizon	96	103	903	0.00	0.14	0.0
			Depth Intervals			
Surface litter	0	0	529	1.13	23.47	20.8
DI 0-3 cm	0	3	657	1.20	19.79	16.4
DI 3-7 cm	3	7	847	1.04	13.27	12.8
DI 3-7 cm	3	7	581	1.08	15.38	14.3
DI 7-10 cm	7	10	613	0.70	9.08	13.0
DI 10-13 cm	10	13	969	0.55	7.00	12.6
DI 13-15 cm	13	15	717	0.42	5.02	12.0
DI 15-18 cm	15	18	789	0.33	4.16	12.6
DI 18-21 cm	18	21	752	0.26	2.96	11.5
DI 21-24 cm	21	24	770	0.13	1.81	13.9
DI 24-31 cm	24	31	824	0.09	1.21	13.4

Table AF.16. Elemental chemistry – Tvärminne_34 Invaded (Tvärminne_34, TW_34)

Sample	Initial (cm)	Final (cm)	Weight (mg)	Org. N (%)	Org. C (%)	C:N
			Horizons			
A1 horizon	0	6	688	0.32	4.46	13.9
A2 horizon	6	13	859	0.22	2.90	13.1
AE horizon	13	25				
E/A horizon	25	31	767	0.01	0.50	84.1
Bt horizon	31	44	829	0.01	0.32	42.0
Bk1 horizon	44	51	745	0.00	0.21	47.8
Bk2 horizon	51	73	901	0.00	0.14	1053.6
			Depth Intervals			
Surface litter	0	0	322	1.10	28.15	25.6
DI 0-2 cm	0	2	598	0.46	8.54	18.7
DI 2-5 cm	2	5	664	0.39	5.07	13.1
DI 5-8 cm	5	8	772	0.29	3.78	12.8
DI 8-11 cm	8	11				
DI 11-14 cm	11	14	964	0.18	2.28	12.6
DI 14-16 cm	14	16	910	0.13	1.76	13.2
DI 16-19 cm	16	19	814	0.08	1.15	14.1
DI 19-22 cm	19	22				
DI 22-25 cm	22	25				
DI 25-27 cm	25	27	875	0.01	0.79	91.1
DI 27-31 cm	27	31	831	0.01	0.45	44.6

Table AF.17. Elemental chemistry – Tvärminne_8 Pre-invasion (Tvärminne_8, TNW_8)

Sample	Initial (cm)	Final (cm)	Weight (mg)	Org. N (%)	Org. C (%)	C:N
			Horizons			
Oi horizon	0	8	368	2.27	47.45	20.9
AO horizon	8	15	664	0.89	19.68	22.2
E horizon	15	21	897	0.01	0.28	23.2
Bw horizon	21	44	956	0.01	0.30	24.0
2Bg horizon	44	53	800	0.15	1.62	11.0
Bw' horizon	53	75	948	0.00	0.13	29.7
BC horizon	75	100	782	0.01	0.09	11.3
			Depth Intervals			
Surface litter	0	0	403	2.16	45.20	20.9
DI 0-2 cm	0	2	421	1.38	26.69	19.3
DI 2-5 cm	2	5	328	2.28	46.72	20.5
DI 5-7 cm	5	7	340	2.36	45.62	19.3
DI 7-10 cm	7	10	691	0.86	18.68	21.7
DI 10-14 cm	10	14	813	0.49	8.99	18.3
DI 14-18 cm	14	18	791	0.05	1.51	28.1
DI 18-21 cm	18	21	926	0.07	1.10	14.7
DI 21-25 cm	21	25	831	0.06	0.68	12.4
DI 25-29 cm	25	29	935	0.05	0.60	11.3
DI 29-33 cm	29	33	998	0.04	0.39	9.3

Table AF.18. Elemental chemistry – Tvärminne_627 (TNW_627) Pre-Invasion soil pit

Sample	Initial (cm)	Final (cm)	Weight (mg)	Org. N (%)	Org. C (%)	C:N
			Horizons			
Oi horizon	0	13	283	2.60	49.33	19.0
Oe1 horizon	13	33	368	2.58	45.56	17.7
Oe2 horizon	33	43	499	3.07	41.43	13.5
AO horizon	43	53	760	0.81	8.84	10.9
Bg1 horizon	53	65	987	0.10	1.13	11.5
Bg2 horizon	65	76	909	0.01	0.12	11.5
BC horizon	76	85	873	0.02	0.10	4.1
			Depth Intervals			
Surface litter	0	0	303	2.52	50.21	19.9
DI 0-3 cm	0	3	355	2.49	47.85	19.2
DI 3-7 cm	3	7	430	2.48	48.78	19.7
DI 7-10 cm	7	10	494	2.07	35.26	17.1
DI 10-13 cm	10	13	327	2.10	35.75	17.0
DI 13-17 cm	13	17	327	2.25	35.13	15.6
DI 17-20 cm	17	20	376	2.47	37.65	15.3
DI 20-30 cm	20	30	499	2.78	47.20	17.0

Appendix G – Mineral specific surface area (SSA) measurements

Methods

Mineral specific surface area (SSA) was measured on fine-earth (<2 mm) soil fraction splits by N_2 gas adsorption using a TriStar 3020 Surface Area and Porosity Analyzer in the Department of Soil, Water and Climate at the University of Minnesota-Twin Cities. Samples were degassed at 423 K in a flow of He for at least 6 hours to purge adsorbed water from mineral surfaces prior to analysis. Surface area contents (m^2 g^{-1}) were calculated from the Brunauer-Emmett-Teller (BET) equation using 11 measurements made at different relative pressure points (P_o/P max = 0.3) under cryogenic temperatures (77 K). After sample processing, adsorption isotherms were monitored for their shape (e.g. Brunauer *et al.,* 1940) and only the linear portions of the isotherm were utilized as suggested by Heister *et al.* (2014).

Mineral SSA measurements were made prior to and after removal of organic matter by muffling. Soils were placed in ceramic crucibles and heated in a Lindberg/Blue 1100 °C box furnace (model BF51800) at 623 K for 12 hours to expose mineral surfaces previously occluded by organic matter. Following muffling, we repeated degassing at 423 K in a flow of He before measuring samples following the same procedure. The SSA covered by sorbed organic matter ($SSA_{occluded}$) and the surface area free of organic coatings was calculated using previously outlined methods (Mayer and Xing, 2001; Wagai *et al.,* 2009) described further in the calculations section below. See Appendix D for additional discussion pertaining to our correction and (re-) presentation of erroneous SSA data published by Lyttle *et al.* (2011, 2015).

Table AG.1. Mineral surface area (SSA) data for the Jierpen Invaded (JW_1) soil profile

Sample	**Initial** (cm)	**Final** (cm)	**$SSA_{exposed}$** (m^2 g^{-1})	**SSA_{total}** (m^2 g^{-1})	**$SSA_{occluded}$** (m^2 g^{-1})	**$\%_{occluded}$** (%)
			Horizons			
A1 horizon	0	10	3.76	12.50	8.74	69.9
AB horizon	10	18	4.80	11.74	6.93	59.1
Bw1 horizon	18	35	7.18	10.74	3.56	33.2
Bw2 horizon	35	63	5.90	8.64	2.74	31.7
			Depth Intervals			
DI 0-3 cm	0	3	3.21	12.92	9.71	75.1
DI 3-6 cm	3	6	3.93	12.95	9.03	69.7
DI 6-9 cm	6	9	4.37	11.88	7.51	63.2
DI 9-12 cm	9	12	4.21	12.31	8.10	65.8
DI 12-16 cm	12	16	4.68	10.67	5.99	56.1
DI 16-20 cm	16	20	5.39	8.43	3.05	36.1
DI 20-30 cm	20	30				

Table AG.2. Mineral SSA data for the JDI_2 (Jierpen Intermediate Invasion) soil profile

Sample	Initial (cm)	Final (cm)	$SSA_{exposed}$ (m^2 g^{-1})	SSA_{total} (m^2 g^{-1})	$SSA_{occluded}$ (m^2 g^{-1})	$\%_{occluded}$ (%)
			Horizons			
Oi horizon	0	5	– [a]	–	–	–
A horizon	5	10	4.64	11.10	6.45	58.2
Bw1 horizon	10	21	6.24	7.60	1.36	18.0
Bw2 horizon	21	42	6.28	6.70	0.41	6.2
			Depth Intervals			
DI 0-3 cm	0	3	– [a]	–	–	–
DI 3-6 cm	3	6	–	–	–	–
DI 6-9 cm	6	9	4.29	10.79	6.50	60.3
DI 9-12 cm	9	12	7.59	9.58	1.98	20.7
DI 12-16 cm	12	16	8.30	9.82	1.52	15.4
DI 16-20 cm	16	20	7.85	8.63	0.78	9.0
DI 20-30 cm	20	30				

[a] Mineral SSA values were not determined for organic horizons and depth intervals

Table AG.3. Mineral SSA data for the JNW_3 (Jierpen Pre-Invasion) soil profile

Sample	Initial (cm)	Final (cm)	$SSA_{exposed}$ (m^2 g^{-1})	SSA_{total} (m^2 g^{-1})	$SSA_{occluded}$ (m^2 g^{-1})	$\%_{occluded}$ (%)
			Horizons			
Oi horizon	0	6	*0.39* [a]	*32.36*	*31.97*	*98.8*
Oe/Oa horizon	6	13	*0.37*	*12.15*	*11.79*	*97.0*
Bw2 horizon	13	51	3.58	6.37	2.79	43.8
			Depth Intervals			
DI 0-3 cm	0	3	*0.43* [a]	*29.93*	*29.50*	*98.6*
DI 3-6 cm	3	6	*0.38*	*27.47*	*27.09*	*98.6*
DI 6-9 cm	6	9	*0.50*	*28.13*	*27.62*	*98.2*
DI 9-12 cm	9	12	*0.84*	*8.78*	*7.94*	*90.5*
DI 12-16 cm	12	16	1.23	7.56	6.32	83.7
DI 16-20 cm	16	20	3.74	6.62	2.88	43.5
DI 20-30 cm	20	30	3.95	6.90	2.96	42.8

[a] Mineral SSA values for organic horizons and depth intervals (*italics*) are invalid because <1 m^2 of total SSA was measured for $SSA_{exposed}$

Table AG.4. Mineral SSA data for the KW_1 (Kopparåsen Heavily Invaded) soil profile

Sample	Initial (cm)	Final (cm)	$SSA_{exposed}$ ($m^2\ g^{-1}$)	SSA_{total} ($m^2\ g^{-1}$)	$SSA_{occluded}$ ($m^2\ g^{-1}$)	$\%_{occluded}$ (%)
			Horizons			
A1 horizon	0	4	4.03	10.35	6.32	61.0
A2 horizon	4	11	3.61	10.16	6.54	64.4
Bw1 horizon	11	21	10.63	12.51	1.88	15.0
Bw2 horizon	21	30	8.92	10.57	1.65	15.6
			Depth Intervals			
DI 0-3 cm	0	3	3.09	10.55	7.45	70.7
DI 3-6 cm	3	6	4.07	11.45	7.39	64.5
DI 6-9 cm	6	9	5.59	11.23	5.64	50.2
DI 9-12 cm	9	12	6.50	10.85	4.35	40.1
DI 12-16 cm	12	16	7.59	10.51	2.92	27.8
DI 16-20 cm	16	20	8.92	9.55	0.63	6.6
DI 20-30 cm	20	30				

Table AG.5. Mineral SSA data for the KW_3 (Kopparåsen Pre-Invasion) soil profile

Sample	Initial (cm)	Final (cm)	$SSA_{exposed}$ ($m^2\ g^{-1}$)	SSA_{total} ($m^2\ g^{-1}$)	$SSA_{occluded}$ ($m^2\ g^{-1}$)	$\%_{occluded}$ (%)
			Horizons			
Oi horizon	0	7	*0.56* [a]	*2.97*	*2.41*	*81.1*
A horizon	7	9	5.95	11.01	5.06	46.0
Bw1 horizon	9	14	12.52	13.87	1.36	9.8
Bw2 horizon	14	25	12.62	12.94	0.32	2.5
			Depth Intervals			
DI 0-3 cm	0	3	*0.56* [a]	*3.32*	*2.75*	*83.0*
DI 3-6 cm	3	6	*1.98*	*6.79*	*4.81*	*70.8*
DI 6-9 cm	6	9	7.96	9.42	1.47	15.6
DI 9-12 cm	9	12	8.75	8.79	0.04	0.5
DI 12-16 cm	12	16	7.89	9.24	1.35	17.1
DI 16-20 cm	16	20	7.61	7.64	0.03	0.4
DI 20-30 cm	20	30				

[a] Mineral SSA values for organic horizons and depth intervals (*italics*) are invalid because <1 m^2 of total SSA was measured for $SSA_{exposed}$

Table AG.6. Mineral SSA data for the Kuhmo Invaded (Kuhmo_176, KW_176) profile

Sample	**Initial** (cm)	**Final** (cm)	**$SSA_{exposed}$** ($m^2\ g^{-1}$)	**SSA_{total}** ($m^2\ g^{-1}$)	**$SSA_{occluded}$** ($m^2\ g^{-1}$)	**$\%_{occluded}$** (%)
			Horizons			
Oi horizon	0	5	*0.42* [a]	*9.21*	*8.79*	*95.4*
AO horizon	5	12	0.19	3.57	3.38	94.7
E horizon	12	21	0.29	0.82	0.53	64.6
Bs horizon	21	32	8.35	14.22	5.87	41.3
Bw horizon	32	45	3.66	4.87	1.21	24.8
BC horizon	45	78	1.16	1.51	0.35	23.0
C horizon	78	102	0.93	1.16	0.23	19.9
			Depth Intervals			
DI 0-3 cm	0	3	*0.32* [a]	*6.48*	*6.16*	*95.0*
DI 3-5 cm	3	5	*0.35*	*6.92*	*6.57*	*94.9*
DI 5-8 cm	5	8	0.30	4.53	4.24	93.4
DI 8-11 cm	8	11	0.28	3.36	3.07	91.5
DI 11-13 cm	11	13	0.23	1.23	1.01	81.7
DI 13-17 cm	13	17	0.28	0.80	0.52	65.5
DI 17-20 cm	17	20	0.51	1.34	0.83	61.7
DI 20-23 cm	20	23	2.56	4.01	1.45	36.1
DI 23-25 cm	23	25	10.97	15.44	4.48	29.0
DI 25-29 cm	25	29	8.49	9.99	1.50	15.0
DI 29-34 cm	29	34				

[a] Mineral SSA values for organic horizons and depth intervals (*italics*) are invalid because <1 m^2 of total SSA was measured for $SSA_{exposed}$

Table AG.7. Mineral SSA data for the Kuhmo Pre-Invasion (Kuhmo_k02, KNW_02) pit

Sample	Initial (cm)	Final (cm)	$SSA_{exposed}$ (m^2 g^{-1})	SSA_{total} (m^2 g^{-1})	$SSA_{occluded}$ (m^2 g^{-1})	$\%_{occluded}$ (%)
			Horizons			
Oi horizon	0	6	*0.29* [a]	*16.38*	*16.09*	*98.2*
Oe horizon	6	8	*0.50*	*19.73*	*19.23*	*97.5*
A horizon	8	10	0.57	2.15	1.58	73.4
E horizon	10	25	0.99	2.30	1.31	57.1
Bhs1 horizon	25	32	2.44	8.04	5.60	69.7
Bhs2 horizon	32	60	3.24	7.99	4.75	59.5
			Depth Intervals			
DI 0-2 cm	0	2	*0.50* [a]	*16.46*	*15.96*	*97.0*
DI 2-5 cm	2	5	*0.51*	*25.55*	*25.04*	*98.0*
DI 5-8 cm	5	8	*0.65*	*25.10*	*24.45*	*97.4*
DI 8-11 cm	8	11	0.44	1.89	1.45	76.7
DI 11-14 cm	11	14	0.40	1.52	1.12	73.7
DI 14-16 cm	14	16	0.44	1.23	0.78	63.8
DI 16-19 cm	16	19	0.91	1.74	0.83	47.8
DI 19-23 cm	19	23	0.99	1.98	0.99	50.0
DI 23-26 cm	23	26	2.28	4.30	2.02	46.9
DI 26-30 cm	26	30	2.58	8.26	5.68	68.8
DI 30-37 cm	30	37	2.22	6.01	3.79	63.1
DI 37-43 cm	37	43				
DI 43-60 cm	43	60				

[a] Mineral SSA values for organic horizons and depth intervals (*italics*) are invalid because <1 m^2 of total SSA was measured for $SSA_{exposed}$

Table AG.8. Mineral SSA data for the Hyytiälä_1A Invaded (Hyytiälä_1A, HW_1A) pit

Sample	**Initial** (cm)	**Final** (cm)	**$SSA_{exposed}$** ($m^2\ g^{-1}$)	**SSA_{total}** ($m^2\ g^{-1}$)	**$SSA_{occluded}$** ($m^2\ g^{-1}$)	**$\%_{occluded}$** (%)
			Horizons			
A horizon	0	9	2.24	14.22	11.98	84.2
E/A horizon	9	17	11.89	12.74	0.85	6.7
Bt horizon	17	27	10.37	11.14	0.78	7.0
Bw horizon	27	60	12.36	11.56	-0.80	-6.9
			Depth Intervals			
DI 0-3 cm	0	3	2.12	15.69	13.58	86.5
DI 3-5 cm	3	5	3.53	12.94	9.41	72.7
DI 5-7 cm	5	7	3.44	12.41	8.97	72.3
DI 7-10 cm	7	10	6.91	13.88	6.98	50.2
DI 10-12 cm	10	12	7.67	12.96	5.30	40.9
DI 12-14 cm	12	14	10.78	13.29	2.51	18.9
DI 14-16 cm	14	16	11.58	14.48	2.90	20.0
DI 16-19 cm	16	19	11.26	13.63	2.37	17.4
DI 19-21 cm	19	21	11.89	12.40	0.51	4.1
DI 21-24 cm	21	24	10.21	11.54	1.32	12.9
DI 24-27 cm	24	27				
DI 27-29 cm	27	29				
DI 29-33 cm	29	33				

Table AG.9. Mineral SSA data for Hyytiälä Pre-Invasion (Hyytiälä_4C, HNW_4C) pit

Sample	Initial (cm)	Final (cm)	$SSA_{exposed}$ (m^2 g^{-1})	SSA_{total} (m^2 g^{-1})	$SSA_{occluded}$ (m^2 g^{-1})	$\%_{occluded}$ (%)
			Horizons			
Oi/Oe horizon	0	9	*0.79* [a]	*36.25*	*35.46*	*97.8*
Oa horizon	9	14	*0.83*	*7.72*	*6.90*	*89.3*
E horizon	14	16	2.15	8.88	6.72	75.7
Bs horizon	16	25	10.77	13.70	2.93	21.4
Bw1 horizon	25	44	6.33	8.74	2.42	38.2
Bw2 horizon	44	54	7.92	5.78	-2.14	-37.0
Bw3 horizon	54	79	7.75	6.83	-0.93	-13.5
BC horizon	79	115	7.32	6.25	-1.07	-17.1
			Depth Intervals			
DI 0-3 cm	0	3	– [b]	–	–	–
DI 3-6 cm	3	6	–	–	–	–
DI 6-10 cm	6	10	–	–	–	–
DI 10-14 cm	10	14	*0.54* [a]	*8.10*	*7.56*	*93.4*
DI 14-17 cm	14	17	3.02	8.75	5.73	65.5
DI 17-20 cm	17	20	10.87	16.32	5.45	33.4
DI 20-23 cm	20	23	11.30	18.40	7.09	38.6
DI 23-25 cm	23	25	11.41	11.89	0.47	4.0
DI 25-28 cm	25	28	10.52	11.05	0.53	5.0
DI 28-32 cm	28	32	9.99	10.38	0.39	3.9

[a] Mineral SSA values for organic horizons and depth intervals (*italics*) are invalid because <1 m^2 of total SSA was measured for $SSA_{exposed}$
[b] Mineral SSA values were not determined for organic layer depth intervals

Table AG.10. Mineral SSA data for Tvärminne_8 Pre-invasion (Tvärminne_8, TNW_8)

Sample	Initial (cm)	Final (cm)	$SSA_{exposed}$ (m^2 g^{-1})	SSA_{total} (m^2 g^{-1})	$SSA_{occluded}$ (m^2 g^{-1})	$\%_{occluded}$ (%)
			Horizons			
Oi horizon	0	8	*0.88* [a]	*109.78*	*108.91*	*99.2*
AO horizon	8	15	1.14	22.52	21.38	94.9
E horizon	15	21	0.17	0.59	0.42	70.8
Bw horizon	21	44	0.39	0.91	0.51	56.6
2Bg horizon	44	53	14.06	21.95	7.89	35.9
Bw' horizon	53	75	3.62	3.48	-0.14	-3.9
BC horizon	75	100	0.52	0.97	0.45	46.2
			Depth Intervals			
DI 0-2 cm	0	2	– [b]	–	–	–
DI 2-5 cm	2	5	–	–	–	–
DI 5-7 cm	5	7	–	–	–	–
DI 7-10 cm	7	10	0.52	9.40	8.88	94.5
DI 10-14 cm	10	14	0.54	7.35	6.81	92.6
DI 14-18 cm	14	18	0.18	1.07	0.89	83.0
DI 18-21 cm	18	21	0.19	0.88	0.69	78.2
DI 21-25 cm	21	25	0.20	0.70	0.50	71.1
DI 25-29 cm	25	29	0.18	0.64	0.46	71.6
DI 29-33 cm	29	33	0.21	0.56	0.35	62.2

[a] Mineral SSA values for organic horizons and depth intervals (*italics*) are invalid because <1 m^2 of total SSA was measured for $SSA_{exposed}$
[b] Mineral SSA values were not determined for organic layer depth intervals